

Dry Preservation of Heavy Metal Contaminants  
Using Cation Exchange Resins for Improved Water  
Quality Monitoring

by

Emily B. Hanhauser

B.S., University of Wisconsin - Madison, 2012

Submitted to the Department of Mechanical Engineering  
in partial fulfillment of the requirements for the degree of

Master of Science in Mechanical Engineering

at the

MASSACHUSETTS INSTITUTE OF TECHNOLOGY

June 2017

© Massachusetts Institute of Technology 2017. All rights reserved.

**Signature redacted**

Author .....

Department of Mechanical Engineering

May 16, 2017

**Signature redacted**

Certified by .....

Rohit Karnik

Associate Professor of Mechanical Engineering

Thesis Supervisor

**Signature redacted**

Certified by .....

A. John Hart

Associate Professor of Mechanical Engineering

Thesis Supervisor

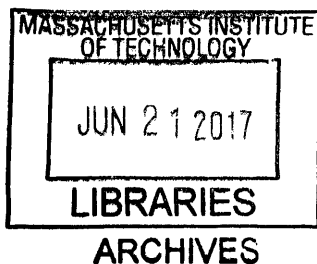
**Signature redacted**

Accepted by .....

Rohan Abeyaratne

Professor of Mechanical Engineering

Chairman, Committee on Graduate Students





# Dry Preservation of Heavy Metal Contaminants Using Cation Exchange Resins for Improved Water Quality Monitoring

by

Emily B. Hanhauser

Submitted to the Department of Mechanical Engineering  
on May 16, 2017, in partial fulfillment of the  
requirements for the degree of  
Master of Science in Mechanical Engineering

## Abstract

Water quality monitoring is crucial to identifying and sustaining safe drinking water sources, tracking contamination events and remediating polluted sources. Monitoring of water sources is usually performed using a combination of field test kits and centralized laboratory analysis. While field test kits are easy and rapid to use, they are often inaccurate and cannot test for all parameters of interest. On the other hand, centralized laboratory testing can quantify parameters at trace levels using high throughput instrumentation, but preserving and transporting large volume water samples to these labs is time consuming and labor intensive. These challenges are especially problematic for rural or resource-limited settings, such that monitoring of drinking water sources in these areas is limited.

Inspired by dried blood spotting, which revolutionized centralized testing for clinical trials, this thesis seeks to explore and develop a dry preservation technology for improved water quality monitoring. The technology includes a dry preservation device incorporating a sorbent, which collects and preserves contaminants from a water sample in a format that is easily transported or shippable. When the device arrives at a centralized lab, the contaminants can be removed from the device using a simple solvent elution step, yielding contaminants in a ready to test format, or the sorbent from the device can itself be directly analyzed using testing methods that accept solid samples. Such a paradigm has the potential to increase the ease and reach of water quality monitoring.

This thesis describes field work, dry sampling sorbent identification and selection, kinetic parameter testing of the dry sampling sorbent, lab contaminant recovery protocol development and initial dry sampling device design for the dry storage of heavy metal cation contaminants. Heavy metals, such as lead, nickel and copper, are selected because they cause chronic health issues at very small concentrations and are increasingly found in drinking water sources due to anthropogenic contamination. The technology is developed in the context of India; however, dry sampling technology would likely find use in rural and resource limited communities around the world.

Thesis Supervisor: Rohit Karnik  
Title: Associate Professor of Mechanical Engineering

Thesis Supervisor: A. John Hart  
Title: Associate Professor of Mechanical Engineering



## Acknowledgments

My time thus far at MIT has been nothing short of fantastic and I have many people to thank for this experience.

First, to Professor Rohit Karnik — thank you for your advice, endless encouragement and support of my educational and career goals. Your guidance as my advisor is large reason why I have become a successful engineer and why I have decided to continue on for a Ph.D.

To Professor John Hart — thank you for your support, assistance in the ideation process and enthusiasm for my learning. I look forward to working more with you as this project gets to the device design stage.

To Professor Chintan Vaishnav — exploring the systems side and social implications of this project has been valuable and eye-opening because of your expertise and thoughtful insights. Thanks for encouraging me to think about the societal impacts of technology.

To my labmates in the Karnik and Hart labs, and the water exploration team — you make the lab a fun and inviting place. Thank you for the laughs and advice.

To the Center for Materials Science and Engineering and the Institute for Soldier Nanotechnologies, both of which provided core instrumentation for this project — thank you for providing the training and support to me and the MIT community necessary to perform cutting edge research.

To my classmates at MIT, in Mechanical Engineering and beyond — you are some of the smartest, most passionate people I have ever met and your accomplishments never seek to amaze me. Thank you for the camaraderie and support. Grad school would not be as fun without you.

And lastly, to my parents and brother — you have never stopped believing in me and pushing me to achieve my goals while having fun at the same time. I have never been afraid to try things because I know I will always have your love and support. Thanks for instilling in me a passion for science and for people and for fun.



# Contents

|          |  |           |
|----------|--|-----------|
| <b>1</b> | <b>Introduction</b>  | <b>17</b> |
| 1.1      | Motivation . . . . .   | 17        |
| 1.2      | Methods in water quality monitoring . . . . .                                      | 21        |
| 1.2.1    | Water quality parameters and guidelines . . . . .                                  | 21        |
| 1.2.2    | Sample collection and preservation for drinking water quality monitoring . . . . . | 24        |
| 1.2.3    | Laboratory test methods for water quality parameters . . . . .                     | 25        |
| 1.3      | Drinking water quality in India . . . . .  | 29        |
| 1.3.1    | Government water quality monitoring scheme in India . . . . .                      | 30        |
| 1.4      | Objectives and outline of thesis . . . . .   | 32        |
| <b>2</b> | <b>Identification of project scope through fieldwork in India</b>                  | <b>35</b> |
| 2.1      | Introduction . . . . .   | 35        |
| 2.2      | Methods . . . . .  | 36        |
| 2.3      | Results . . . . .  | 36        |
| 2.3.1    | Sub-district laboratories . . . . .  | 38        |
| 2.3.2    | District level labs . . . . .  | 40        |
| 2.3.3    | State level labs . . . . .   | 41        |
| 2.4      | Conclusion . . . . .   | 42        |
| <b>3</b> | <b>Identification of sorbent materials for dry sampling of heavy metals</b>        | <b>47</b> |
| 3.1      | Introduction . . . . .   | 47        |

|          |   |           |
|----------|---|-----------|
| 3.2      | Literature review: The potential for adsorptive water purification technologies as dry preservation materials . . . . . | 48        |
| 3.2.1    | Adsorption isotherms and equilibrium . . . . .  | 50        |
| 3.2.2    | Cellulosic adsorbents for heavy metal removal . . . . .   | 53        |
| 3.2.3    | Ion exchange resins for heavy metal removal . . . . .   | 55        |
| 3.3      | Materials and methods . . . . .   | 57        |
| 3.3.1    | Reagents . . . . .  | 57        |
| 3.3.2    | Equilibrium adsorption experiments: Cellulose and ion exchange resin capacity for heavy metal contaminants . . . . .    | 58        |
| 3.3.3    | Specific experiment details . . . . .   | 62        |
| 3.4      | Results . . . . .   | 66        |
| 3.4.1    | Effect of pH on copper adsorption on Grade 1 Whatman filter paper . . . . .   | 66        |
| 3.4.2    | Effect of filter paper grade on adsorption capacity of copper . . . . .   | 69        |
| 3.4.3    | Effect of cellulose modifications on adsorption capacity of copper . . . . .  | 70        |
| 3.4.4    | Cation exchange resin copper adsorption capacity . . . . .  | 72        |
| 3.4.5    | Effect of hardness on ion exchange resin and filter paper performance . . . . .   | 73        |
| 3.5      | Conclusion . . . . .  | 77        |
| <b>4</b> | <b>Kinetics of heavy metal uptake by G-26 ion exchange resin</b>  | <b>79</b> |
| 4.1      | Introduction . . . . .  | 79        |
| 4.2      | Kinetics of ion uptake in ion exchange resins: a diffusion controlled process . . . . .                                 | 80        |
| 4.2.1    | Types of diffusion control in ion exchange . . . . .  | 81        |
| 4.2.2    | Kinetic models used in describing ion exchange . . . . .  | 84        |
| 4.3      | Materials and Methods . . . . .   | 88        |
| 4.3.1    | General kinetic experiment protocol . . . . .   | 88        |
| 4.3.2    | Experiment specific protocols . . . . .   | 89        |
| 4.3.3    | Data analysis . . . . .   | 91        |

|          |   |            |
|----------|---|------------|
| 4.4      | Results . . . . .   | 94         |
| 4.4.1    | Uptake of copper, nickel and lead on Dowex G-26 ion exchange resin from very hard water . . . . .   | 95         |
| 4.4.2    | Interruption test and effect of stir speed variation . . . . .                                      | 96         |
| 4.4.3    | Effect of resin dosing on uptake time from very hard water . . . . .                                | 99         |
| 4.4.4    | Effect of water matrix on uptake rate . . . . .   | 101        |
| 4.4.5    | Intraparticle diffusivity estimation . . . . .  | 103        |
| 4.4.6    | Estimation of Nernst film thickness from concentration decay data . . . . .                         | 105        |
| 4.5      | Conclusion . . . . .  | 106        |
| <b>5</b> | <b>Recovery of heavy metal ions after dry preservation on G-26 ion exchange resin</b>               | <b>109</b> |
| 5.1      | Introduction . . . . .  | 109        |
| 5.2      | Materials and methods . . . . .   | 111        |
| 5.2.1    | Materials from previous experiments . . . . .   | 111        |
| 5.2.2    | Sample preparation for testing of long term preservation . . . . .                                  | 111        |
| 5.2.3    | Regeneration of G-26 resin using hydrochloric acid . . . . .  | 112        |
| 5.2.4    | Recovery calculations . . . . .   | 112        |
| 5.3      | Results . . . . .   | 113        |
| 5.3.1    | Initial recovery trial: 5% hydrochloric acid regeneration for G-26 resin and filter paper . . . . . | 113        |
| 5.3.2    | Recovery from the same starting solution after different dry preservation periods . . . . .         | 115        |
| 5.3.3    | Effect of hydrochloric acid concentration on cation recovery . . . . .                              | 118        |
| 5.4      | Conclusion . . . . .  | 119        |
| <b>6</b> | <b>Dry sampling device conceptualization and design</b>   | <b>121</b> |
| 6.1      | Introduction . . . . .  | 121        |
| 6.2      | Ideal device characteristics . . . . .  | 121        |
| 6.3      | Conceptualized ideas . . . . .  | 123        |

|          |  |            |
|----------|--|------------|
| 6.4      | Materials and methods . . . . .  | 125        |
| 6.4.1    | Fabrication of resin coated fabrics, meshes and strings . . . . .                              | 125        |
| 6.4.2    | Thermal testing of G-26 resin . . . . .  | 126        |
| 6.4.3    | Fabrication of ion exchange resin tea bags and tea bag testing<br>in very hard water . . . . . | 126        |
| 6.5      | Results . . . . .  | 127        |
| 6.5.1    | Swelling and stability of resin coated materials . . . . .                                     | 127        |
| 6.5.2    | Thermal formability of native G-26 ion exchange resin . . . . .                                | 130        |
| 6.5.3    | Initial tea bag testing . . . . .  | 131        |
| 6.6      | Conclusion . . . . .   | 133        |
| <b>7</b> | <b>Conclusion</b>  | <b>135</b> |
| 7.1      | Summary of thesis . . . . .  | 135        |
| 7.2      | Future work . . . . .  | 138        |

# List of Figures

|     |  |    |
|-----|--|----|
| 1-1 | Number of people worldwide lacking access to drinking water . . . . .  | 18 |
| 1-2 | Map of water quality labs in the Malda district in the state of West Bengal, India . . . . .                       | 19 |
| 1-3 | Cost of bacterial testing and sampling compliance by site . . . . .  | 20 |
| 1-4 | Water hardness and TDS in the United States measured by the United States Geological Survey . . . . .              | 22 |
| 1-5 | Detection limits of atomic spectroscopy methods . . . . .  | 27 |
| 1-6 | Schematic of most probable number technique . . . . .  | 28 |
| 1-7 | Portfolio of water quality and soil solutions currently in development in Karnik, Hart and Vaishav labs . . . . .  | 30 |
| 1-8 | Schematic of feedback structure for water quality monitoring, suggested by the UDWQMP . . . . .                    | 31 |
| 2-1 | Sampling from open well in Maharashtra . . . . .   | 38 |
| 2-2 | Physical and chemical parameter testing equipment at sub-district water quality monitoring labs in India . . . . . | 39 |
| 2-3 | Bacterial testing equipment at a sub-district water quality lab in Maharashtra . . . . .                           | 40 |
| 2-4 | Water quality sampling and testing equipment at a district lab in Maharashtra . . . . .                            | 41 |
| 2-5 | Current monitoring framework and proposed monitoring framework enabled by dry sampling technology . . . . .        | 45 |
| 3-1 | Asymmetrical surface forces that cause adsorption phenomena . . . . .  | 49 |

|      |   |     |
|------|---|-----|
| 3-2  | Molecular structure of cellulose . . . . .  | 53  |
| 3-3  | Cellulose modification reactions . . . . .  | 55  |
| 3-4  | Structure of cation exchange resin . . . . .  | 56  |
| 3-5  | ICP-OES instrument at the CMSE . . . . .  | 59  |
| 3-6  | Example of ICP-OES calibration curve used for data analysis . . . . .   | 61  |
| 3-7  | Effect of pH on amount of copper adsorbed onto cellulose Grade 1 filter<br>paper . . . . .  | 67  |
| 3-8  | Example of isotherm fitting to experimental data using MATLAB . . . . .   | 68  |
| 3-9  | Modified cellulose performance as a copper adsorbent . . . . .  | 71  |
| 3-10 | Citric acid modified filter paper performance as a copper adsorbent in<br>trials of two modification batches . . . . .              | 72  |
| 3-11 | Copper adsorption isotherm on DOWEX G-26 cation exchange resin . . . . .  | 73  |
| 3-12 | Filter paper versus G-26 resin performance as a copper sorbent in hard<br>water matrices . . . . .                                  | 74  |
| 3-13 | Performance of cation exchange resins in adsorption of multiple heavy<br>metal cations from different hard water matrices . . . . . | 75  |
| 3-14 | Chemical structure of ion exchange resins . . . . .   | 76  |
| 4-1  | Steps in the ion exchange process . . . . .   | 80  |
| 4-2  | Characteristics of particle diffusion and film diffusion . . . . .  | 82  |
| 4-3  | Electrical transference effect on ion exchange . . . . .  | 87  |
| 4-4  | Example exponential decay curve fit to concentration versus time data<br>using MATLAB . . . . .                                     | 92  |
| 4-5  | Kinetics of heavy metal uptake on G-26 resin, initial experiment . . . . .  | 95  |
| 4-6  | Interruption test . . . . .   | 97  |
| 4-7  | Stir speed test . . . . .   | 98  |
| 4-8  | Effect of resin mass/particle number on uptake rate . . . . .   | 100 |
| 4-9  | Comparison between number of resin particles in experiment and decay<br>time constant . . . . .                                     | 100 |
| 4-10 | Effect of water matrix on copper uptake on G-26 resin dosed at SF1.0 . . . . .  | 102 |



|   |     |
|---|-----|
| 4-11 Uptake of sodium and potassium on G-26 resin dosed at SF1.0 from very hard water . . . . .                         | 103 |
| 4-12 Graphical analysis of combined calcium/magnesium intraparticle diffusivities in different water matrices . . . . . | 104 |
| 4-13 Graphical determination of Nernst film thickness . . . . .   | 107 |
| 5-1 Generic ion exchange reaction with hydrogen form resin and reaction quotient . . . . .                              | 110 |
| 5-2 Initial recovery of copper from dry preservation sorbents after 12 days of dry storage . . . . .                    | 114 |
| 5-3 Heavy metal cation recovery from G-26 resin after up to 4 months of dry preservation . . . . .                      | 116 |
| 6-1 Sketches of dry sampling device geometry . . . . .  | 124 |
| 6-2 Polypropylene tea bag testing setup . . . . .   | 127 |
| 6-3 Resin coated fabrics in dry and wet swelled form . . . . .  | 129 |
| 6-4 Comparison of G-26 resin in native form and after incremental heating to 260°C . . . . .                            | 130 |
| 6-5 Fabricated nylon tea bags and their kinetic performance . . . . .   | 131 |
| 6-6 Fabricated polypropylene tea bags and their kinetic performance . . .   | 132 |



# List of Tables

|      |  |    |
|------|--|----|
| 1.1  | Heavy metal contaminants of water, their maximum acceptable limits and health effects . . . . .                                | 24 |
| 1.2  | Sampling and preservation guidelines for common drinking water parameters . . . . .  | 25 |
| 1.3  | Testing methods for common drinking water parameters . . . . .   | 26 |
| 2.1  | Water quality monitoring labs visited in India, January 2016 . . . . .   | 37 |
| 3.1  | Ideal characteristics for a dry preservation device . . . . .  | 48 |
| 3.2  | Cellulose filter paper grades tested . . . . .   | 58 |
| 3.3  | Cation exchange resins tested . . . . .  | 58 |
| 3.4  | ICP-OES instrument settings for analysis . . . . .   | 60 |
| 3.5  | Wavelengths monitoring during ICP-OES analysis . . . . .   | 60 |
| 3.6  | Cellulose modifications attempted in this investigation . . . . .  | 63 |
| 3.7  | Synthetic water recipes . . . . .  | 66 |
| 3.8  | Isotherm best fit parameters for copper adsorption onto cellulose Grade 1 filter paper at various pH . . . . .                 | 68 |
| 3.9  | Amount of Grade 1 filter paper needed to adsorb 80% of copper from a 1L water sample . . . . .                                 | 69 |
| 3.10 | Amount of filter paper of different grades needed to adsorb 80% of copper from a 1L water sample . . . . .                     | 70 |
| 3.11 | Mass of cation exchange resins needed to remove 80% of copper at a concentration of 0.050mg/L from a 1L water sample . . . . . | 73 |

|     |  |     |
|-----|--|-----|
| 4.1 | Fick's Laws of diffusion . . . . .   | 84  |
| 4.2 | Synthetic water recipes used in kinetic testing . . . . .  | 90  |
| 4.3 | Masses of G-26 resin used in kinetic experiments . . . . .   | 91  |
| 4.4 | Decay constants for divalent ions in uptake on G-26 resin from very<br>hard water dosed at SF1.0 . . . . .   | 101 |
| 4.5 | Decay constants for divalent ions in uptake on G-26 resin dosed at<br>SF1.0 from waters of various matrices . . . . .  | 102 |
| 4.6 | Estimated combined calcium/magnesium intraparticle diffusivities . .   | 104 |
| 4.7 | Free solution diffusivities of metal cations at 25°C . . . . .   | 106 |
| 5.1 | Removal efficiency, recovery and overall preservation efficiency for ini-<br>tial preservation testing using G-26 resin and filter paper . . . . .                               | 114 |
| 5.2 | Starting and ending concentration of heavy metals in solution after<br>incubation for 24 hours with no sorbent . . . . .   | 115 |
| 5.3 | Removal efficiency, recovery and overall preservation efficiency for ini-<br>tial preservation testing using G-26 resin for dry preservation periods<br>up to 4 months . . . . . | 117 |
| 5.4 | Comparison of 5% and 10% hydrochloric acid in recovery of heavy<br>metal cations from G-26 resin . . . . .   | 118 |
| 6.1 | Ideal characteristics for dry preservation device, revisited . . . . .   | 122 |
| 6.2 | Tea bag dimensions . . . . .   | 126 |

# Chapter 1

## Introduction

### 1.1 Motivation

Drinking water availability and quality are a major global concerns. As defined by the World Health Organization (WHO), safe drinking water does not cause significant risk to human health during a lifetime of consumption [1]. Accordingly, safe drinking water is free of biological contaminants (bacteria, viruses and protozoa), contains low levels of toxic heavy metals and organic contaminants and should be tasteless, odorless and colorless.

The United Nations (UN) Millennium Development Goals, ratified in 2000, set a target of halving the number of people without access to a safe drinking water source by 2015 [2]. This goal was met, with 2.6 billion people acquiring safe drinking water access between 1990 and 2015 [2]. However, an estimated 660 million people still lack access to an improved water source and 1.75 billion people continue to drink from fecally contaminated sources (Figure 1-1, [3]). There is a clear urban-rural divide in improved source access; 80% of those who lack access to an improved source live in rural settings [3].

Additionally, the natural source of drinking water on earth, freshwater, faces increasing usage pressures from other sectors. Agriculture is the biggest of these sectors, with the largest fraction of worldwide freshwater use [4]. With the global population expected to increase to 9 billion people by 2050, agricultural freshwater withdrawal

## Billions lack safe drinking water

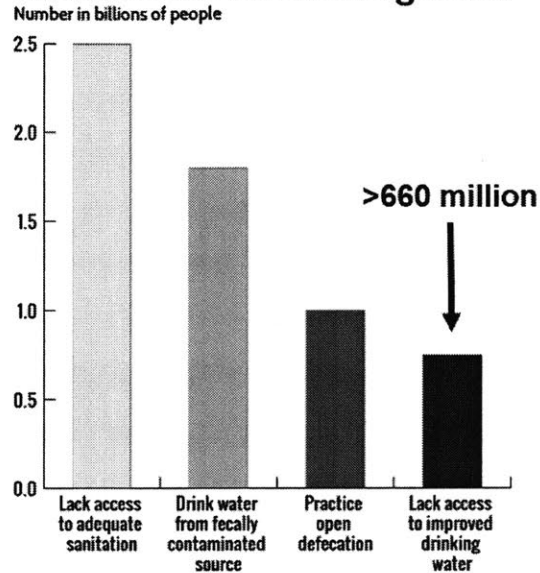


Figure 1-1: Number of people worldwide that lack satisfactory access to drinking water [3].

will need to increase by 19% to produce the food needed to sustain this projected population [5]. This competition in freshwater usage is predicted to force the use and consumption of poor quality, contaminated water.

Together, these projections and current statistics clearly highlight the need for technological solutions in order to ensure safe drinking water for current and future generations. These solutions include sustainable water treatment and reuse technologies, as well as cost effective water purification methods. Although often overlooked, an equally important area in need of improvements is water quality monitoring, including water sampling, preservation and testing technologies and data management.

Water quality monitoring identifies and sustains safe water sources, helps in the management and understanding of disease outbreaks and addresses sources of contamination. Testing for physical, chemical and biological contaminants usually occurs using a combination of field test kits, mobile and/or local laboratories and more centralized local laboratories, as typically specified by a governmental water quality monitoring scheme.

Significant challenges in each type of testing can hamper overall water quality

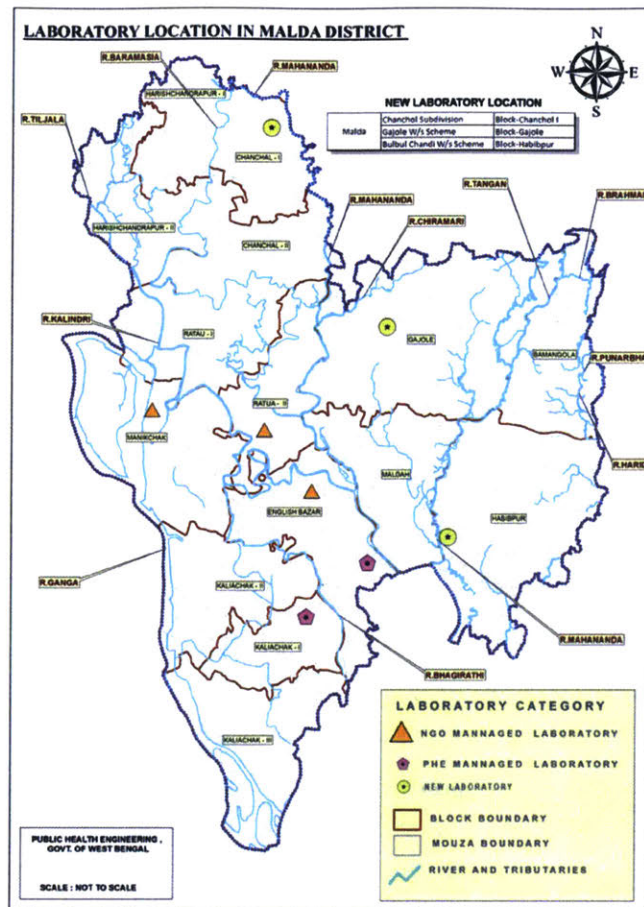


Figure 1-2: Map of water quality labs in the Malda district of West Bengal, India. The district only has two government water quality labs, denoted by pink pentagons [9].

monitoring, especially of sources in rural settings. While field test kits provide rapid results and require minimal training to use, they suffer from low accuracy and inadequate limits of detection, making testing for low level toxic pollutants virtually impossible in the field. Also, field test kits have low throughput and are not available for all relevant parameters [6]. For example, a field test kit for arsenic does exist, with a limit of detection ten times that of the maximum acceptable level, but no test kits exist for mercury, lead or other heavy metal contaminants. Additionally, field test kits for bacteria have been found to be inaccurate and are easily contaminated [7, 8].

On the other hand, laboratory based testing is often high throughput and can

quantify contaminants with high accuracy and precision at very low levels. However, laboratory instrumentation is expensive, preventing the widespread availability of such analyses. Further, preserving large volumes of water (up to 1 liter (L)) and timely transporting water samples from rural localities to these centralized labs for analysis is cumbersome and costly (Figure 1-2). For example, Crocker et al. found that the cost of transporting bacterial samples to the lab was usually the most expensive part of bacterial water quality monitoring in rural settings and resulted in a wide range of testing compliance (Figure 1-3, [10]). Combined, the challenges in field based testing and lab based testing place significant limitations on the ability to collect and disseminated water quality data.

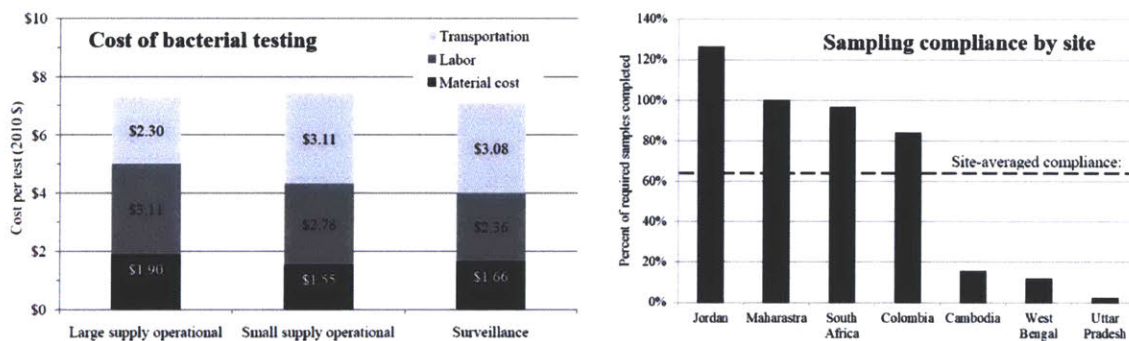


Figure 1-3: Cost of bacterial testing and sampling compliance by site. The transportation cost is the highest cost in two out of three monitoring schemes [10].

Similar challenges in sampling, preservation and accurate testing in clinical trials in rural and resource limited settings were alleviated with the introduction of dried blood spotting (DBS) technology. This technique involves the spotting of a low volume blood sample on a cellulose card and subsequent drying [11]. Bioanalytes can be recovered and quantified accurately from the dried blood spot after card storage at a wide variety of temperatures and over a period of years [12, 13]. Due to its low blood volume requirement and material cost, transportation and storage without special conditions and high analyte stability, usage of DBS has been associated with enhanced cooperation in clinical trials and reduced exposure to biohazards [14, 15]. DBS avoids issues with long distance shipping of blood and point-of-use diagnostics. The method is now used in testing for a wide range of biological molecules, including



blood sugar, pharmaceutical and illicit drugs, viral proteins and DNA [16, 17, 18].

Inspired by DBS technology, rural water quality monitoring could benefit from a similar dry preservation technology for water contaminants, circumventing issues in liquid preservation and transport. The goal of this thesis is to develop a low cost, compact dry preservation technology for heavy metal contaminants in water to facilitate their ambient temperature shipping, storage and testing at centralized government labs in order to improve the ability to monitor water quality. This includes device and usage protocol development for reproducible and accurate operation, as well as for easy integration in current governmental water quality monitoring schemes, specifically the system which is present in India. While the device will be developed in the context of India, a dry sampling device could also find use in other resource limited or rural settings around the globe.

The following sections outline common contaminants of water and current water quality monitoring schemes in India. It is necessary background for understanding the potential for dry preservation technology in drinking water quality monitoring.

## **1.2 Methods in water quality monitoring**

Determination of water quality involves the broad measurement of physical, chemical and biological parameters in water samples. To ensure accurate enumeration, general protocols exist for water sample collection, preservation and quantification by applicable methods. While the protocols for heavy metals are the most relevant for this thesis, a general overview of other parameters is presented for completeness.

### **1.2.1 Water quality parameters and guidelines**

Comprehensive water quality guidelines are published by the WHO and most countries follow these standards with slight modifications for local variation [1, 19].

All water contains some level of a naturally occurring dissolved species, which when present at or below the acceptable limit, do not affect human health detrimentally. These dissolved species include cations (calcium, magnesium, sodium and

potassium), halogen ions (fluoride, chloride and bromide), polyatomic anions (nitrate, phosphate, sulfate and carbonate) and dissolved oxygen. Two common measurements quantify the levels of these dissolved species are:

- **Total Hardness (TH)** is the total concentration of cations in water. As calcium and magnesium are usually present at levels much higher than other cations, hardness is most commonly a measure of calcium and magnesium only. Hardness is measured in parts per million (ppm, equivalent to milligrams per liter (mg/L)) of calcium carbonate. Water is categorized based on its hardness level into one of four categories: soft (less than 60ppm), hard (60-120ppm), moderately hard (120-180ppm) and very hard (greater than 180ppm).
- **Total Dissolved Solids (TDS)** is the total concentration of all dissolved inorganic salts in water

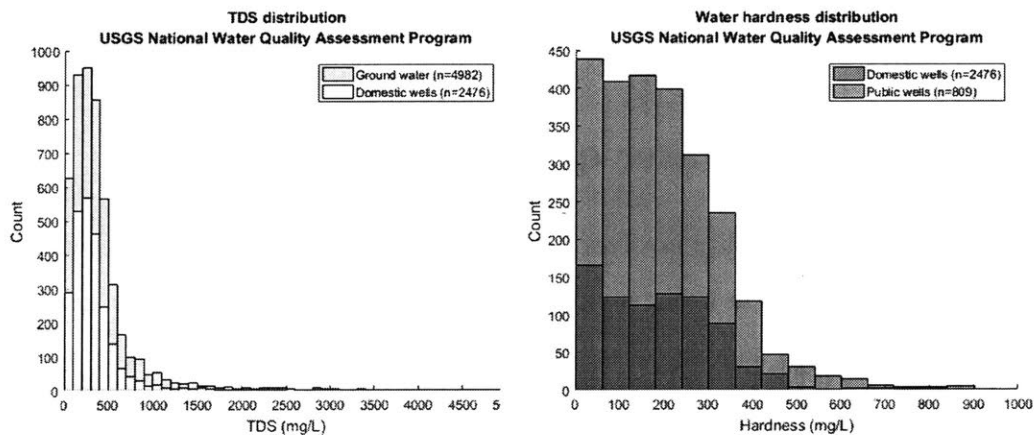


Figure 1-4: Water TDS and hardness in the United States measured by the United States Geological Survey [20, 21].

Figure 1-4 shows the distribution of hardness and TDS in several thousand sources in the United States, as measured by the United States Geological Survey [20, 21]. Hardness and TDS levels are generally affected by geological parameters, with higher hardness and TDS found in locations where there are large limestone deposits [22].

Many dissolved species are beneficial to human health. For example, dissolved fluoride in water helps to prevent cavities by promoting remineralization of teeth

after acid induced demineralization [23]; fluoride is added to water in some localities through fluoridation to reach the optimal 0.7ppm concentration for these health benefits [24].

Long term consumption of water containing higher than recommended levels of these naturally occurring ions can cause health problems. An example is dental and skeletal fluorosis caused by the long term intake of high levels of fluoride, which builds up in tooth and bone, causing bone hardness and joint calcification [25, 26]. Another example mainly affecting infants is methemoglobinemia caused by consumption of high levels of nitrate, which impairs oxygen transport due to the strong association between hemoglobin and nitrogen [27].

However, there are some ions and compounds that do not naturally occur in water and are harmful to human health even at extremely low levels. These 'micropollutants' or trace contaminants include heavy metals and organic molecules. These species are most commonly introduced into water systems through anthropogenic contamination as a result of human activities. Some heavy metals, including arsenic, can be geogenic contaminants, arising from erosion of rocks and sediments; this type of contamination is most commonly found in ground water. Prolonged exposure to these contaminants cause a variety of cancers, developmental disorders and enzymatic deficiencies [28]. A partial listing of heavy metal contaminants relevant to this work, their maximum acceptable limits as set by the Bureau of Indian Standards [29] and their health effects are shown in Table 1.1.

In addition to containing no heavy metals or organic pollutants, drinking water should be free of biological contaminants such as bacteria (such as *Escherichia coli*), viruses (such as Enteroviruses), protozoa (such as *Cryptosporidium*) and other parasites (such as *Schistosomiasis*). Human and animal fecal matter is the largest source of biological water contamination [30]. Consumption of these pathogens causes acute gastrointestinal illness. Despite improvements in biological water quality, diarrheal disease remains the second largest cause of childhood death worldwide [31].

Table 1.1: Heavy metal contaminants of water, their maximum acceptable limit set by the Bureau of Indian Standards and their associated health effects [1, 29]

| Element   | Maximum acceptable limit (ppm) | Health effects                         |
|-----------|--------------------------------|--|
| Arsenic   | 0.010                          | Kidney and liver cancer                |
| Cadmium   | 0.003                          | Kidney disease and cancer; acute edema |
| Chromium  | 0.050                          | Nasal and lung cancer                  |
| Copper    | 0.050                          | Liver damage; kidney disease           |
| Lead      | 0.010                          | Developmental abnormalities            |
| Manganese | 0.100                          | Nervous system disorders               |
| Mercury   | 0.001                          | Nervous system disorders               |
| Nickel    | 0.020                          | Cancers                                |
| Silver    | 0.100                          | Lung disorders; skin discoloration     |
| Zinc      | 5.000                          | Digestive disorders                    |

### 1.2.2 Sample collection and preservation for drinking water quality monitoring

Ensuring public health depends on a functioning water quality monitoring system able to accurately and reproducibly quantify trace and biological contaminants. Sample collection and preservation is the first step in testing for any of these parameters. Sample volumes, containers, preservation method and maximum holding time (MHT) for quantification vary by contaminant type (Table 1.2). In-depth ideal specifications for location of sample and method of collection are available for each source type of water [32]. For drinking water, the most complicated sampling method involves sampling ground water sources by using different pressure and displacement apparatuses. For drinking water from surface water and piped water supplies, the simpler "grab" sample is used, in which a clean sampling container is immersed in the water and allowed to fill. Essential to all sampling methods is the use of clean, sterilized containers to prevent outside contamination from affecting results [32, 33].

As shown in Table 1.2, all samples should ideally be chilled to 4°C immediately after collection to promote preservation of analytes. This is especially important for microbial samples, as elevated temperatures promote bacterial proliferation [1, 19, 34]. Addition of concentrated hydrochloric acid or nitric acid after sample collection is

Table 1.2: Sampling and preservation guidelines for common drinking water parameters [32]

| Contaminant class | Volume (L) | Container type   | Preservation                  | MHT       |
|-------------------|------------|------------------|-------------------------------|-----------|
| Physical          | 1.0        | Plastic or glass | None                          | 1 hour*   |
| Heavy metals      | 1.0        | Plastic          | Acidify to pH 2; chill to 4°C | 6 months  |
| Organics          | 1.0        | Glass            | Chill to 4°C                  | 7-14 days |
| Bacteria          | 0.250      | Glass            | Chill to 4°C                  | 30 hours  |

crucial for keeping metal ions in solution for analysis. Plastic bottles are used for heavy metal samples to facilitate their preservation, as metal ions can adsorb to the negatively charged surface of glass, thereby decreasing their concentration in the sample [35]. Samples should be transported to the laboratory and analyzed within the MHT to ensure quantification accuracy.

### 1.2.3 Laboratory test methods for water quality parameters

Common laboratory testing methods for chemical and physical water quality parameters include ion-selective electrode, titration, ultraviolet or visible spectroscopy, atomic absorption spectroscopy, inductively coupled plasma optical emission spectroscopy and inductively coupled plasma mass spectroscopy (Figure 1.3 [36, 37]). Microbial contamination is measured by the most probable number technique or the membrane filtration technique. Understanding quantification methods is crucial for determining the recovery protocol for dryly preserved contaminants, to make the recovered analyte compatible with the relevant quantification protocols and instrumentation.

Ion selective electrodes exist for a large variety of ionic species, but in water quality monitoring, they are most commonly used for pH and fluoride measurement. Measurement of the potential difference between a selectively permeable working electrode and a reference electrode allows quantification of a specific ion. This method is relatively rapid and inexpensive after upfront costs, but can suffer from interferences from other ions in solution, which can become a major source of error in high TDS

Table 1.3: Methods for commonly tested drinking water parameters.

| Parameter      | Test method   |
|----------------|---|
| pH             | Ions selective electrode<br>Colorimetric strips       |
| Turbidity      | Nephelometer<br>Turbidimeter                          |
| Organic carbon | UV/Vis spectroscopy                                   |
| TDS            | Conductivity meter<br>Gravimetric method              |
| Fluoride       | UV/Vis spectroscopy<br>Ion selective electrode        |
| Hardness       | Titration<br>Atomic spectroscopy<br>Mass spectroscopy |
| Metals         | Titration<br>Atomic spectroscopy<br>Mass spectroscopy |
| Organics       | Liquid or gas chromatography-<br>mass spectroscopy    |
| Bacteria       | Most probable number<br>Membrane filtration           |

samples [38].

Titration methods measure the concentration of a target ion in a solution of known volume by reaction with another solution of known concentration and volume. The degree of the reaction is often measured chromogenically and the concentration of the target ion is back calculated using the known stoichiometry of the reaction. Titrations exist for many different analytes and do not require special expertise to perform. They are, however, time-consuming and not high throughput, requiring many different reagents.

In ultraviolet or visible spectroscopy (UV/Vis spectroscopy), the unknown concentration of analyte in solution calculated using the Beer-Lambert law based on the amount of absorbance of specific known wavelength. Crucial to this method is a contaminant-specific reagent that produces a change in color or absorbance spectra. The technique requires a calibration curve, is not high throughput and suffers from limited accuracy, but it is not technically challenging.

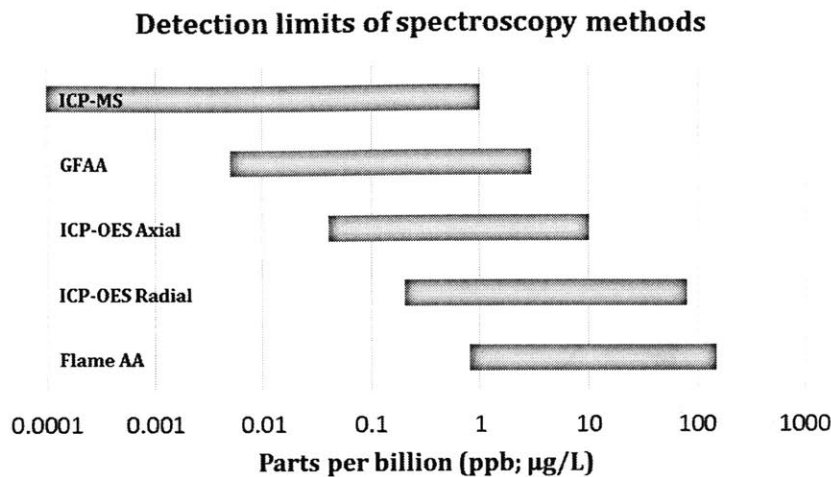


Figure 1-5: Detection limits of atomic spectroscopy methods [39].

Atomic absorption spectroscopy (AAS) and inductively coupled plasma optical emission spectroscopy (ICP-OES) measure concentrations based upon characteristic electronic transitions of a specific element. In both methods, a sample is vaporized, atomized and/or ionized using either a furnace (AAS) or a high temperature argon plasma (ICP-OES). AAS measures the absorbance of the atomized sample at a specific wavelength and the concentration of the element is calculated based upon the Beer-Lambert law. ICP-OES measures the light emitted at characteristic wavelengths by elements; the intensity of the light is linearly proportional to the concentration of the element in the sample. Both AAS and ICP-OES require expensive instrumentation and a technically trained operator, but both can measure multiple elements in one sample and there is usually minimal sample preparation required beyond acidification. ICP-OES achieves lower limits of detection, in parts per billion (ppb) to ppm range, than AAS due to the increased degree of atomization achieved by the higher temperature of the argon plasma [39].

Inductively coupled plasma mass spectroscopy (ICP-MS) uses the same argon plasma atomization as ICP-OES, but the ions in the sample are subsequently sorted by mass to charge ratio through the application of an electric field. ICP-MS is the most sensitive of the spectroscopy methods, with detection limits in the sub-ppb range

(Figure 1-5, [39]). Like AAS and ICP-OES, measurement using ICP-MS requires a trained technician and the instrumentation is very expensive. But its low limits of detection and high throughput capabilities make the method increasingly widely used for trace contaminant analysis.

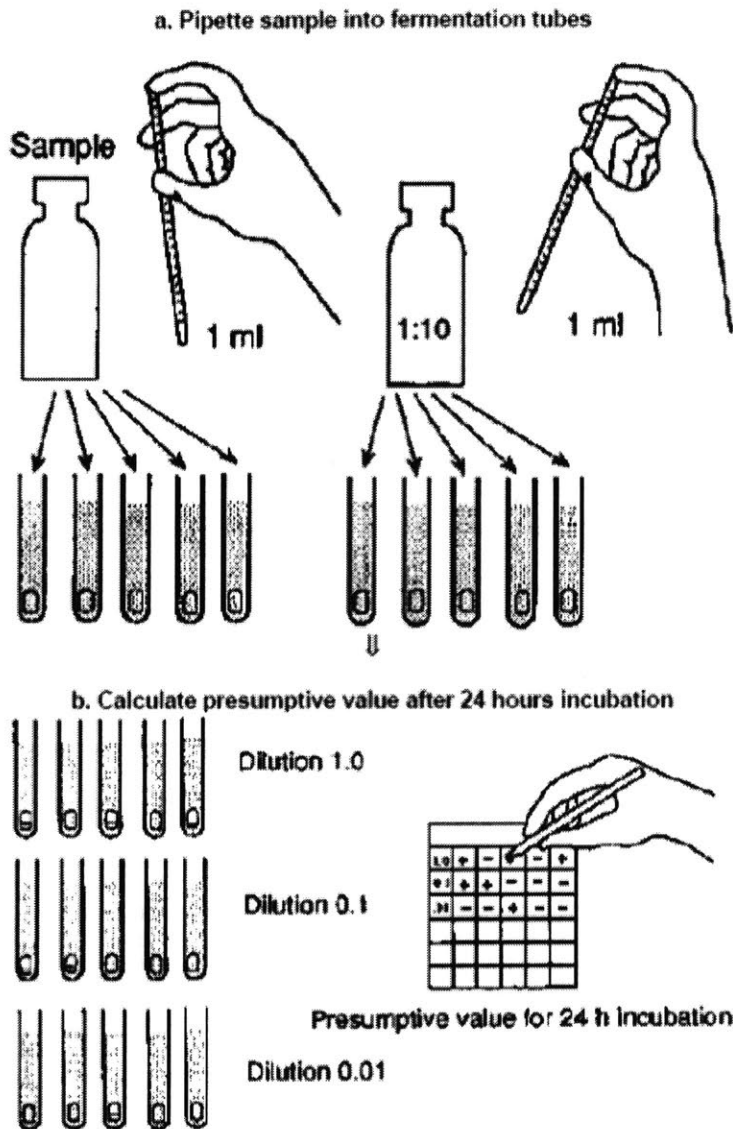


Figure 1-6: Schematic of most probable number technique showing dilution scheme [19].

For microbial contaminants, two culture based techniques are used. In the most probable number technique (MPN), selective culture medium is inoculated with serial



dilutions of the water sample (Figure 1-6). After 48 hours of incubation, culture tubes are examined for turbidity and/or gas production, which are signs of bacterial growth. The most probable number of bacteria present in the original undiluted sample is calculated using established statistical tables based upon the number of tubes at each dilution that show bacterial growth.

In the less quantitative membrane filtration technique (MF), bacteria are extracted from water samples on a nitrocellulose filter using vacuum filtration. The filters are deposited on to selective medium and incubated for 48 hours, after which the number of colonies grown on the medium are counted and recorded. Both MPN and MF suffer from limited accuracy and inadequate limits of detection.

### **1.3 Drinking water quality in India**

India is chosen as the initial context of application for the proposed dry sampling technology for a few reasons. Drinking water in India faces both problems of quality and quantity, with 30% of India's rural population receiving less than 40 liters per person per day, the required amount to maintain an acceptable level of individual health and sanitation [40]. Out of 11,274,819 documented sources, only 1,734,882 (15.38%) had water quality data available for the year 2013-2014, of which 8% percent were found to be contaminated [41].

The Government of India (GOI) recognizes water as a public good and access to safe water as a fundamental right. As such, it has implemented an elaborate regulatory scheme, described below, for monitoring water quality and providing safe water that employs government and community collaboration. However, even with the network of water quality laboratories mandated by the government, the National Rural Drinking Water Program (NRDWP) admits that is impossible to meet the overall prescribed water quality testing of twice a year for chemical and microbial contaminants, which amounts to a total of 0.5 million water samples every year [40].

Dry sampling technology could complement India's water quality monitoring system by improving the reach and ease of testing rural sources. Additionally, dry

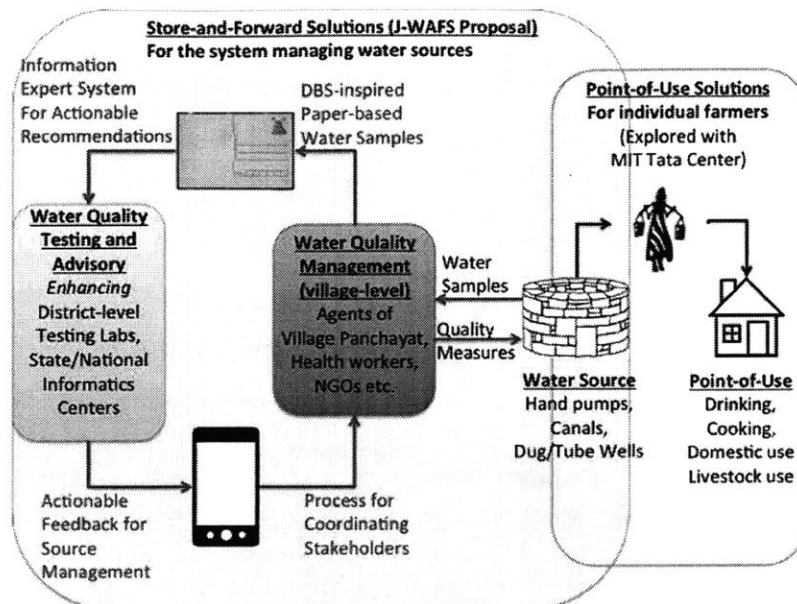


Figure 1-7: Portfolio of complementary water quality and soil solutions currently in development in Karnik, Hart and Vaishav labs, supported by the Water and Food Security Lab (J-WAFS) and the MIT Tata Center

sampling technology is part of a larger portfolio of water and soil quality solutions for India currently being developed in conjunction with the MIT Tata Center for Technology and Design and the Jamal Abdul Latif Jameel Water and Food Security Lab (Figure 1-7). Developing dry sampling technology for use in India allows for easy integration of the technology both into the governmental scheme and with these other technological solutions.

### 1.3.1 Government water quality monitoring scheme in India

In India, drinking water quality monitoring is overseen by the government, which mandates water quality standards, protocols and testing frequency. The Ministry of Drinking Water and Sanitation (MDWS) is the governmental entity that specifies these regulations for all types of water quality monitoring in coordination with state governments.

In 2005, the GOI published a Uniform Water Quality Management Protocol as a guideline for general water quality monitoring, irrespective of intended use. In re-

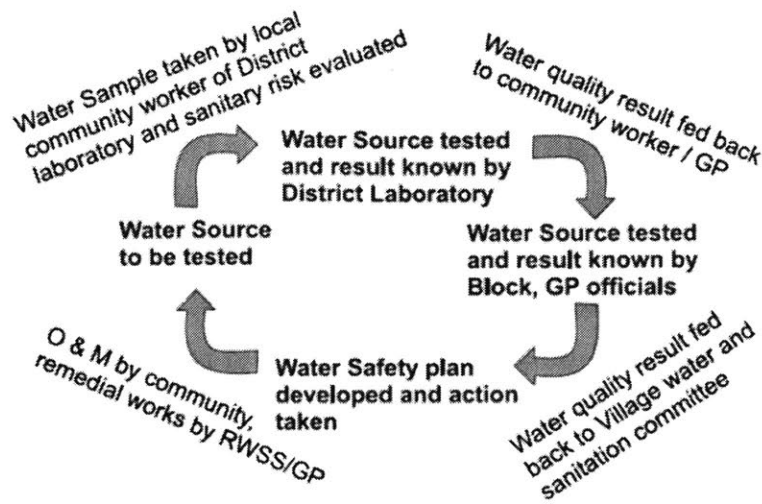


Figure 1-8: Schematic of testing and feedback structure suggested by the UDWQMP [42]

response to the increased pollution found in drinking water, the GOI implemented a separate Uniform Drinking Water Quality Monitoring Protocol (UDWQMP), outlining procedures specific to drinking water [42]. Guidelines for rural drinking water management are further specified in the National Rural Drinking Water Program (NRDWP) [40].

The UDWQMP mandates a hierarchical structure of government run water quality monitoring laboratories at two levels: block/sub-district and district, and state (Figure 1-8). It is a community centric protocol, relying upon the participation of villages, and in particular a village water and sanitation committee (VWSC), as the first monitoring entity in the chain. Additionally, the UDWQMP outlines the role of other departments in the water quality monitoring process, including the Public Health Engineering Department in the remediation of contaminated sources and the maintenance of piped water systems, and Accredited Social Healthcare Advocates (ASHA) workers in the public education of the risks of drinking contaminated water.

The water quality monitoring protocol detailed in the UDWQMP consists of the following hierarchy of water quality testing:

- At the village level, the VWSC should use distributed field testing kits to test quality of the drinking water sources within their jurisdiction. This testing

should be performed at least twice every year, once in the months before the monsoon and one in the months after the monsoon. The VWSC is required to notify the appropriate district or sub-district lab for confirmation testing if a field test returns an out of range result.

- District and sub-district labs provide support to the VWSCs. Twice a year, these labs are required to carry out their own testing of all water sources in their jurisdiction for 13 recommended parameters using basic chemistry and microbiological techniques.
- State level labs possess the advanced instrumentation needed for monitoring of micropollutants including heavy metals, pesticides and viruses. The state level lab should itself collect and test samples from every source once a year. Beyond this, it serves as the "referral institute for new/emerging contamination issues". Additionally, the state lab monitors the operations of the district and sub-district labs and administers parts of the NRDWP.

All labs are required to periodically upload test results to the MDWS Integrated Management Information System (IMIS), which is publicly accessible, thereby making water quality data transparent to the public.

## 1.4 Objectives and outline of thesis

The main objectives of this thesis, as outlined by chapter, are as follow:

- **Identification of project scope through interviews with stakeholders in India:** In order to choose the contaminants to focus on for this initial demonstration of dry preservation, an understanding of the current water quality monitoring scheme and challenges is necessary. **Chapter 2** details the data gathering during and conclusions drawn from visiting with government laboratories in India that led to the selection of heavy metals as the focus contaminant.

- **Materials selection and capacity for dry preservation of heavy metal cations:** After reviewing literature of absorptive technology for heavy metal removal, cellulose and ion exchange resins were tested for their dry preservation potential. **Chapter 3** includes all relevant experimental details and results that led to ion exchange resins being selected as the material for dry preservation.
- **Characterization of kinetics of heavy metal uptake on ion exchange resins:** The dry-preservation device should collect heavy metals in a short time scale in order to make a device that is easily and rapidly operable. Therefore, an investigation of the kinetics of this uptake process was carried out using different water matrices and correlated to different theoretical models. **Chapter 4** presents this testing in depth.
- **Recovery and quantification of heavy metals after long periods of dry storage:** The device should be able to reliably preserve and release heavy metal cations so that they are quantifiable after dry preservation over long periods of time. In **Chapter 5**, recovery experiments from up to 4 months of dry preservation are described.
- **Selection of device geometry and operation protocol:** Potential for a shippable dry preservation system, as well as aspects of the operational protocol, means that the device must be made of certain materials and in certain geometry. **Chapter 6** discusses the selection and testing of geometries with comparison to free bead resin performance.



## Chapter 2

# Identification of project scope through fieldwork in India

### 2.1 Introduction

The scope of drinking water quality monitoring encompasses all physical, chemical and biological parameters, some of which may be more amenable to dry sampling technology than others. Due to the novelty of the proposed dry sampling technology, it is crucial to examine the existing systems, protocols and regulations for water quality monitoring in order to determine the correct and most impactful implementation of the technology. Not only does such an investigation lead to greater understanding about drinking water management in general, but it also guides laboratory experiments and decides device design parameters.

Therefore, to define the initial scope of this project, visits to various water quality stakeholders in India and interviews with personnel were carried out in January 2016. With a focus on rural drinking water monitoring, the goal was to better understand the hierarchical system of government water quality monitoring labs as set forth in the UDWMQP and NRDWP, detailed in Chapter 1.3.1. This included a survey of:

1. Contaminants tested for at each lab level
2. Protocols for sampling and testing each contaminant

3. Laboratory personnel capacity
4. Water quality data management and information flow
5. Relationships among villages and local labs, and between hierarchical lab levels

## 2.2 Methods

In January 2016, in conjunction with other water quality researchers from the MIT Tata Center, project staff traveled to three states in India: Maharashtra, Karnataka and Gujarat. Stakeholders were identified through contacts at the MIT Tata Center and were contacted before international travel to arrange meetings.

In meetings with each stakeholder, a variety of personnel were interviewed and their responses were summarized and hand recorded by project staff. Pertinent questions for each stakeholder or category of personnel were collected in advance. In the discussion that follows, stakeholders and government labs are anonymized to protect identities.

## 2.3 Results

In total, nine water quality labs were visited over the course of the trip. Not all of these labs were drinking water quality labs; India has an additional network of 2500 monitoring stations for ground water and surface water that is not intended as a drinking water source. This network is over seen by the Central Pollution Control Board (CPCB), a division of the Ministry of Environment, Forest and Climate Change. An overview of the labs visited is presented in Table 2.1.



Table 2.1: Water quality monitoring labs visited in India, January 2016. Table lists the parameters for which each lab tests and the method that is used.

| State                          | Maharashtra                   |                                | Karnataka     |                                | Gujarat       |                                |
|--------------------------------|-------------------------------|--------------------------------|---------------|--------------------------------|---------------|--------------------------------|
|                                | District                      | Sub-district                   | District      | Sub-district                   | District      | District                       |
| <b>Volumes collected</b>       | 1L (plastic)<br>300mL (glass) | 1L (plastic)<br>300mL (glass)  | 2L (plastic)  | 1L (plastic)<br>250mL (glass)  | 1L (plastic)  | 1L (plastic)<br>300mL (glass)  |
| <b>Physical parameters</b>     |                               |                                |               |                                |               |                                |
| pH                             | Electrode                     | Electrode                      | Electrode     | Electrode                      | Electrode     | Electrode                      |
| Conductivity                   | Electrode                     |                                | Electrode     | Electrode                      | Electrode     | Electrode                      |
| Hardness                       | Titration                     | Titration                      | Titration     | Titration                      | Titration     | Titration                      |
| Alkalinity                     | Titration                     | Titration                      | Titration     | Titration                      | Titration     | Titration                      |
| Turbidity                      |                               | Nephelometer                   | Nephelometer  | Nephelometer                   | Nephelometer  | Nephelometer                   |
| TDS                            |                               | Electrode                      | Electrode     | Electrode                      | Electrode     | Electrode                      |
| <b>Cations</b>                 |                               |                                |               |                                |               |                                |
| Calcium                        | Titration                     |                                | Titration     |                                | Titration     | Titration                      |
| Magnesium                      |                               |                                | Titration     |                                |               | Titration                      |
| Sodium                         | Flame photometry              |                                |               |                                |               |                                |
| Potassium                      | Flame photometry              |                                |               |                                |               |                                |
| Iron                           | UV/Vis spec                   | UV/Vis spec                    | UV/Vis spec   | UV/Vis spec                    | UV/Vis spec   | UV/Vis spec                    |
| Manganese                      |                               |                                |               | UV/Vis spec                    |               |                                |
| <b>Anion</b>                   |                               |                                |               |                                |               |                                |
| Carbonate                      | Titration                     |                                |               |                                |               |                                |
| Chloride                       | Titration                     | Titration                      | Titration     | Titration                      | Titration     | Titration                      |
| Fluoride                       | UV/Vis spec                   | UV/Vis spec                    | UV/Vis spec   | Electrode                      | UV/Vis spec   | UV/Vis spec                    |
| Nitrate                        | UV/Vis spec                   | UV/Vis spec                    | UV/Vis spec   | UV/Vis spec                    | UV/Vis spec   | UV/Vis spec                    |
| Sulfate                        | UV/Vis spec                   |                                | UV/Vis spec   | UV/Vis spec                    | UV/Vis spec   | UV/Vis spec                    |
| Residual chlorine              |                               | Orthotolidine test             |               | Orthotolidine test             |               | Orthotolidine test             |
| Arsenic                        |                               |                                |               | Test kit                       |               |                                |
| Cyanide                        |                               |                                |               |                                |               | Titration                      |
| <b>Microbial</b>               |                               |                                |               |                                |               |                                |
| Total coliform                 |                               | MPN                            | ?             | MPN                            |               | MPN                            |
| <i>E. coli</i>                 |                               | MPN                            | ?             | MPN                            |               | MPN                            |
| <b>TOTAL PARAMETERS TESTED</b> | 13 (chemical)                 | 10 (chemical)<br>2 (microbial) | 13 (chemical) | 14 (chemical)<br>2 (microbial) | 12 (chemical) | 15 (chemical)<br>2 (microbial) |

### 2.3.1 Sub-district laboratories

According to the UDWQMP, sub-district labs should carry out testing of all sources for chemical and bacteriological contamination twice a year (pre- and post-monsoon), as well as address and respond to issues that arise during village scale testing using field testing kits.

In general, it was found that the communication between the villages and the sub-district labs was quite good. Most villages usually had one "water protector", or *jalsurakshak* in Marathi, the local language of Maharashtra. This individual is responsible for testing of sources using field testing kits, the distribution of bleaching powder for disinfection of water sources, and collection and transport of bi-yearly samples for testing at sub-district labs (Figure 2-1). Both sub-district labs and the villagers reported adequate compliance with water quality monitoring as laid out by the UDWQMP. The most common complaint heard regarding sample collection and testing was that samples sometime arrived to the lab in unacceptable condition, either due to the sampling container or the volume of sample collected.



Figure 2-1: Sampling from open well source in Maharashtra.

Although the UDWQMP mandates a common set of 13 parameters that should be tested for at sub-district laboratories, it was found that the actual parameters tested at sub-district level varied. This discrepancy seemed to be due to state level policies that mandate testing for parameters of local concern over some of the parameters



Figure 2-2: Physical and chemical parameter testing equipment at sub-district water quality monitoring labs in India. Sub-district labs are equipped with basic chemistry equipment including pH electrodes, turbimeters, UV/Vis spectrophotometers (left) and hardness titrations (right).

outlined in the UDWQMP. For example, the sub-district lab in Maharashtra, tested for iron in all samples received, but did not test for conductivity. This contrasts with the sub-district lab in Karnataka, where all 13 UDWQMP parameters are tested plus manganese, sulfate and arsenic (Table 2.1). Additionally, the Maharashtra sub-district lab employed both a chemist and a microbiologist (although the microbiologist position was unfilled during the visit), while one chemist worked at the Karnataka sub-district lab and performed all chemical and biological assays, as well as data entry. Laboratory staff at both labs confirmed that their jobs were demanding due to the number of samples required to be tested daily. For example, at the sub-district lab in Karnataka, the chemist provided records that showed 666 samples tested for all 16 parameters in 2 months.

The testing methods for parameters at the sub-district labs are similar. Labs used electrodes or titration methods for most chemical contaminants (Figure 2-2), as well as the most probable number technique for bacterial testing (Figure 2-3). Surprisingly, both sub-district labs visited were equipped with an ultraviolet/visible spectroscopy instrument and used it for some chemical analyses. Additionally, at the Karnataka sub-district lab, the reported method used for arsenic testing was a field test kit. Although no field test kit was seen, this seems plausible, as earlier in the

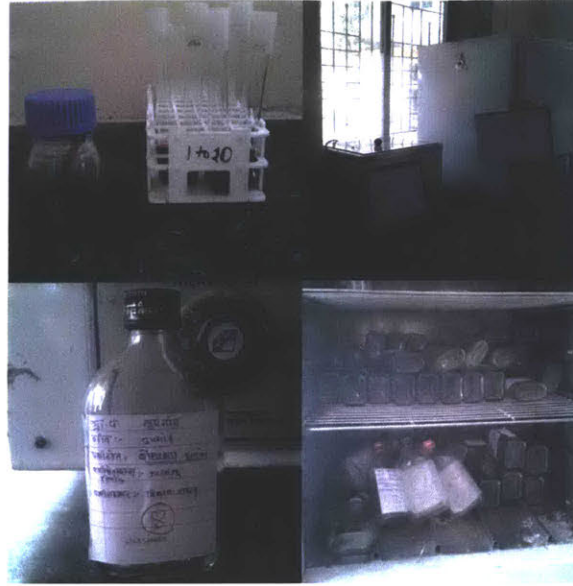


Figure 2-3: Bacterial testing equipment at a sub-district water quality testing laboratory in Maharashtra, India. The lab uses the most probable number technique to test water samples for bacteria (top left) and has a designated bacterial testing room with an incubator and water bath (top right). Additionally, the lab provides all bacterial sample collection bottles to the communities (bottom left) and sterilizes them in an oven (bottom right).

trip, the chemist and manufacturer of all the field test kits in Karnataka was visited in Huballi. This company also makes an arsenic field testing kit, which is in use in some locals across the state.

### 2.3.2 District level labs

The UDWQMP mandates that district labs test all sources in their jurisdiction twice a year, perform verification testing of water from sources that return unacceptable results from field testing kits or laboratory tests at sub-district labs and oversee administration of sub-district labs.

Greater variation was found between district labs than sub-district labs. The exact role of the district lab was unclear; in some cases, the district lab seemed to function as another sub-district lab, monitoring only of a subset of drinking water sources, whereas other labs tested all sources in their district. At the district lab in Maharashtra, this was compounded by the fact that the government organization





Figure 2-4: Water quality sampling and testing equipment at a district lab in Maharashtra. The lab provides plastic bottles for water samples to be collected for chemical testing (left) and the lab contains basic chemical testing equipment (right) but does not test for bacteria.

running the lab had just taken over responsibility for drinking water quality monitoring in Maharashtra, where it had previously only monitored ground water. One district lab in Karnataka was found to be under repair and in transition and was not currently collecting or testing samples.

While all district labs measured the majority of the UDWQMP chemical parameters, not all district labs performed bacterial testing and no bacterial testing equipment was present at the lab in Maharashtra (Figure 2-4). When questioned about this discrepancy between what the UDWQMP prescribes and what the district lab performs, the general response was the bacterial testing was performed at sub-district labs. At the district lab in Karnataka, it was reported that sources that were found to contain bacteria by testing at the sub-district lab were immediately resampled and sent on ice to the state lab in Bangalore. Chemical testing methods were similar across labs, with ion selective electrode, titration and UV/Vis spectroscopy being the most commonly employed methods.

### 2.3.3 State level labs

No state level drinking water quality labs were visited in this trip. In some cases, state level labs were reported to be under construction and not yet testing samples.

Communication between the sub-district/district labs and the state lab seemed to be lacking. Aside from the mention of state laboratory confirmatory bacterial testing in Karnataka, there was no mention of contact with the state level laboratories during the rest of the trip.

The opportunity did arise to visit a pollution control board lab in Maharashtra. The mandate of this lab is to test the state's fresh water resources, including industrial effluents. About 250 sources are sampled monthly and tested for contaminants for which the source is most likely to contain, based upon its location, proximity to industry and geology. The lab has the capacity to test for 9 physical parameters, 44 chemical parameters (including heavy metals and organic compounds), 2 bacteriological parameters and 1 toxological parameter. As such, it was the only lab visited during the trip that had AAS, ICP-OES and MS.

## 2.4 Conclusion

Visiting with potential stakeholders in India led to the following conclusions about drinking water quality testing in India:

- Basic drinking water quality monitoring for physical and chemical parameters, as prescribed by the UDWQMP, is adequately functioning. Introduction of a dry sampling technology to this subset of drinking water quality monitoring would likely negatively impact the system and so should not be the focus of technology development.
- Bacteriological testing is performed as prescribed in most areas visited. There is no advanced molecular biological testing via polymerase chain reaction present, at least at the district and sub-district level. Although technicians generally were interested in a dry sampling device for bacteria, the applicability to the water quality monitoring system was not clear from this trip. Additionally, preserving whole live bacteria in order to test sources for bacteria using the current culture based methods is a technical challenge in itself.

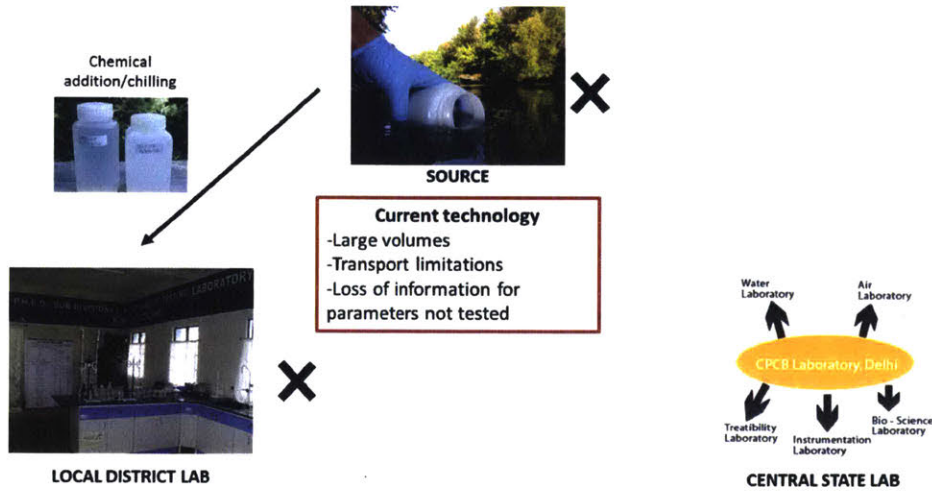
- The lack of connection and communication between the state level laboratories and the lower level laboratories is very apparent. In some cases, this is due to the lack of a state level lab and in others, it is not clear. However, in either case, the contaminants mandated for state level lab drinking water testing — namely heavy metals, pesticides and pathogens other than bacteria — are not being tested. This was anecdotally demonstrated by a public health engineer at the sub-district lab in Maharashtra, who had been notified of possible industrial mercury contamination of a drinking water source that supplies multiple villages. He was uncertain of how or where should send a sample to be tested for this contamination.

Based on these conclusions, the initial scope of the project was refined to the dry preservation of heavy metal contaminants. Because of the lack of current monitoring for heavy metal contaminants, as well as the dearth of communication between lower level labs and state labs, a device that dryly preserves heavy metal contaminants is the most impactful in the current water quality monitoring scheme in India. Such a device would allow increased monitoring of rural sources for heavy metals, which are emerging contaminant threats in many areas, by bridging the gap between local lab sampling and state lab testing capability, without negatively impacting the current basic parameter testing (Figure 2-5). Additionally, dry sampling for heavy metal pollutants could find usage in water quality monitoring of surface and ground waters not necessarily used as drinking water source and especially in the monitoring of industrial effluents.

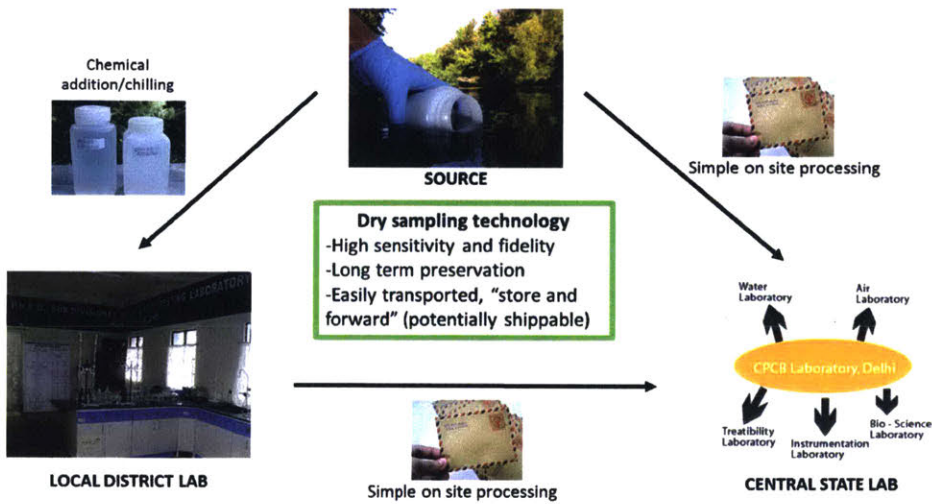
Dry preservation technology could, in the future, be expanded to encompass organic and biological contaminants. Indeed, as was seen from the visit, these are also two classes of contaminants that are not routinely tested (besides *E.coli*) and they are emerging contamination concerns worldwide. However, characteristics of organic and biological pollutants make them harder to dryly preserve. Some organic molecules decay much more quickly than heavy metals, which would need to be taken into account for a dry preservation device. Given the current lack of molecular testing methods, biological contaminants would need to be preserved in live form to be compatible

with culture based testing. If molecular testing was standard, it would be easier to dryly preserve DNA or proteins for biological analysis, as is done with dried blood spotting. These challenges were also taken into account during the initial focusing of the project and heavy metals were partially selected due to their not possessing these characteristics. It is envisioned that, if heavy metal dry sampling finds good use in water quality monitoring, dry preservation devices for organics and biologics will also be explored.





(a) Current monitoring framework



(b) Dry sampling monitoring framework

Figure 2-5: Visual schematic of current monitoring framework and proposed monitoring framework enabled by dry sampling technology.



## Chapter 3

# Identification of sorbent materials for dry sampling of heavy metals

### 3.1 Introduction

In order to preserve heavy metals in a dry form, a suitable sorbent material needs to be identified which can bind large amounts of heavy metal cations, preserve the bound cations reliably in a dry form over a long period of time and, most crucially, release the heavy metals after treatment at a lab. Additional ideal attributes, including low cost and wide availability, are listed in Table 3.1. Therefore, after extensive literature review, cellulose and commercially available ion exchange resins were selected and tested in their ability to selectively take up copper, nickel and lead from waters of different matrices. This chapter presents both the background information obtained from literature review as well as the experiments that led to the selection of a commercially available cation exchange resin, DOWEX G-26 from Dow Chemical Company, as the material for further investigation of heavy metal cation dry preservation.

Table 3.1: Ideal characteristics for dry preservation device.

| Characteristic       | Ideal  |
|----------------------|--|
| Contaminant capacity | Adsorb 1-10mg of contaminant per gram of material<br>High fidelity/specificity for heavy metals over other ions<br>Consistent over relevant pH range (6.5-8) |
| Preservation process | Minimal addition of other reagents<br>Fast adsorption kinetics (<30min)  |
| Geometry             | Compact; flat if possible<br>Total weight less than 10 grams   |
| Availability         | Commercially available components or simple synthesis protocol<br>Low cost   |

### 3.2 Literature review: The potential for adsorptive water purification technologies as dry preservation materials

In the water purification literature, adsorptive technologies are widely seen as the most promising purification materials. This is due to their low cost, fast operation time, limited production of harmful byproducts and the wide range of materials that can serve as adsorbents [43]. Further, adsorptive technologies are often also able to be regenerated to their original form through treatment with acidic or basic reagents, making them reusable and sustainable alternative to other purification technologies [43]. Naturally occurring polymers, such as cellulose, lignin, chitin and polyamino acids, as well as synthetic materials, have adsorptive properties. Adsorptive materials have been widely used for heavy metal and organic pollutant removal from drinking water; some of the most common sorbents include silica and activated carbon or charcoal [44]. For these reasons, adsorptive materials are also promising as dry preservation materials.

Adsorption is a surface phenomenon. Adsorptive materials work through physical or chemical associations between adsorbent surfaces and species in solutions targeted for removal. Atoms or molecules at the surface of a material differ from the bulk of the material by their surroundings; unlike the bulk of the material, these particles are not

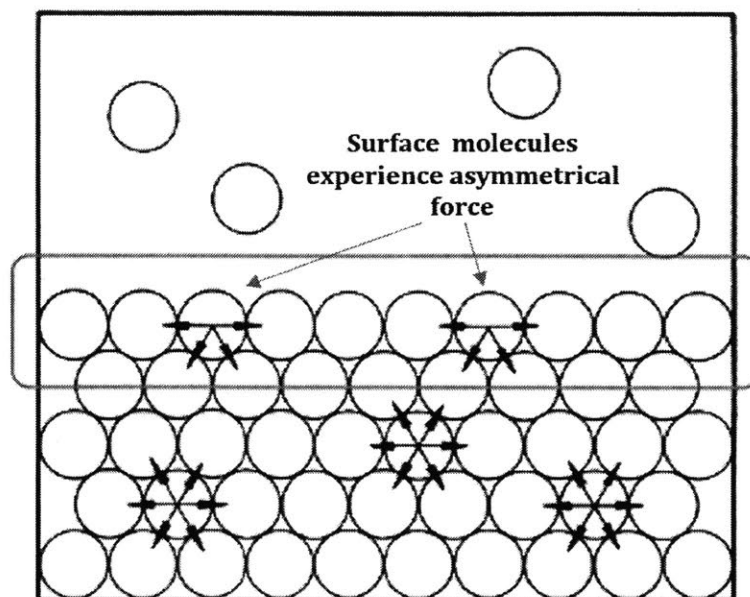


Figure 3-1: Adsorption phenomena are caused by asymmetrical surface forces. Surface molecules attempt to reduce the surface energy through associations with other atoms or molecules.

completely surrounded by other atoms, resulting in asymmetrical forces experienced by the surface molecules (Figure 3-1, [45]). This results in surface free energy, which the surface molecules attempt to lower through interactions with other atoms or molecules.

Physisorption, also known as Van der Waals adsorption, occurs when the interaction between surface and adsorbate is purely due to weak long range energetic reactions, such as Van der Waals forces or hydrogen bonding. Physisorption is characterized as being readily reversible, usually non-specific and having adsorption enthalpies in the range of 5-50 kilojoules/mole [45].

On the other hand, chemisorption is characterized by stronger interactions (heat of adsorption in the range of 40-800 kilojoules/mole) involving chemical bonding, which can be irreversible. However, the difference between physisorption and chemisorption is not usually clear and many adsorptive processes exhibit elements of both types of sorption mechanisms [45].

Because adsorption is a surface phenomenon, effective adsorbents typically have

large surface areas often on the order of 200 square meters per gram or more [45]. This means that adsorbents are often in powdered or granular form and can have an extensive interconnected pore structure. Pores are classified according to their size, with macroporous adsorbents containing pores larger than 50 nanometers (nm) in diameter, mesoporous adsorbents having pores 2 to 50nm in diameter and microporous sorbent having pores smaller than 2nm in diameter [45].

From an extensive literature review of adsorbent materials, cellulose and ion exchange resins were selected to test as dry preservation sorbents. As discussed in depth below, raw materials for cellulosic adsorbents are cheap and widely available. Preserving contaminants on a card or paper strip is appealing for this application. Numerous types of ion exchange resins exist and they are cheap when bought in bulk. Other common adsorbents, namely activated carbon and silica, were not explored due to their relatively high cost. Additionally, activated carbon is known to require a high energy input for regeneration, which is not desirable for dry preservation devices to be operated in laboratories with minimal instrumentation.

### **3.2.1 Adsorption isotherms and equilibrium**

The most important characteristic of adsorbents is their capacity to adsorb different species from solution. Knowledge of the adsorbent capacity aids in selecting effective adsorbents for a particular application as well as estimating the amount of adsorbent needed to achieve removal of the desired contaminant. Capacity is defined as the maximum amount of contaminant that can be adsorbed by the material, commonly expressed in milligrams or moles of contaminant per gram of material (mg/g or mole/g).

To determine the capacity that an adsorbent has for a particular compound or species, equilibrium adsorption experiments are performed in which the adsorbent contacts contaminated solutions for a period of time long enough to achieve equilibrium. Two versions of this experiment exist. In one version, the mass of the adsorbent is varied, while the starting concentration contaminant in solution is kept constant. Alternatively, the mass of the adsorbent can be kept constant while varying

the concentration of the contaminant in solution.

Initial and equilibrium contaminant concentration in solution is measured by an appropriate technique and an adsorption isotherm is constructed from the experimental results. Adsorption isotherms plot the equilibrium capacity ( $q_e$ , in mg/g) versus the equilibrium concentration of contaminant in solution. In a version of these experiments where a certain amount of sorbent is added to a volume  $V$  [L] of solution containing contaminant at initial concentration  $C_i$  [ppm or mg/L], the equilibrium capacity is given by:

$$q_e = \frac{(C_i - C_e)V}{m} \quad (3.1)$$

where  $C_e$  is the equilibrium concentration of contaminant in the solution [mg/L] and  $m$  is the mass of adsorbent [g]. By fitting isotherm models to the experimental data, the system behavior can be predicted and applied to the desired application. Many isotherms models exist to describe adsorption phenomena; two of the most common are outlined here.

Derived first in 1916 to describe gas adsorption on solid surfaces, the Langmuir isotherm is also widely applicable to fluid-solid systems. The isotherm takes the following form:

$$q_e = \frac{Q_{max}K_L C_e}{1 + K_L C_e} \quad (3.2)$$

where  $Q_{max}$  is the maximum predicted adsorption capacity and  $K_L$  is the Langmuir constant. This model of adsorption assumes that adsorption takes place in a monolayer, there are a fixed number of homogenous adsorption sites, and all adsorption occurs through the same mechanism. Also, the Langmuir model assumes that the enthalpy of adsorption is independent of the amount of adsorbate adsorbed.

The Langmuir constant,  $K_L$ , is a equilibrium constant for the adsorption, reflecting the favorability of the adsorption interaction over the desorption reaction; the larger the Langmuir constant, the more favorable the adsorption. Additionally, the Langmuir isotherm predicts the maximum amount of contaminant that can be taken

up as  $Q_{max}$ , a useful parameter in quickly evaluating an adsorbent's relevance to a particular application [45, 46].

The Freundlich adsorption isotherm is a purely empirical power law model, derived also to express the variation in amount of gas adsorbed on a solid surface due to gas pressure. It also can be applied to liquid-solid systems. More accurate at low pressures or concentrations, it takes the following form:

$$q_e = K_F C_e^{\frac{1}{n}} \quad (3.3)$$

where  $K_F$  is the Freundlich constant and  $n$  is the index of adsorption intensity, usually less than one. A higher  $K_F$  and  $\frac{1}{n}$  value signify favorable and strong adsorption. The Freundlich model makes no assumptions as to the nature or distribution of adsorption sites [45, 46].

Once the isotherm has been determined, the amount of adsorbent necessary to decrease the contaminant concentration to a particular equilibrium concentration can be determined by a mass balance, resulting in the following equation for mass of adsorbent needed (assuming no adsorbate is initially bound to the adsorbent):

$$m = \frac{V(C_i - C_f)}{q_e} \quad (3.4)$$

where  $V$  is the volume of the solution to be treated,  $C_i$  is the initial concentration of the contaminant in solution,  $C_f$  is the desired final concentration in the solution and  $q_e$  is the equilibrium capacity of the adsorbent at the desired  $C_f$ .

Adsorption isotherms are only applicable to the experimental conditions tested because adsorptive processes are highly affected by temperature and pH. Because adsorption is an exothermic interaction, lowering temperatures tends to increase adsorption. pH affects the surface charge density of the adsorbent, as hydrogen ions are susceptible to the same attractive forces as other cations in solution. At low pH, adsorption of a specific cationic species can decrease. Therefore, it is important to experimentally determine isotherms at conditions that as closely match application operation conditions as possible to make accurate predictions.



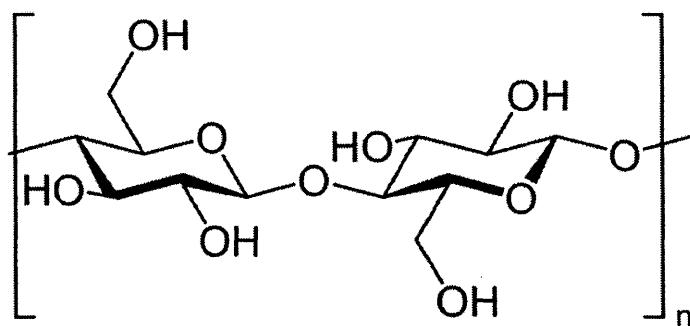


Figure 3-2: Molecular structure of cellulose. Cellulose is a polymer of beta glucose. Lone electron pairs and reactive hydroxyl groups make cellulose a reactive polymer and give it its adsorption capacity [43].

### 3.2.2 Cellulosic adsorbents for heavy metal removal

Cellulose is the most abundant natural polymer on earth, composed of beta glucose monomers linked together by 1-4 glycosidic linkages (Figure 3-2, [43]). Hydroxyl groups and lone electron pairs on oxygens involved in monomer linkage as well located in the ring structure give cellulose a high chemical reactivity and are the main participants in the adsorption of cationic species on cellulose [43].

Various forms of pure cellulose have been investigated for their adsorption of heavy metals from drinking water and industrial waste effluents. These include cellulose nanocrystals, nanowhiskers and beads [44]. Additionally, due to the abundance of cellulose in natural materials, many sources of cellulose have been applied for heavy metal adsorption including sawdust of various trees, corn cob waste, sugarcane bagasse and cotton [47]. Many of these materials are waste from other industrial processes, which increases the appeal of using cellulosic sorbents as a sustainable adsorbent. Also, many of these materials are made up of cellulose as well as other polysaccharides containing different additional active sites for adsorption [43].

While pure cellulose intrinsically can adsorb heavy metals, much of the research in cellulose adsorbents has focused on increasing adsorption capacity through chemical modifications of cellulose in order to increase adsorbent efficiency. For example, activation of poplar sawdust by sulfuric acid treatment increased the material's copper adsorption capacity from 5.4mg/g of untreated sawdust to 13.5mg/g of activated

sawdust [48].

Modifications of cellulose are possible due to the reactivity of the hydroxyl groups in the glucose monomer ring. Cellulose modifications are generally classified into two kinds of functionalization. The first involves the direct chemical modification of the highly reactive hydroxyl groups. In hydroxyl groups, the highly electronegative oxygen pulls electrons away from both carbon and hydrogen, resulting in polarized covalent bonds and electrophilic hydrogens susceptible to electrophilic addition reactions [43]. Due to this electrophilic activity, hydroxyl groups are readily converted into carboxylic acids, esters and acyl chlorides, all functional groups with higher electron density and negative charge (Figure 3-3, [43]). These reactions can be very simple, such as the heating of cellulose in the presence of concentrated citric acid to promote esterification which creates a sorbent capable of adsorbing 20 to 30 milligrams of copper or lead per gram of material [49, 50].

The other class of modification is grafting of functional groups onto the cellulose backbone through covalent bonds. These reactions are often more involved and use more dangerous chemicals, but yield adsorbents with similar capacities for heavy metals as direct chemical modification methods. Grafting is achieved using various initiators that introduce reactive radicals into the cellulose backbone, which further react with compounds in the reaction mixture to result in modified cellulose. Typical initiators used include ultraviolet radiation and chemical initiators, such as ceric ammonium hydrate and various persulfates [43].

Cost and effectiveness of the sorbents strongly depends upon the chemicals needed to induce the modification and reliability of modification chemistry. However, many modified cellulose sorbents are able to be regenerated using acidic or basic treatment. As such, cellulosic sorbents are cheaper than activated carbon or charcoal, which has a high raw material cost and requires high energy inputs for both creation and regeneration [44].

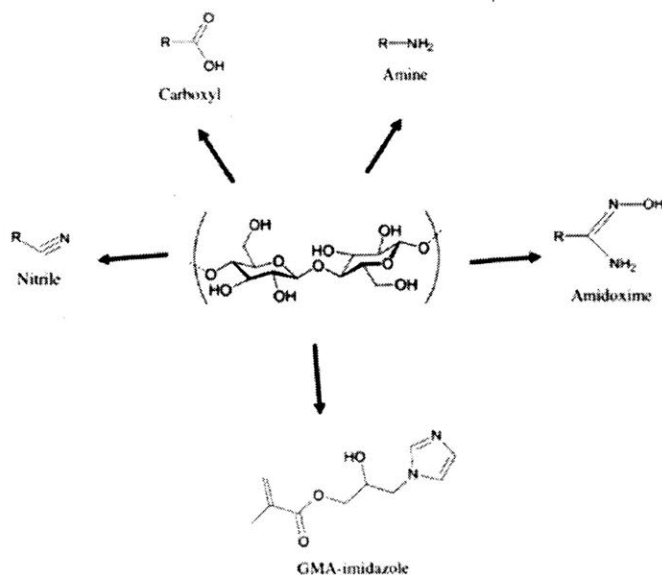


Figure 3-3: Cellulose modifications reactions. Cellulose is able to be modified through a variety of chemical and grafting reactions due to its chemical reactivity [43].

### 3.2.3 Ion exchange resins for heavy metal removal

Ion exchange resins remove pollutants through exchanging one ion for another due to the difference in matrix chemical group affinity for different ions (Figure 3-4, [51]). This makes ion exchange inherently different from adsorption; in ion exchange, the concentration in equivalents in the resin phase and the bulk solution phase remains constant throughout the whole process, due to the stoichiometry of the exchange process, whereas in adsorption, the total equivalent concentration in solution decreases [52].

Resin specificity usually increases with the size and atomic weight of the ion; in the case of heavy metals, cation exchange resins are well known to show high selectivity for lead, iron and cobalt [51]. Resins take the form of synthetic crosslinked polymer spheres, usually several hundred microns in diameters. Both anion and cation exchange resins exist and are widely commercially available for many applications from companies such as DOW Chemical and Purolite.

Cation exchange resins are generally made of polystyrene crosslinked with divinyl benzene and synthesized by inversion polymerization followed by functionalization

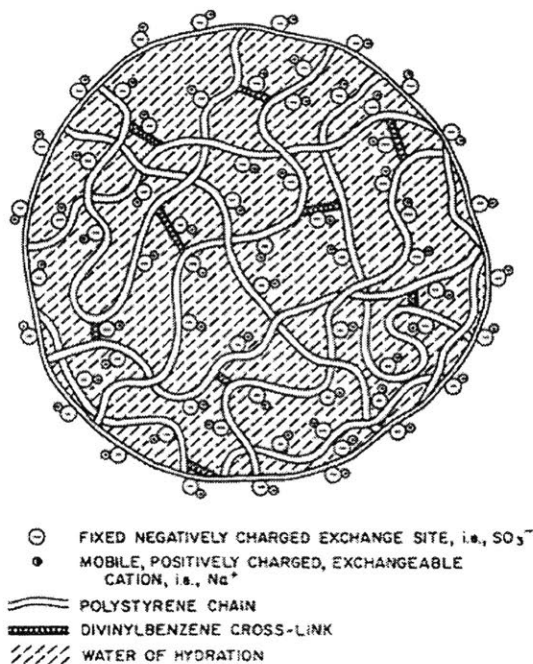


Figure 3-4: General structure of a strong acid ion exchange resin. The resin is a crosslinked polymer with stationary negatively charged groups, which bind and release cations of interest [51].

with the reactive exchange group. The degree of cross linkage determines the porosity of the bead; the higher the crosslinking, the smaller the pores of the resin beads [51]. Their porosity gives them a larger surface area per mass (up to  $500 \text{ m}^2/\text{g}$ ) and promotes their high exchange capacity. Due to their porous structure and fixed charged group content, resins are swollen in their wet form by water molecules that are attracted to the fixed groups.

Cation exchange resins are classified by their stationary resin phase functional group into strong acid and weak acid resins. Both functional groups exchange hydrogen or sodium for metal cation. Strong acid resins possess sulfonic acid functional groups can be used in solutions of any pH. Weak acid resins contain carboxylic acid functional groups and are only useful in solutions of pH 5 to 14.

Additionally, ion exchange resins are able to be regenerated to their original form by the application of concentrated acid. The large concentration of hydrogen ions in solution promotes the exchange of immobilized metal ions by reversal of the thermo-

dynamic driving potential. Protocols for resin regeneration are well established and resins can be used multiple times before needing replacement.

Many studies have demonstrated the use of ion exchange resins in removing heavy metals from various solutions, including drinking water and industrial effluent. As an example, DOWEX 50W, a strong acid hydrogen form ion exchange resin, has been used for removal of copper, chromium, cadmium, lead and nickel from drinking water and industrial effluents [53].

### 3.3 Materials and methods

#### 3.3.1 Reagents

Copper nitrate, lead nitrate and nickel nitrate ( $\text{Cu}(\text{NO}_3)_2$ ,  $\text{Pb}(\text{NO}_3)_2$  and  $\text{Ni}(\text{NO}_3)_2$ , respectively), inorganic salts and buffer salts were purchased from Sigma Aldrich. Ultrapure water, with  $18.2\text{M}\Omega$  resistivity produced from a Millipore Direct Q3 laboratory water purification system, was used in all experiments.

For the preparation and analysis of metal ion concentration, TraceMetal Grade nitric acid (Fisher Scientific or Sigma Aldrich) was used. Single ion spectroscopy standards for ICP-OES or ICP-MS were purchased from Inorganic Ventures or from SPEX Certiprep at concentrations of 1000 mg/L or 10000 mg/L.

All grades of cellulose filter paper were purchased from General Electric Life Sciences. Filter paper grades and their pore sizes are shown in Table 3.2. DOWEX G-26 strong acid ion exchange resin, Marathon C strong acid ion exchange resin and MAC-3 weak acid ion exchange resin were purchased from Sigma Aldrich. Characteristics of ion exchange resins are shown in Table 3.3.

Table 3.2: Cellulose filter paper grades tested.

| Filter paper grade | Particle retention ( $\mu\text{m}$ ) |
|--------------------|--------------------------------------|
| 1                  | 11                                   |
| 2                  | 8                                    |
| 3                  | 6                                    |
| 4                  | 25                                   |
| 5                  | 2.5                                  |
| 6                  | 3                                    |
| 42                 | 2.5                                  |
| 50                 | 2.7                                  |

Table 3.3: Characteristics of cation exchange resins tested [54, 55, 56].

| Resin      | Form                      | Functional group | Diameter ( $\mu\text{m}$ ) | Minimum exchange capacity (Eq/L) | Bulk cost (\$/gram) |
|------------|---------------------------|------------------|----------------------------|----------------------------------|---------------------|
| Marathon C | Strong acid, $\text{H}^+$ | Sulfonic acid    | 550-650                    | 1.8                              | 0.12                |
| G-26       | Strong acid, $\text{H}^+$ | Sulfonic acid    | 600-700                    | 2.0                              | 0.04                |
| MAC 3      | Weak acid, $\text{H}^+$   | Carboxylic acid  | 300-1200                   | 3.8                              | 0.13                |

### 3.3.2 Equilibrium adsorption experiments: Cellulose and ion exchange resin capacity for heavy metal contaminants

#### General protocol

In order to determine the capacity of cellulose sorbents or ion exchange resins for copper, lead and nickel, equilibrium adsorption experiments were performed similarly for all materials, unless otherwise noted.

1000mg/L stock solutions of heavy metal ion were made by dissolving the necessary amount of heavy metal nitrate salt in ultrapure water in a volumetric flask. These solutions were kept in 50 milliliter (mL) polypropylene conicals for a maximum of 6 months before new stocks were made.

30mL of synthetically contaminated water with a known concentration of heavy metal contaminant was added to a known mass of adsorbent in a non-tissue culture treated polypropylene petri dish. Solutions contained one or all three heavy metals of interest. The filled dishes were placed on an orbital shaker, moving at 100 rotations

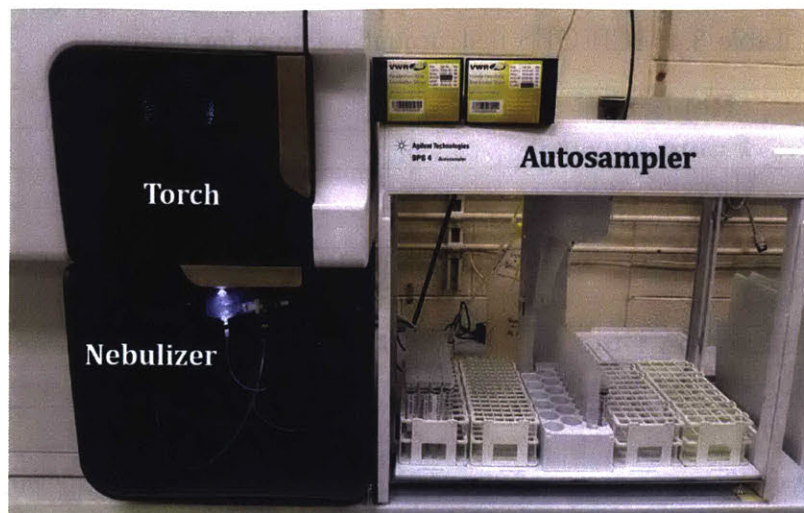


Figure 3-5: ICP-OES instrument at MIT's CMSE. The instrument is equipped with an autosampler for easy sample introduction. The sample is taken up through the autosampler, and vaporized in a quartz nebulizer, from which it is drawn into the argon plasma torch chamber.

per minute (rpm), and allowed to come to equilibrium at room temperature over a period of 20 hours. After incubation, 10mL of solution were removed from each dish and placed into a 15mL polypropylene conical previously filled with 2mL of 10% TraceMetal grade nitric acid and 3mL of ultrapure water. This way, the 15mL resulting total sample volume had a final concentration of 2% nitric acid, the required concentration for metal ion preservation [32]. A 10mL sample of initial synthetically contaminants water was also preserved for analysis in order to accurately quantify the amount of metal in the starting solution.

### **Analysis of metal concentration using ICP-OES**

Preserved samples were analyzed as soon as possible using an Agilent 5100 Inductively Coupled Plasma Optical Emission Spectroscopy (ICP-OES) instrument located at MIT's Center for Materials Science and Engineering (CMSE) in autosampler mode (Figure 3-5). In between samples, the machine was flushed with a 3% nitric acid solution made in house. The standard machine settings for all runs are shown in Table 3.4 and the wavelengths used for each element are shown in Table 3.5. Radial and axial view intensities were collected for each element.

Table 3.4: ICP-OES instrument settings for analysis.

|                              |       |                        |           |
|------------------------------|-------|------------------------|-----------|
| <b>Replicates</b>            |       | 3                      |           |
| <b>Pump speed</b>            |       | 10rpm                  |           |
| <b>Uptake delay</b>          |       | 25s                    |           |
| <b>Rinse time</b>            |       | 30s                    |           |
| <b>Read time</b>             | 5s    | <b>Nebulizer flow</b>  | 0.70L/min |
| <b>RF power</b>              | 1.2kW | <b>Plasma flow</b>     | 12L/min   |
| <b>Stabilization time</b>    | 15s   | <b>Auxilliary flow</b> | 1.0L/min  |
| <b>Radial viewing height</b> | 8mm   | <b>Makeup flow</b>     | 0L/min    |

For all ICP-OES runs, a set of standards was analyzed first for generation of calibration curves. Depending upon the experiment and the water matrix tested, the standards were either single or multi-ion. All standards were diluted from certified 1000 mg/L or 10000mg/L stock solutions using volumetric flasks, ultrapure water and TraceMetal Grade nitric acid at a final concentration of 2%. Standards were kept and used for 6 months maximum before a new set of standards was diluted from certified stock solutions.

Table 3.5: Elements and wavelengths monitoring during ICP-OES analysis of water samples. Data from bolded wavelengths was used in analysis.

| <b>Element</b> | <b>Wavelength (nm)</b>           |
|----------------|----------------------------------|
| Calcium        | <b>315.887</b> , 396.847         |
| Copper         | <b>324.754</b> , 327.795         |
| Potassium      | <b>766.491</b> , 769.847         |
| Magnesium      | 279.078, 279.553, <b>280.270</b> |
| Sodium         | <b>588.995</b> , 588.592         |
| Nickel         | <b>231.604</b>                   |
| Lead           | <b>220.353</b>                   |

Calibration curves were generated using a MATLAB script implementing a weighted least squares linear regression algorithm. Each calibration point was weighted by the variance of three successive measurements. This is different from the weighting that is performed by the ICP-OES software when it attempts to fit the standard data; standard deviation is used as the weights in the fitting algorithm. Weighting by variance is the more usual statistical method and was thus used in this analysis. Standard curves were required to have a correlation coefficient of greater than 0.9990 to be



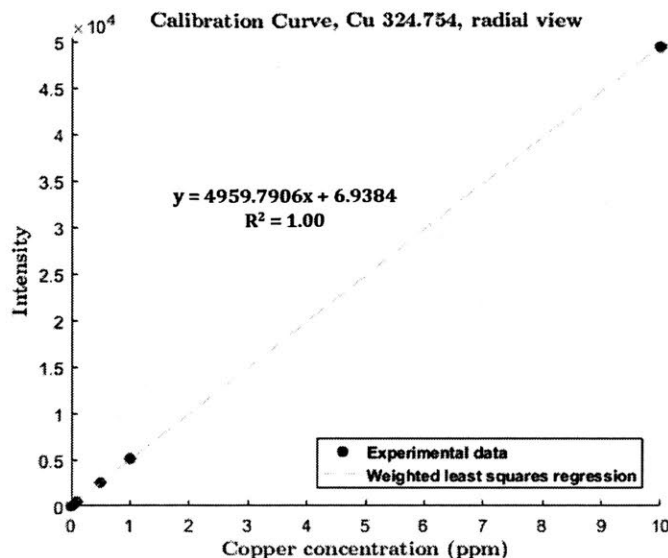


Figure 3-6: Example ICP calibration curve used for data analysis.

acceptable for data analysis. An example calibration curve for copper is shown in Figure 3-6.

### Isotherm fitting and adsorbent mass prediction

Using a MATLAB algorithm for nonlinear weighted least squares curve fitting, the Langmuir and Freundlich isotherm models were fit to each experimental data set. The code uses MATLAB's built-in *lsqcurvefit()* function using the Levenberg-Marquardt nonlinear least squares fitting algorithm to fit user specified curve equations to the data on a linear scale. This method of isotherm fitting was selected over the more traditional log-log plot method to give more accurate parameter estimation. The isotherm that gave the best fit, as judged by the regression coefficient, at the relevant low concentrations was used to predict the amount of adsorbent that would be needed to remove 80% of a contaminant at the maximum acceptable concentration from 1L of drinking water using Equation 3.4.

Additionally, most adsorption experiments were performed in triplicate. Error in the experimental measurement was estimated using the standard deviation of the three replicates. Graphs in the results section plot these error bars for experiments

in which replicates were performed.

### **3.3.3 Specific experiment details**

#### **pH dependent adsorption on cellulose filter paper**

As an initial screen of pH effect on heavy metal adsorption, experiments with a single ion, copper, were carried out. Ultrapure water was spiked with 10 various concentrations of copper ranging from 0.05ppm to 5ppm (from copper nitrate stock solutions) and buffered with 0.10mM pH buffer to precisely control the pH of the solution over the entire course of the experiment. The adsorbent for all of these experiments was a single 47 millimeter (mm) diameter Whatman Grade 1 cellulose filter paper disk, with an average mass of 0.1550g.

Solution pHs from 6-9 were tested, as this is the most relevant range for drinking water pH. Buffers were selected for their compatibility with heavy metal ions; all were from the family of Good's N-substituted aminosulfonic acids, used extensive in biological experiments and reported to not precipitate or complex heavy metal ions [57]. The following pH buffers were made in house from the free acid and free base:

- **pH 6:** 2-(N-morpholino)ethanesulfonic acid (MES)
- **pH 7 and pH 8:** 4-(2-hydroxyethyl)-1-piperazineethanesulfonic acid (HEPES)
- **pH 9:** N-cyclohexyl-3-aminopropanesulfonic acid (CAPSO)

Each experiment was performed in triplicate. The initial and final pH of each dish was monitored to be sure the pH did not significantly vary over the course of the experiment.

#### **Effect of cellulose filter paper grade on adsorption capacity**

Eight grades of filter paper were tested for their ability to adsorb copper from ultrapure water with no pH control. 47mm disks of filter paper were used in each experiment. Three concentrations of copper, 0.250ppm, 0.500ppm and 0.750ppm,

were tested in triplicate. Pore sizes for the different grades of filter paper are given in Table 3.2.

### Adsorption capacity of modified cellulose

Eight different modifications of grade 1 cellulose filter paper were performed, as described below. 47mm modified disks were tested in triplicate in their ability to adsorb copper from two or three different solution concentrations (either 0.250ppm and 0.750ppm or the same three concentrations used in Section 3.3.2). A summary of modifications and their references in literature is shown in Table 3.6.

Table 3.6: Cellulose modifications attempted in this investigation.

| Starting material from literature | Modification  | Maximum reported capacity (mg/g) | Reference |
|-----------------------------------|---|----------------------------------|-----------|
| Microfibrillated cellulose        | Silylation (APTES)  | Copper: 200.17                   | [58]      |
| Wood shavings                     | Activation (HCl, NaOH, $\text{Na}(\text{CO}_3)_2$ , $\text{NaH}_2\text{PO}_4$ ) | Methylene blue: 52               | [59, 60]  |
| Wood shavings                     | Esterification (Citric acid)  | Copper: 23.7                     | [49]      |
| Sawdust                           | Activation (NaOH)   | Copper: 13                       | [61]      |
| A4 paper                          | Amine linking (PEI)   | Copper: 435                      | [62]      |
| Wood chips                        | Sulfonation ( $\text{Na}_2\text{SO}_3$ )  | Cadmium: 17                      | [63]      |

**Activation of filter paper by acidic or alkaline treatment** Acidic and alkaline treatment have been reported to change the cellulose supramolecular structure from cellulose I to cellulose II. Cellulose II has a more open and exposed structure, which is hypothesized to cause the increased adsorption capacity observed in acidic or alkaline treated cellulose [64].

Activation of cellulose was performed by room temperature treatment of filter paper for a range of times, based on previously reported protocols [59, 60, 65]. Filter paper was immersed in the modification solution in a non-tissue culture treated polypropylene dish and placed on an orbital shaker with gentle rocking for the duration of the incubation period. The concentrations and incubations used were:

- 1M sodium hydroxide (NaOH) for 10min, 20min, 30min, 2hr or 24hr

- 0.05M, 0.10M or 0.20M sodium hydrogen phosphate ( $\text{Na}_2\text{HPO}_4$ ) for 24hr
- 0.1M, 0.5M or 1M hydrochloric acid (HCl) for 24hr
- 0.1M, 0.5M or 1M sodium carbonate ( $\text{Na}_2\text{CO}_3$ ) for 24hr

After incubation, filter paper was washed 5 times for 5 minutes each with ultrapure water before being dried in an oven at 50°C overnight.

**Citric acid esterification** Heating citric acid solution promotes the formation of citric acid anhydride, a reactive species, which further attacks cellulose hydroxyl groups in an esterification reaction and results in a cellulose backbone enriched with carboxyl groups [49, 50, 66].

Citric acid solutions, 1M or 0.5M in concentration, were heated to 90°C in glass beakers immersed in a water bath. Filter paper was incubated in the solutions for 90 minutes with gentle stirring. After incubation, filter paper was removed from beakers and washed 5 times for 5 minutes each with ultrapure water. The modified papers were then placed in a 50°C oven for overnight drying.

**Silylation with (3-aminopropyl)triethoxysilane (APTES)** Silylation involves the formation and attachment of silanol groups to reactive surfaces. In the specific procedure attempted, a silane is hydrolyzed to silanol monomers in the presence of alcohol. After condensation of the silanol monomers, the silanol polymer associates with the cellulose hydroxyl groups through hydrogen bonding. Heating promotes a condensation reaction between the two groups, during which a bond is formed and a water molecule is liberated. Adsorption functionality is proposed to come from the amino side chain attached to the silicon atom in the silanol [58].

Briefly, filter paper was placed in a Pyrex beaker with an 80:20 (v/v) ethanol: water mixture with 40% APTES added at 40% of the total filter paper weight. The mixture was incubated at room temperature on an orbital shaker with gentle shaking for 2 hours. After incubation, the filter paper was removed from solution and rinsed first with 80:20 (v/v) ethanol:water for 10 minutes. This was followed by two ultrapure

water washes for 10 minutes each. The filter paper was then placed in an oven at 60°C for overnight drying.

### **Polyethyleneimine (PEI) coated paper with glutaraldehyde crosslinking**

PEI is a large branched polymer with amine groups that can aid in the adsorption of positively charge species. Coating PEI onto substrates can increase their adsorption capacity. However, PEI is water soluble and will leach out of coated substrates; crosslinking using glutaraldehyde helps to stabilize and strengthen the PEI-filter paper association [62].

First, pieces of filter paper were activated through alkaline and acidic treatment. An 8 minute treatment with 1M NaOH was first, followed by a 1 minute water wash. Subsequently, filter paper was treated with 0.01M sulfuric acid for 8 minutes and another 1 minute water wash followed. Filter paper was then placed in a 50°C oven for drying for 24 hours.

Activated filter paper was then incubated 50mL of 1% (v/v) PEI:water solution for 24 hours at room temperature. 0.5mL of 50% aqueous glutaraldehyde and 0.5mL of 50% phosphoric acid were added dropwise to each solution during 250rpm orbital mixing. After 2 hours, the filter paper was removed, washed with 200mL of water and dried at 50°C for 24 hours.

### **Adsorption capacity of ion exchange resins**

0.0030g of ion exchange resin was incubated with ultrapure water spiked with various concentrations of copper ion (from copper nitrate), with final concentrations ranging from 2ppm to 100pm, following the general protocol described above. Resins are shipped in their wet form and can therefore be used directly in this application without preparatory steps. The mass of the resin chosen was based upon the published maximum exchange capacity of each resin (shown in Table 3.3).

Table 3.7: Synthetic water recipes used in testing ion exchange resins and cellulose. Masses shown are adequate to make one liter of synthetic water.

|   | Soft water | Hard water | Very hard water |
|---|------------|------------|-----------------|
| <b>Hardness (mg CaCO<sub>3</sub>/L)</b>               | 60         | 150        | 400             |
| <b>CaCl<sub>2</sub> 2H<sub>2</sub>O (g)</b>           | 0.0550     | 0.1284     | 0.2751          |
| <b>Ca<sup>+2</sup> concentration (ppm)</b>            | 15         | 35         | 75              |
| <b>MgCl<sub>2</sub> (g)</b>                           | 0.0215     | 0.0597     | 0.2030          |
| <b>Mg<sup>+2</sup> concentration (ppm)</b>            | 5.49       | 15.24      | 51.83           |
| <b>KCl (g)</b>  | 0.0076     | 0.0076     | 0.0076          |
| <b>K<sup>+</sup> concentration (ppm)</b>              | 4          | 4          | 4               |
| <b>NaNO<sub>3</sub> (g)</b>                           | 0.1553     | 0.1553     | 0.1553          |
| <b>Na<sup>+</sup> concentration (ppm)</b>             | 42         | 42         | 42              |
| <b>Cl<sup>-</sup> concentration (ppm)</b>             | 46         | 110        | 288             |
| <b>NO<sub>3</sub><sup>-</sup> concentration (ppm)</b> | 120        | 120        | 120             |

### Effect of water hardness on cellulose and ion exchange resin adsorption capacity

Waters of different calcium and magnesium content were synthesized, as summarized in Table 3.7. Salts used to create hard water were chosen so as to not induce precipitation of lead, whose inorganic salts outside of nitrate are very insoluble.

In these experiments, the initial concentration of copper, nickel and lead were not varied, while the mass of adsorbent varied. Six grades of filter paper and three ion exchange resins were tested following the general protocol.

## 3.4 Results

### 3.4.1 Effect of pH on copper adsorption on Grade 1 Whatman filter paper

A graph of experimental data showing the effect of pH on adsorption of copper from solution is shown in Figure 3-7. Data from pH 9 experiments is not shown, as it was found that the CAPSO buffer did not adequately control pH for the entire experiment.

In a promising finding, it is clear the cellulose filter paper can adsorb copper from solution, reaching equilibrium capacities in the 0.10-0.20mg/g range, depending on

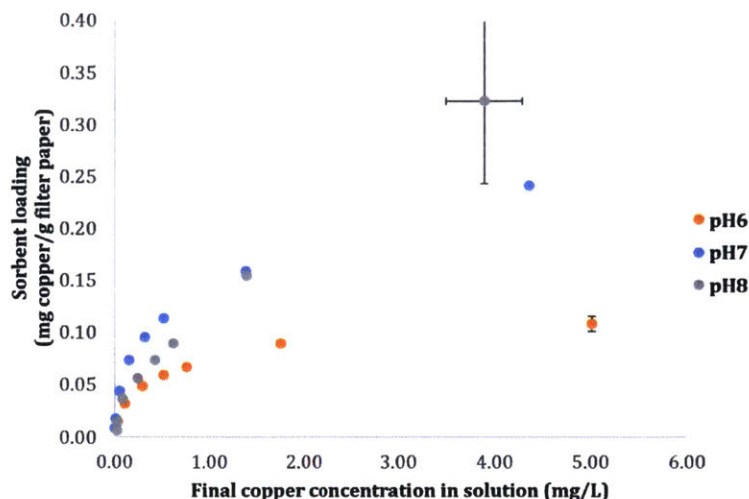


Figure 3-7: Effect of pH on amount of copper adsorbed onto cellulose Grade 1 filter paper. Error bars represent the standard error of three replicates. Filter paper can adsorb 0.10-0.20mg/g, depending on the solution pH.

the pH of the solution. The pH highly affects this capacity, however. A trend of capacity decrease is seen from decreasing pH from 7 to 6. This agrees with hypotheses that the higher the concentration of hydrogen ion (the lower the pH), the less negatively charged the cellulosic surface becomes due to aggregation of positively charged hydrogen ions that compete for adsorption.

However, an unexpected trend is seen when increasing pH from 7 to 8; pH 8 shows an overall lower adsorption capacity than pH 7, opposite of what is expected. While the source of this discrepancy is unclear, a possible explanation is that the buffer molecules may be either partly complexing the copper ions or partially adsorbing on to the surface itself. The reason for this effect was not further investigated.

Isotherms were fit to each experimental data set; an example of a fitted isotherm is shown in Figure 3-8. Fit parameters are shown in Table 3.8. The Langmuir model best overall described the pH 6 data, while the Freundlich model was more relevant for the pH 7 and pH 8 experiments. However, at low concentrations most relevant for this application (it is rare to find drinking water contaminated with greater than 0.500ppm of copper), the Freundlich isotherm fit all experiments the best.

For the purposes of predicting how much adsorbent would be needed to remove

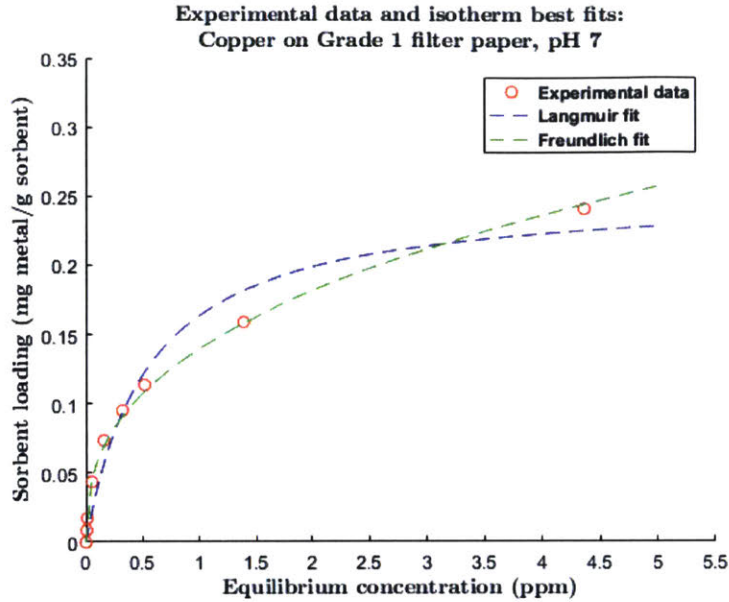


Figure 3-8: Example of isotherm fitting to experimental data using MATLAB. Script uses a nonlinear weighted least squares algorithm to fit the data with Langmuir (Equation 3.2) and Freundlich (Equation 3.3) isotherms.

Table 3.8: Isotherm best fit parameters and estimated sorbent mass needed for copper adsorption onto cellulose Grade 1 filter paper at various pH.

| Experiment | Langmuir Isotherm |           |        | Freundlich Isotherm |        | $R^2$  |
|------------|-------------------|-----------|--------|---------------------|--------|--------|
|            | $K_L$             | $Q_{max}$ | $R^2$  | $K_F$               | $n$    |        |
| pH6        | 2.3955            | 0.1126    | 0.9851 | 0.0679              | 0.3329 | 0.9681 |
| pH 7       | 1.8344            | 0.2534    | 0.9641 | 0.14                | 0.3784 | 0.9941 |
| pH 8       | 0.2759            | 0.6154    | 0.9856 | 0.1287              | 0.1287 | 0.997  |

80% of copper from 1L of water with 0.050ppm initial copper concentration, the Freundlich isotherm parameters were used. Calculated amounts are also shown in Table 3.9. The amount of Grade 1 filter paper is greater than 1 gram in all cases and is above 6 grams in the worst case scenario of pH 8.

While this data is encouraging, it is clear that pure cellulose in filter paper form does not possess adequate capacity for the dry sampling application. Without any additional cations added to solution, which could negatively impact the capacity, the amount of filter paper needed is already trending towards the upper end of the design goal set forth in Table 3.1. For this reason, other grades of filter paper and modified cellulose were tested for their adsorption capacities.



Table 3.9: Amount of Grade 1 filter paper needed to adsorb 80% of copper from a 1L water sample. Mass is estimated using Freundlich isotherm parameters shown in Table 3.8.

| Solution pH | Mass of Grade 1 filter paper needed (g) |
|-------------|---|
| pH 6        | 2.728                                   |
| pH 7        | 1.632                                   |
| pH 8        | 6.824                                   |

### 3.4.2 Effect of filter paper grade on adsorption capacity of copper

Filter paper grades vary in thickness and pore size, and therefore will vary in cellulose content and surface area available for adsorption. It was hypothesized that different grades of filter paper would adsorb different amounts of copper.

Estimated masses of filter paper needed to remove 80% of copper from a 1L sample with an initial concentration of 0.05mg/L are listed in Table 3.10. Of note, these experiments only included three copper concentrations and so there were less points for isotherm fitting than in the experiments described in Section 3.3.2. However, experiments were performed in triplicate and there was good agreement between the triplicates. Thus, the isotherms generated give good preliminary evidence as to which grades of filter paper may be more efficient adsorbents.

There does not seem to be a clear association between adsorption capacity and pore size or thickness of filter paper. The hypothesis was that papers with lower pore size should have higher cellulose content, and should show an increased capacity over papers of larger pore size. This is not the case, however. For example, Grade 3 filter paper is has an intermediate porosity, with a particle retention of 6  $\mu\text{m}$ , but requires the greatest mass to adsorb the copper. Greater cellulose content may not necessarily translate into greater available surface area for adsorption, which is the major determinant of adsorbent performance and may be partially a reason for the results seen here. This could be further confirmed with an experimental determination of surface area via Brunnauer Emmett Teller (BET) surface area analysis.

Table 3.10: Amount of filter paper of different grades needed to adsorb 80% of copper from a 1L water sample. Masses were estimated using Freundlich isotherm best fit parameters (isotherms not shown).

| Grade | Particle retention ( $\mu\text{m}$ ) | Mass needed (g) |
|-------|--------------------------------------|-----------------|
| 1     | 11                                   | 2.93            |
| 2     | 8                                    | 1.56            |
| 3     | 6                                    | 7.46            |
| 4     | 25                                   | 3.79            |
| 5     | 2.5                                  | 1.10            |
| 6     | 3                                    | 0.226           |
| 42    | 2.5                                  | 2.74            |
| 50    | 2.7                                  | 1.41            |

Interestingly, the two low porosity papers made of different cellulose or treated differently in manufacturing, Grade 42 and Grade 50, have relatively low copper capacity. Grade 42 filter paper is ashless and contains the highest cellulose content (95%) of all papers; it is also acid treated during processing to promote low ash content. Grade 50 filter paper is acid treated to promote high wet strength. This is interesting, given the body of literature supporting acid treatment of cellulose to activate the material and increase its adsorption capacity [64].

These estimated masses are still in the range of 1-10 grams and thus are adequate for the dry-sampling application, although lower mass sorbents are desired. The exception to this Grade 6 filter paper, with an estimated mass needed of around 200 milligrams. Based on these experiments, Grade 6 filter paper was selected to move forward in testing, as well as Grade 1 filter paper for comparison purposes.

### 3.4.3 Effect of cellulose modifications on adsorption capacity of copper

All cellulose modifications were first tested in their ability to remove copper from solutions with starting concentrations of 0.250ppm and 0.750ppm. The most promising materials from this screen were then tested further using three different copper concentrations to see if performance was reproducible. Performance was compared to that of the baseline material, Grade 1 filter paper.

Results of the first two solution screen are shown in Figure 3-9. A majority of the treated filter papers performed similarly or better than untreated Grade 1 filter paper. Contrary to published literature, treatment with hydrochloric acid negatively impacted the adsorption capacity. The most promising treatment tested was citric acid esterification, which significantly outperformed untreated filter paper. As an adsorbent with better capacity than untreated filter paper was sought, it was decided that the only treatment worth re-testing was citric acid.

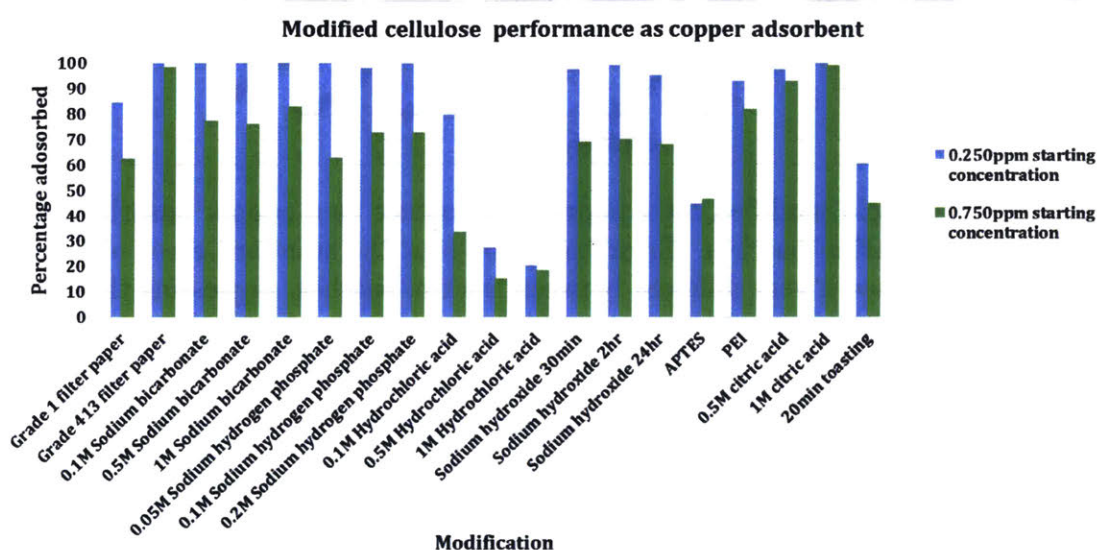


Figure 3-9: Modified cellulose performance as a copper adsorbent. Most modification performed similarly, if not better, compared to untreated filter paper.

However, the citric acid modification chemistry was not reliable, as shown in the comparison between the two experiment sets in Figure 3-10. Not only did the capacity of the citric acid treated filter paper decrease in the second experiment, but the error between replicates was very high. The reason for this irreproducibility of the citric acid modification is unclear; both modifications were carried out using the same protocol and conditions. These results were discouraging, as reproducible performance of dry sampling technology is very important. Due to this, cellulose modification was not explored further and attention turned to commercially available materials that do not rely on in house chemistry.

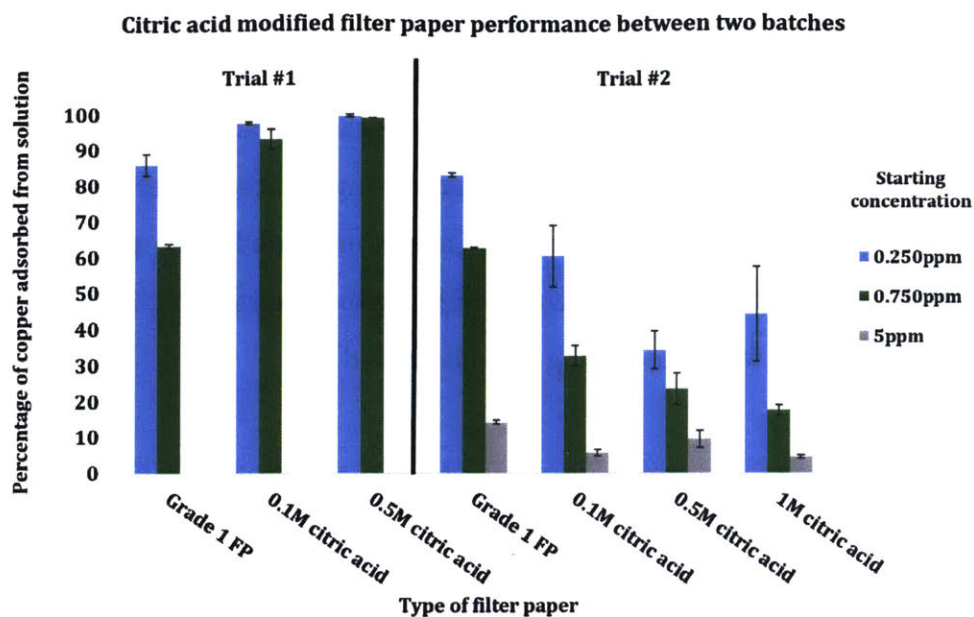


Figure 3-10: Citric acid modified filter paper performance as a copper adsorbent in trials of two modification batches. Error bars represent the standard error of three replicates. Performance is very different between the two batches, suggesting that the modification chemistry is not reliable.

### 3.4.4 Cation exchange resin copper adsorption capacity

According to published material data sheets, a very small amount of the cation exchange resin should be able to remove large amounts of copper ion. This makes ion exchange resins appealing as a dry preservation material, especially if the device is to be shippable. To test this, three ion exchange resins were tested in equilibrium capacity experiments.

An example isotherm is shown in Figure 3-11 and estimated resin masses needed for 80% adsorption of copper at a concentration of 0.050mg/L in a 1L water sample is shown in Table 3.11. These results confirm this high capacity for copper, with maximum experimental capacities greater than 70mg of copper per gram of resin. This translates into 100mg of resin or less needed to remove copper from a 1L sample, as predicted using best fit Langmuir isotherm parameters. This is further confirmed by the amount of resin needed predicted by the reported maximum exchange capacity in product literature. MAC-3 weak acid cation exchange resin shows the lowest capacity for copper; there is literature evidence suggesting weak acid ion exchange

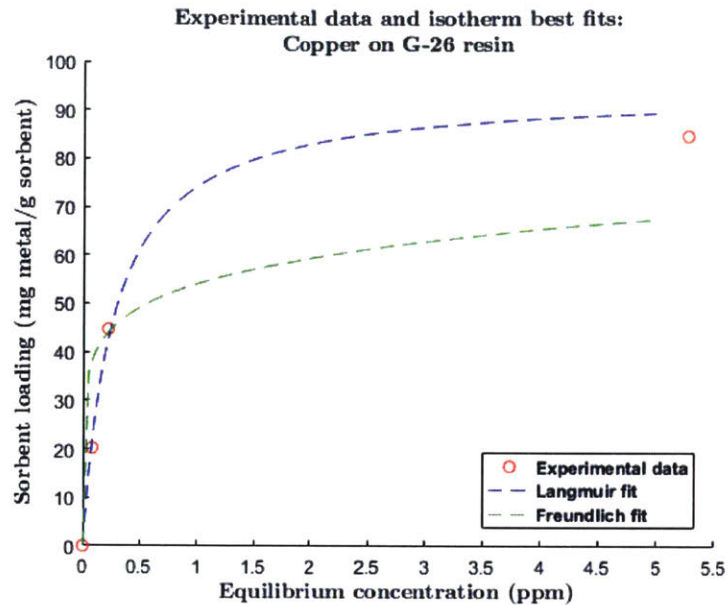


Figure 3-11: Copper adsorption isotherm on DOWEX G-26 cation exchange resin. G-26 resin has a very large capacity for copper, much larger than that of cellulose filter paper.

resins usually associate less strongly with metal ions, especially when the resin is used in hydrogen form [45].

Table 3.11: Mass of cation exchange resins needed to remove 80% of copper at a concentration of 0.050mg/L from a 1L water sample. Masses are estimated using Langmuir isotherm best fit parameters (not shown).

| Resin      | Mass needed (g) |
|------------|-----------------|
| MAC 3      | 0.1360          |
| Marathon C | 0.0133          |
| G-26       | 0.0119          |

### 3.4.5 Effect of hardness on ion exchange resin and filter paper performance

The two main divalent cations in water, calcium and magnesium, may negatively impact the adsorption capacity of adsorbents for heavy metal cations by competition for adsorption sites. For this reason, the adsorption capacity in ultrapure water spiked with heavy metals is not the most realistic measure, since drinking water samples will



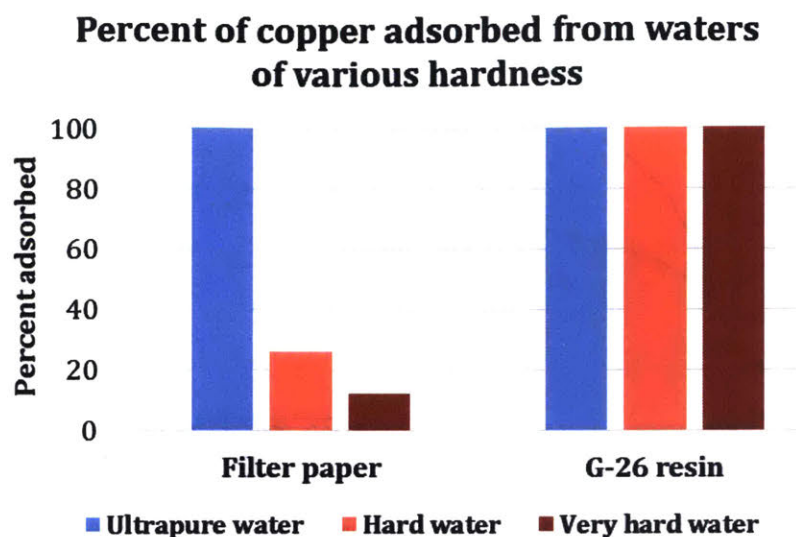


Figure 3-12: Filter paper versus G-26 resin performance as a copper sorbent in hard water matrices. G-26 resin outperforms filter paper due to its much greater capacity for copper.

undoubtedly have some level of hardness in them. Ion exchange resins are known to bind calcium and magnesium and are used extensively in softening applications [67], whereas the effects of calcium and magnesium on the adsorptive properties of cellulose are less reported.

While filter paper and ion exchange resins perform similarly in ultrapure water spiked with copper, the performance of filter paper drops precipitously as water hardness increases (Figure 3-12). This further confirms that the capacity of filter paper is not sufficient for the dry-sampling application since it cannot protect against uncertainties in water hardness.

Of note, pH control was not performed in this experiment. As it was shown that pH is crucial for optimum filter paper performance as an adsorbent, it may be that these results would be different if was precisely controlled over the course of the experiment by use of a buffer. However, from the perspective of a dry sampling device, buffer addition as a step in the protocol adds more cost, time and potential error to the dry sampling process; strong acid ion exchange resins are more appealing over cellulose for this reason.

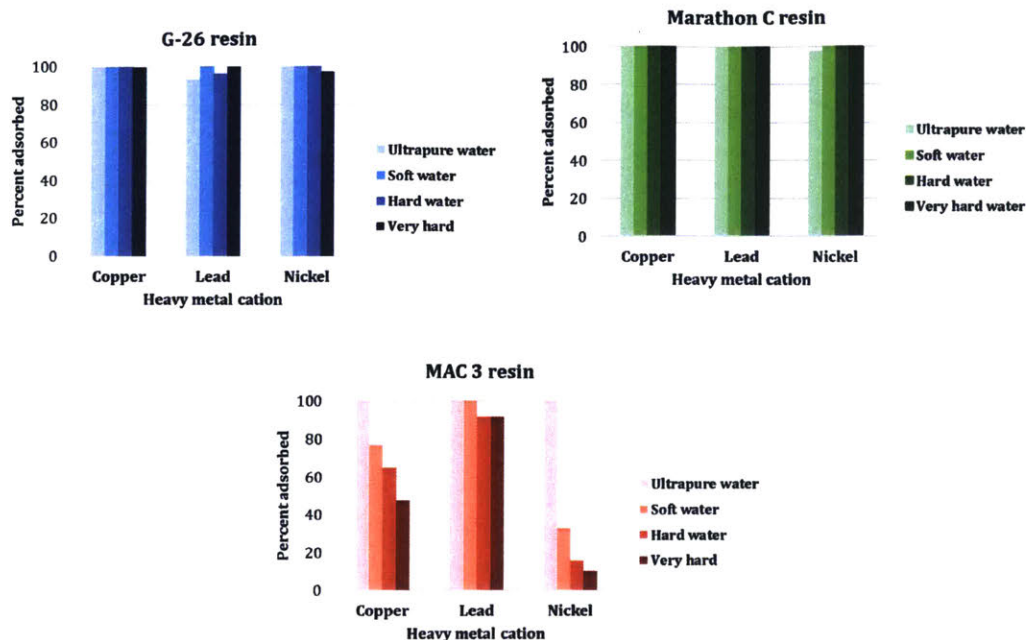


Figure 3-13: Performance of cation exchange resins in adsorption of copper, lead and nickel from different hard water matrices. Cation exchange resins have enough capacity to adsorb multiple heavy metal cations from solution, increasing their appeal as a dry sampling sorbent.

Cation exchange resins also perform well in solutions spiked with three heavy metal cations, copper, nickel and lead, as shown in Figure 3-13. Among the ion exchange resins, the weak acid resin, MAC 3, performed the worst. Its already low capacities for copper and nickel decrease as hardness increases. The capacity for lead remains relatively unchanged, however. Ion exchange resins, regardless of their form, tend to show a higher capacity for ions with higher valences and atomic masses, which could partly explain the performance discrepancy in this case, as the atomic mass of lead is more than three times that of copper and nickel [67].

Also, differences in functional group and affinity for hydrogen may contribute to this difference in performance. Strong acid cation exchange resins are essentially fully ionized in solution, due to the polarization of the bond between hydrogen and sulfonate because of differences in electronegativity [67]. On the other hand, carboxylic acid functional groups in weak acid ion exchange resins have a much greater affinity for the hydrogen ion and thus have slower hydrogen release kinetics (Figure 3-14). Addi-

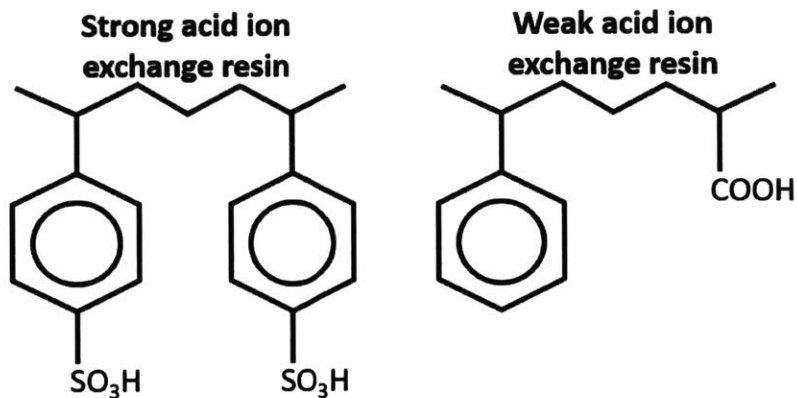


Figure 3-14: Chemical structure of ion exchange resins. Strong acid resins contain a sulfonic acid group, which fully ionizes in water. Weak acid resins contain carboxylic acids, which do not completely ionize. This difference in structure can help explain the difference in resin performance in some circumstances.

tionally, without a larger amount of alkalinity in solution to neutralize the dissociated hydrogen ion, the carboxylic acid groups will remain protonated [67]. As there was no alkalinity present in the test solutions, this could be a reason why MAC 3 performed poorly in copper and nickel removal. It is, however, also a reason why a weak acid exchange resin may not be the best option for the dry sampling application, since the alkalinity content of water samples is unpredictable. In retrospect, a weak acid cation exchange resin in the salt form (as opposed to hydrogen form) may have been a better choice to test in these experiments.

Marathon C and G-26 strong acid exchange resins performed similarly for all heavy metal ions of interest. The main difference between the two resins is their particle size, maximum exchange capacity and bulk cost. Marathon-C is slightly smaller than G-26, which could result in faster exchange kinetics, but also has a smaller minimum exchange capacity. G-26 is the cheaper of the two resins and has a higher minimum exchange capacity. Therefore, G-26 was selected as the material to pursue as a dry preservation sorbent.



### 3.5 Conclusion

The first step in creating a dry sampling device is the screening of sorbents for heavy metal capacity. An ideal dry sampling sorbent has a high capacity for heavy metals, is commercially available, needs minimal additional reagents to promote adsorption and is low cost.

The experiments described in this chapter helped to narrow down the pool of potential materials to ion exchange resins. While cellulose filter paper showed promise in early experiments, modifications to increase its capacity were not reproducible and its performance decreased significantly when tested in waters with varying hardness. As real water samples contain a certain amount of hardness that is unknown at the time of dry preservation, filter paper is not an effective material for the dry preservation of heavy metal cations.

Ion exchange resins are commercially available, have high heavy metal capacities, are low cost materials when purchased in bulk and have consistent removal performance even in waters of varying hardness. Therefore, strong acid exchange resins are natural choices for heavy metal cation sorbents. Additionally, there are a wide range of resins available, which opens the potential for custom combinations of resins to remove wide ranges of contaminants in future device and application development.

DOWEX G-26 hydrogen form strong acid cation exchange resin is chosen as the material for further development and is the subject of further characterization and experimentation in the next chapters.



## Chapter 4

# Kinetics of heavy metal uptake by G-26 ion exchange resin

### 4.1 Introduction

Ideally, a dry preservation device would be able to collect all heavy metal cations from a water sample in a relatively short amount of time, on the order of minutes. This is important, not only for user experience, but also for adoption of the device into the current monitoring system. A dry preservation device that needs hours to achieve preservation will not provide as much of a benefit to water quality monitoring as a technology that is rapid and easy to use.

For this purpose, an examination of the kinetics of heavy metal uptake on G-26 ion exchange resin in waters with background ionic content similar to that of drinking water was performed. The goal was to determine the rate limiting step in cation uptake in order to obtain predictive capability for the time needed to operate a dry preservation device. Knowledge of kinetic parameters also aid in later device design, as the geometry of the dry preservation device can be optimized to minimize resistance to cation uptake.

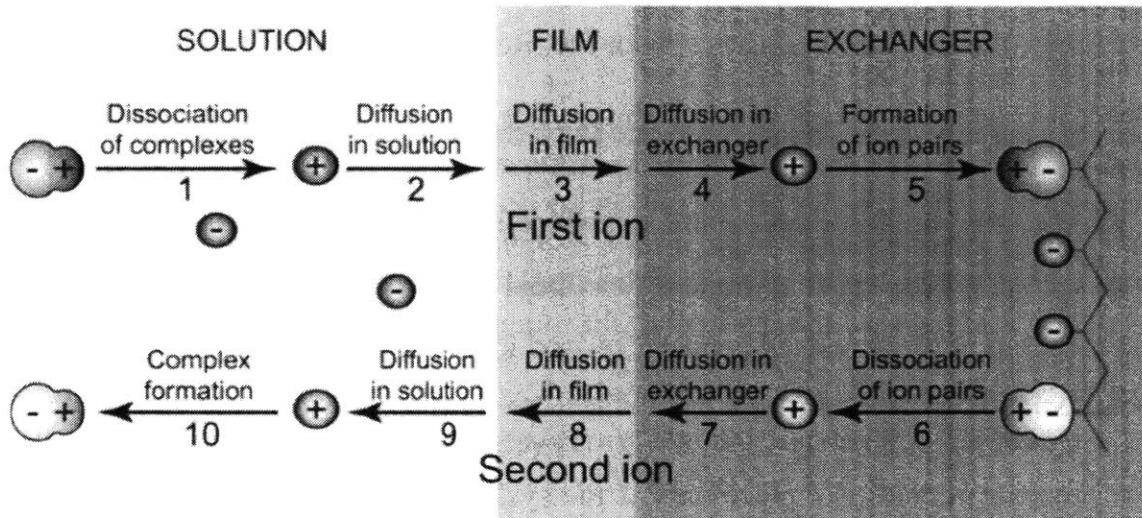


Figure 4-1: Steps in the ion exchange process. Usually, diffusion through the film or diffusion within the particle is limiting [68].

## 4.2 Kinetics of ion uptake in ion exchange resins: a diffusion controlled process

Ion exchange processes are inherently diffusion mass transport processes: the ions to be removed must migrate from the solution bulk to the interior of the resin polymer bead, where they are bound by a stationary charged group. This process can be broken down into a series steps, as shown in Figure 4-1.

In the bulk solution, the species to be removed must first dissociate from any complex in which it is involved to become a freely charged ion. Then it diffuses through the bulk solution to the surface of a stationary film of fluid that surrounds the bead, known as the Nernst film. Diffusion through the film to the bead surface is followed by diffusion through the solid resin matrix to an ion exchange site, to which the ion binds. The resin ion, which the contaminant ion displaces from the exchange site, follows the reverse of this process in migration to the bulk solution.

In free beads in well stirred batch reactors, usually either diffusion through the film or diffusion through the solid resin matrix governs how fast the removal process can proceed. These two regimes are called film limited diffusion and particle limited

diffusion, respectively. Knowledge of which regime is rate limiting allows for prediction of the time necessary for removal of contaminant, and thus provides an estimation of the operating time for a dry preservation device.

In this analysis, the rate of the ion binding chemical reaction in the interior of the bead is assumed to be fast relative to the diffusion processes and is therefore neglected; diffusive transport is the focus. In the discussion of this section, the following nomenclature is adopted:

- **Counter-ions:** ions to be removed from solution (in the case of the dry preservation device, heavy metal cations)
- **Co-ions:** ions of opposite charge that also exist in solution from the dissolution of salts and preserve overall electroneutrality (i.e. anions for the system at hand)
- **Resin ion:** the ion initially present in the exchanger, which is exchanged for the counter-ions (i.e. hydrogen in the DOWEX G-26 system)

#### 4.2.1 Types of diffusion control in ion exchange

When diffusion of the species through the stagnant liquid film attached to the bead is rate limiting, the ion exchange process is said to be controlled by film diffusion (Figure 4-2). The film layer is an idealization of the actual situation, which involves a growing boundary layer due to action of viscous surface forces on the advecting liquid around the bead. First proposed by Walther Nernst, the stagnant thin film approximation replaces this boundary layer with a layer of defined thickness, which is convection free and has a sharp boundary separating it from the agitated solution [69]. While it is a simplification of the actual phenomena, the Nernst film is a very accurate approximation and is used widely in mass transfer diffusion modeling. In this model, all resistance to mass transfer to the bead surface is due to the liquid film.

On the other hand, if the diffusion of the counter-ion through the porous resin phase is slower, the process is said to be particle diffusion controlled. Resin matrix diffusivities are usually lower than free solution diffusivity due to the spatial resistance imposed by the porous resin structure.

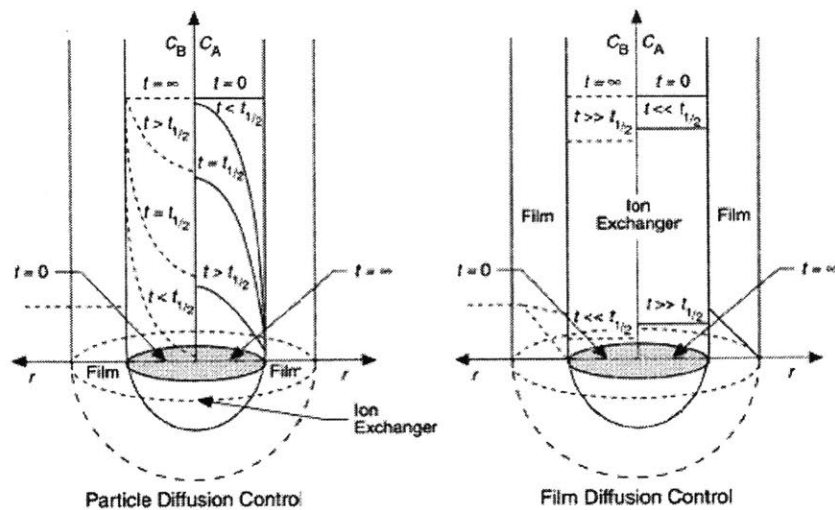


Figure 4-2: Characteristics of particle and film diffusion. In film diffusion, transport in the bead is negligible and all resistance to transport lies within the stagnant liquid layer surrounding the bead. In particle diffusion, resistance to mass transport is due to transport within the bead itself [69].

System parameters that influence which diffusive mechanism is rate limiting include:

1. **Solution concentration of the counter-ion** The diffusive flux of any ion  $i$ ,  $J_i$  [moles/m<sup>2</sup>s], is related to the concentration gradient of that ion through Fick's first law:

$$J_i = -D\nabla C_i \quad (4.1)$$

where  $D_i$  is the mass diffusivity of the ion [m<sup>2</sup>/s]. The larger the concentration gradient, the larger the flux of the ion. In ion exchange systems, kinetics of exchange in low concentration solutions are generally film diffusion limited, because the concentration gradient from the outer edge of the film to the surface of the bead is low and thus the driving force for diffusion through the stagnant film is low. Higher solution concentrations favor particle diffusion, since the concentration gradient across the liquid film is higher, making the film diffusion resistance lower and the diffusional flux across the film faster as compared to diffusion within the particle.

2. **Ion exchange capacity** The capacity of the ion exchange resin, or how many counter-ions the resin can exchange and remove from solution, affects the rate of diffusion within the ion exchanger. If the ion exchange capacity is high, the counter-ion does not have to travel far within the resin to find a binding site, which makes the resistance to diffusion within the particle lower. Therefore, film diffusion is often rate limiting with higher capacity resins.
  
3. **Porosity and crosslinking of ion exchange resin** The porosity of ion exchange resins is controlled by the degree of crosslinking, expressed as a percentage of the crosslinking agent used in synthesis (usually divinylbenzene (DVB) in the case of strong acid cation exchange resins such as G-26). The higher this percentage, the less porous the resin matrix is. Therefore, resins with higher crosslinking have greater resistance to counter-ion diffusion within the resin matrix. In these situations, particle diffusion is generally the rate determining mechanism.
  
4. **Agitation and advection of the solution** The film thickness surrounding each spherical bead,  $\delta$ , scales inversely with the flow speed of the bulk liquid. This is shown through correlations of dimensionless parameters in mass transport for a single sphere:

$$Sh = \frac{2r}{\delta} = 0.37Re^{0.6}Sc^{\frac{1}{3}} \quad (4.2)$$

where  $Sh$  is the dimensionless Sherwood number comparing convective and diffusive mass transport;  $r$  is the ion exchanger bead radius;  $Re$  is the flow Reynolds number; and  $Sc$  is the dimensionless Schmidt number, comparing momentum diffusivity to mass diffusivity [69]. The Reynolds number for flow past a sphere is defined as:

$$Re = \frac{\rho v D}{\mu} \quad (4.3)$$

where  $\rho$  is the fluid density,  $v$  is the flow velocity;  $D$  is the particle diameter and  $\mu$  is the fluid dynamic viscosity. Therefore, higher flow speeds and agitation

rates tend decrease the film thickness surrounding the bead, rendering film diffusion negligible. Such systems are often controlled by particle diffusion.

An additional parameter that influences the rate of exchange, the size of the resin bead, affects both diffusion processes. Smaller beads promote faster diffusion within the particle, since the diffusion path length is reduced. However, smaller beads also have a larger specific surface area, which provides greater area over which film diffusion can occur. While particle diffusion and film diffusion differ mathematically in the extent to which they depend on particle size, experiments varying the resin particle size cannot always reveal which diffusive mechanism is rate limiting.

#### 4.2.2 Kinetic models used in describing ion exchange

Study of diffusive mass transfer begins with Fick's Laws (Figure 4.1). Fick's first law shows that concentration gradients are the driving force for diffusion. At steady state with an unchanging concentration profile, Fick's first law can be used to evaluate the diffusional flux of a species. For systems where the concentration profile is not yet constant, Fick's second law describes how the species concentrations evolves in time.

Table 4.1: Fick's Laws of diffusion

|                     |                                       |
|---------------------|---------------------------------------|
| 1 <sup>st</sup> Law | $J_i = -D_i \nabla C_i$               |
| 2 <sup>nd</sup> Law | $\frac{dC_i}{dt} = -\nabla \cdot J_i$ |

Both equations include the mass diffusivity (or diffusion coefficient),  $D_i$ , a proportionality constant that is experimentally determined for and specific to a binary combination of species in a medium. This binary diffusivity is constant; the diffusivity of species A through B is the same as the diffusivity of species B through A. The larger the diffusion coefficient, the more mobile the species is in the given medium. Additionally, the diffusion coefficient strongly depends on the temperature, necessitating the experimental measurement of diffusivity in systems operated at extreme temperature conditions.

Fick's laws of diffusion are the starting point for the two common models used in analyzing ion exchange systems. The Fick's law model is most applicable to isotopic



species. In the more accurate Nernst Planck model, an additional term is included in the governing equation which accounts for the electrical coupling of ion fluxes.

In both models, governing differential equations are solved for each diffusion controlling mechanism subject to boundary conditions consistent with batch reactor conditions. In the infinite solution volume case, the solution concentration of the counter-ion remains constant for the entire exchange process, thereby enforcing a constant concentration boundary condition at the resin/film interface (for particle diffusion) or at the liquid film/bulk solution interface (for film diffusion). This boundary condition is difficult to enforce experimentally, but can be solved analytically. In contrast, in the finite solution volume case, the solution concentration of the counter-ion changes over time, a common situation found in ion exchange systems. Solving the differential equations for finite solution volumes requires a time dependent (often nonlinear) concentration boundary condition at the interface, which makes analytically solving the equation much more challenging and quite frequently, impossible.

In practice, differentiating between the two boundary condition cases is based upon the application of the following equation [52, 70]:

$$w = \frac{Q_M M_r}{C_o V_o} \quad (4.4)$$

where  $Q_M$  is the exchange capacity of the resin [equivalents/g];  $M_r$  is the mass of the resin [g];  $C_o$  is the initial solution concentration of the counter-ion [equivalents/L]; and  $V_o$  is the solution volume [L]. If  $w$  is less than 1, the infinite solution volume condition is appropriate; if  $w$  is greater than 1, the finite solution volume condition should be used.

For multicomponent systems, with multiple counter-ions to be removed from solution and multiple co-ions existing in the solution, a set of governing equations must be solved for each counter-ion pair and counter-ion-resin-ion pair in order to accurately predict the exchange rate. The result is a set of coupled differential equations which must be solved numerically. As such, there exist relatively few published studies in the literature for multicomponent ion exchange systems [71, 72, 73]. The inher-

ent complexity of modeling ion exchange processes has led to many authors using empirical equations or simplified models to describe data.

### **Fick's law model**

In isotopic exchange, the ions that are exchanging are two elements of the same valence. This means that the system is in equilibrium besides for the distribution of these isotopes. For this simplistic and ideal case, Fick's laws (Table 4.1) are solved in spherical geometry.

Analytical solutions for isotopic exchange exist for all boundary conditions. Despite the existence of these analytical solutions, the isotopic exchange model is often not practically applicable. It can only accurately predict the evolution of species concentration in isotopic exchange. In this case, the diffusion coefficient is the self-diffusion coefficient, or the diffusion coefficient of the ion in the absence of any concentration gradient. Counter-ion diffusivity in solutions that are infinitely dilute is well approximated by the self-diffusion coefficient.

However, in real ion exchange systems, there are usually multiple counter- and co-ions, each of different size and valence; the behavior of these systems cannot be accurately modeled by the Fick's law model because the model does not take into account differences in mobility, molecular interactions or system behavior far from equilibrium. Despite this inaccuracy, the Fick's law model is widely used as a first approximation to ion exchange behavior throughout the literature, since it is relatively easy to apply the analytical equations to experimental data.

### **Nernst Planck model**

Actual ion exchange systems are much more complex, due to the presence and concentration of multiple counter-ions and co-ions. Additionally, due to their charge, moving ions create electrical potentials that influence the diffusion of other species. In such systems, the diffusion of one ion is coupled to the diffusion of another.

A further discussion of this electrical influence is warranted. Charge conservation requires stoichiometric exchange such that the equivalent ionic fluxes of exchanging

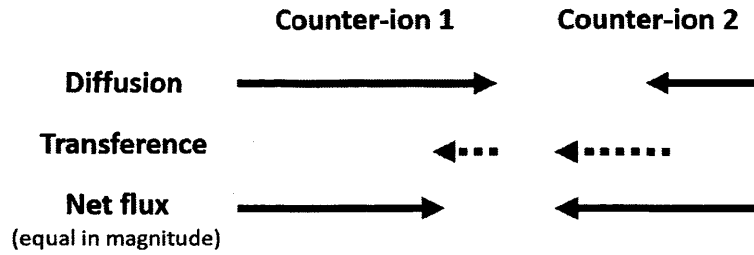


Figure 4-3: Electrical transference effect on ion exchange. This is taken into consideration in the Nernst Planck model. The electrical transference equalizes the fluxes of both exchanging ions.

ions are equal in magnitude. If this were not the case, a net transfer of charge would occur, which would violate charge conservation. The electrical potential set up by moving ionic charges controls these equivalent fluxes by producing an electrical transference in the direction of the slower moving ion (Figure 4-3). The ion with the larger diffusion coefficient diffuses at a faster rate, which leads to a small momentary accumulation of space charge and an accompanying electrical potential field which acts on all ions. This electrical transference is in the direction of the slower diffusing counter-ion, which speeds up the diffusion of the slower ion and retards the diffusion of the faster ion, thereby equalizing the fluxes of the two ions [74]. Therefore, while the individual diffusion coefficients of the counter-ions remain constant, the ions are coupled in an effective "interdiffusion" coefficient, which does not remain constant and changes with concentration changes during the exchange.

The Nernst Planck model takes this electrical transference into account and can be applied to both film diffusion and particle diffusion. Electrical flux (transference) of a species  $i$  is expressed as:

$$J_{i,el} = -u_i z_i C_i \nabla \psi \quad (4.5)$$

where  $z_i$  is the valence of species  $i$  and  $\psi$  is the electric potential. The electrochemical mobility of each species,  $u_i$ , is related to the free solution diffusivity of the species,  $D_{i,free}$  through the Nernst Einstein equation:

$$u_i = \frac{D_{i,free}F}{RT} \quad (4.6)$$

where  $F$  is Faraday's constant,  $R$  is the ideal gas constant and  $T$  is the temperature.

This electrical flux is included as an additional term in a modified Fick's first law for each ion, known as the Nernst-Planck equation:

$$J_i = J_{i,diff} + J_{i,el} = -D_i(\nabla C_i + z_i C_i \frac{F}{RT} \nabla \psi) \quad (4.7)$$

While the Nernst Planck model more accurately describes the ion exchange process and has been used in many theoretical studies of ion exchange [75, 76, 77], its use has been limited in the ion exchange applications in literature due to the complexity involved in solving the above equations. The discussion of the model is presented here for background; however, for the dry preservation application at hand, the Fick's law solutions are used in a first order estimation of the intraparticle diffusivities and film diffusivities.

## 4.3 Materials and Methods

All kinetic experiments were carried out using Nalgene low density polyethylene (LDPE) bottles and Teflon coated 1.5 inch (in) magnetic stir bars. Agitation of the liquid was achieved using VWR hot plate/stirrers. For separating crushed particles based on size, a sieve set from Bel Art, Inc. was used with polypropylene (PP) meshes purchased from McMaster Carr.

### 4.3.1 General kinetic experiment protocol

All kinetic experiments used the same basic experimental set up. 250mL of a synthetic water matrix spiked with 0.250ppm copper, 0.250ppm lead and 0.250ppm nickel was dispensed into a LDPE bottle equipped with a 1.5in stir bar.

A 2mL sample of the starting solution was removed and preserved with TraceMetal Grade nitric acid at a final concentration of 2% in water. With the solution stirring at stir speed 3, a specific mass of G-26 cation exchange resin, weighed out in the wet state, was added to the solution and the timer was started. At set time intervals, 2mL samples of the solution were removed and preserved in 2% nitric acid, as described above for the initial sample. A total of 11 samples were taken over a time period of 2-3hrs, with more frequent sampling at the beginning of the experiment and more sporadic sampling towards the end of the experiment. A 2mL sample volume was chosen to minimize reduction in the liquid volume over the course of the experiment, while still taking enough volume to be able to detect metals in ICP-OES analysis. Eleven 2mL samples corresponds to a volume reduction of 8.8%.

As soon as possible, samples were analyzed via ICP-OES analysis using lab generated standard solutions and standard machine settings, as described in Section 3.3.2. Standard curves were generated each time the instrument was used for analysis.

### **4.3.2 Experiment specific protocols**

#### **Interruption test**

To determine the rate limiting diffusion mechanism, G-26 resin at Safety Factor 1.0 mass (described below) was added to a stirring 250mL sample of water and allowed to mix with the solution for 5 minutes. After this initial contact period, the beads were removed from solution, blotted dry and allowed to sit at room temperature for 15 minutes. After this 15 minute interruption period, the beads were reintroduced to the water sample and the kinetic experiment was allow to proceed with fluid sampling for a total of 2 hours.

#### **Stir speed test**

To evaluate the effect of stir speed and liquid velocity on removal kinetics, three kinetic experiments were run, each with a different stir speed. In all three experiments, the resin was dosed at Safety Factor 0.5 mass (described below) and the water matrix

Table 4.2: Synthetic water recipes used in kinetic testing of G-26 ion exchange resin

|  | Hard water | Very hard water | High TDS water |
|--|------------|-----------------|----------------|
| Hardness (mg CaCO <sub>3</sub> /L)               | 150        | 400             | 400            |
| CaCl <sub>2</sub> 2H <sub>2</sub> O (g)          | 0.1284     | 0.2751          | 0.2751         |
| Ca <sup>+2</sup> concentration (ppm)             | 35         | 75              | 75             |
| MgCl <sub>2</sub> (g)                            | 0.0597     | 0.2030          | 0.2030         |
| Mg <sup>+2</sup> concentration (ppm)             | 15.24      | 51.83           | 51.83          |
| KCl (g)  | 0.0076     | 0.0076          | 0.0076         |
| K <sup>+</sup> concentration (ppm)               | 4          | 4               | 4              |
| NaNO <sub>3</sub> (g)                            | 0.1553     | 0.1553          | 2.79           |
| Na <sup>+</sup> concentration (ppm)              | 42         | 42              | 712            |
| Cl <sup>-</sup> concentration (ppm)              | 46         | 110             | 288            |
| NO <sub>3</sub> <sup>-</sup> concentration (ppm) | 120        | 120             | 1919           |

used was very hard water. Stir speeds used in the experiments were 1, 3 and 5, corresponding to dial settings on the stir plate.

#### Effect of varying water matrix hardness and TDS content

To examine the effect of sample hardness and total dissolved solids on uptake time, three different water matrices were used in kinetic experiments. Two waters of different hardness were tested (hard and very hard water), as well as water with a very large amount of dissolved solids (3206 ppm TDS total). Recipes for these water matrices are given in Table 4.2.

Using the minimum exchange capacity published in product literature, the mass of G-26 required to remove all ions from 250mL of very hard water matrix was calculated. This calculated mass and four additional Safety Factor (SF) masses, based on multiples of the minimum resin mass needed, were weighed out in the wet state and used individually in a set of 5 kinetic experiments, while keeping the water matrix, stir speed and sample volume constant. Resin masses are shown in Table 4.3.

The masses calculated for very hard water were used in testing of all water matrices for data and decay rate comparisons. (In actuality, the minimum mass needed to remove all ions from solution varies depending on components of the solution.)

Table 4.3: Masses of G-26 resin used in kinetic experiments. Masses are calculated based upon the published resin capacity shown in Table 3.3. The amount of resin needed to theoretically remove all cations from a 250mL very hard water sample is SF 1.

| Safety Factor (SF) | Mass  |
|--------------------|-------|
| 0.5                | 0.615 |
| 1                  | 1.23  |
| 1.5                | 1.845 |
| 2                  | 2.46  |
| 2.5                | 3.075 |

### 4.3.3 Data analysis

Intensity data for each element from ICP-OES analysis was converted into concentrations and concentration versus time was plotted for each individual ion to examine the decrease in solution concentration over time. Data was either plotted as milligrams per liter (mg/L) or moles per cubic meter (moles/m<sup>3</sup>) versus time. In some cases, the data was further converted into the dimensionless fractional attainment of equilibrium,  $F(t)$ , for modeling purposes. It is defined as:

$$F(t) = \frac{Q_t}{Q_\infty} = \frac{C_o - C_t}{C_o - C_\infty} \quad (4.8)$$

where  $C_o$  is the initial concentration in solution;  $C_t$  is the concentration in solution at time  $t$ ; and  $C_\infty$  is the concentration in solution at equilibrium.

### Ion exchange time constant estimation

To estimate the ion exchange time constant for each ion, a simple exponential decay curve for solution concentration,  $C(t)$ , in the form of

$$C(t) = Ae^{-Bt} + C \quad (4.9)$$

was fit to the concentration versus time data using a MATLAB program implementing nonlinear weighted least squares curve fitting algorithm to find the constants  $A$ ,  $B$  and  $C$  (Figure 4-4). The concentration decay time constant for the ion exchange

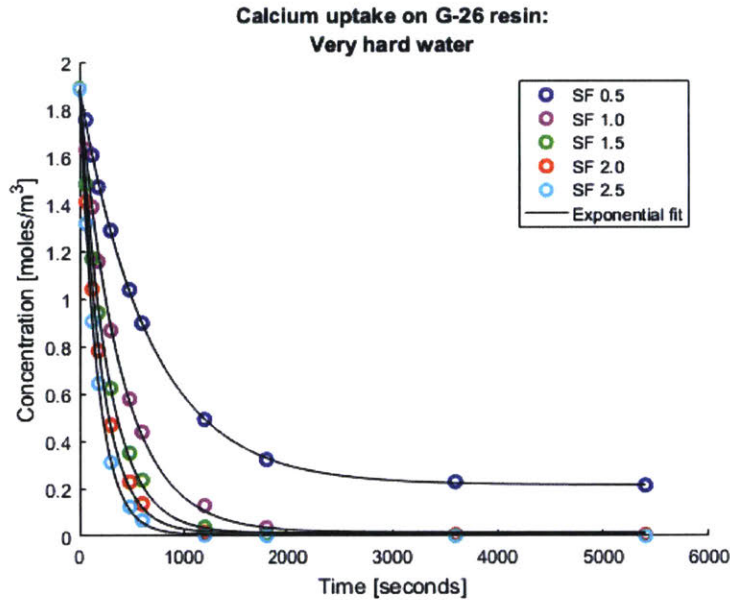


Figure 4-4: Example exponential decay curve fit to concentration versus time data using MATLAB to estimate the diffusion time constant.

process for each ion was calculated from the best fit exponential, equal to the time elapsed when the concentration of ion in the bulk solution was 63% of the initial value  $C_o$ .

### Intraparticle diffusivity estimation

The system at hand involves multicomponent ion exchange from a finite volume; this experimental set up is the hardest to model accurately using the aforementioned Fick's or Nernst Planck models. Additionally, only an estimate of diffusivity for predictive power of operation time is needed; thus a full numerical simulation of the Nernst Planck model using experimental conditions was deemed as unnecessary for this study. Therefore, for a first order estimate of the diffusivities in the resin particle,  $D_p$ , equations from the Fick's law model were used and modified, as follows, to best describe data from experiments varying the number of beads used in solution.

In estimating the intraparticle diffusivity, it is assumed that the cation diffusion within the resin particle is the rate limiting process; diffusion through the Nernst film is so fast comparatively that it can be neglected. The Fick's law solution for diffusion



in a resin particle from an infinite solution volume is [78]:

$$F(t) = 1 - \frac{6}{\pi^2} \sum_{n=1}^{\infty} \frac{1}{n^2} \exp\left(-\frac{D_p t \pi^2 n^2}{r^2}\right) \quad (4.10)$$

where  $r$  is the radius of the resin bead.

To estimate diffusivities of the counter-ions in the resin matrix using the initial slope from the concentration versus time curves, the particle diffusion equation was differentiated with respect to time:

$$\frac{dF(t)}{dt} = \frac{6D_p}{r^2} \sum_{n=1}^{\infty} \exp\left(-\frac{D_p t \pi^2 n^2}{r^2}\right) \quad (4.11)$$

Only the first term of the summation is used in this analysis. Additionally, the analysis uses the initial slope of the decay curve, before selectivity effects emerge, such that  $t$  is small; the exponential term in the above equation then disappears. From the definition of  $F(t)$ , the derivative of  $F(t)$  can be related to the solution concentration as:

$$\frac{dF(t)}{dt} = \frac{d}{dt} \left[ \frac{C_o - C_t}{C_o - C_{\infty}} \right] = -\frac{1}{C_o - C_{\infty}} \frac{dC_t}{dt} \quad (4.12)$$

Putting this all together:

$$-\frac{1}{C_o - C_{\infty}} \frac{dC_t}{dt} = \frac{6D_p}{r^2} \quad (4.13)$$

Equation 4.10 is applicable to a single ion exchange particle. Thus, the above equation is modified to pertain to the bulk solution volume,  $V$ , and to different masses of resins/different numbers of resin particles,  $N$ , by including the amount of counter-ion adsorbed per particle at equilibrium,  $Q_{p,\infty}$ :

$$-\frac{V}{N} \frac{dC_t}{dt} = \frac{V(C_o - C_{\infty})}{N} \frac{6D_p}{r^2} = Q_{p,\infty} \frac{6D_p}{r^2} \quad (4.14)$$

Based on the above equation and using data from the exponential model, plotting the initial slope of the concentration decay curve versus the amount absorbed per

particle should result in a linear relationship, with the slope of the line equal to 6 times the intraparticle diffusivity.

### Estimation of Nernst film thickness

In the estimation of the Nernst film thickness, it is assumed that Fickian diffusion in the boundary layer (or Nernst film) is the rate dominating process. The film diffusion coefficient was estimated by the bulk solution diffusivity for each ion. The following derivation was used to estimate the Nernst Film thickness in experiments.

Assuming a linear concentration profile across the film thickness  $\delta$ , the flux of ion  $i$ ,  $J_i$ , across the film is:

$$J_i = D_i \frac{\Delta C}{\delta} \quad (4.15)$$

The rate of change in the bulk concentration of the solution is:

$$V \frac{dC_t}{dt} = J_i 4\pi r^2 N = D_i \frac{\Delta C}{\delta} 4\pi r^2 N \quad (4.16)$$

For the small times considered,  $\Delta C$  can be approximated by  $C_o$ . Thus, the above equation reduces to:

$$V \frac{dC_t}{dt} = D_i \frac{C_o}{\delta} 4\pi r^2 N \quad (4.17)$$

Using data from the exponential model, the value of  $\delta$  can be estimated.

## 4.4 Results

In some figures in the following results, experimental data for copper is only shown for conciseness. Unless otherwise noted, adsorption phenomena followed similar trends for both nickel and lead.

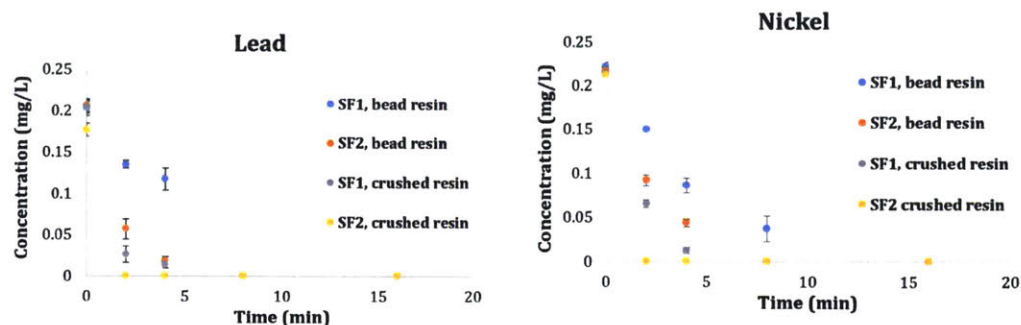


Figure 4-5: Kinetics of nickel and lead uptake on G-26 resin from very hard water. Crushed resin outperforms bead resin, so much so that no nickel or lead can be detected after 3 minutes when using SF2 crushed resin.

#### 4.4.1 Uptake of copper, nickel and lead on Dowex G-26 ion exchange resin from very hard water

In order to initially gauge the kinetics of uptake on G-26 resin, a resin sample was mixed with 250mL of very hard water containing 0.250ppm each of copper, nickel and lead. Resin was dosed at SF1 and SF2, both bead and crushed form. For this initial experiment, the crushed resin was not sieved by particle size; the bulk crushed resin was used.

Concentration decay curves for nickel and lead are shown in Figure 4-5. Copper concentrations were also monitored during the experiment but are not shown here because the sieves initially used in separation of whole beads from crushed particles were made of phosphor bronze, which contaminated the crushed resin with copper, leading to erroneous results.

In all resin dosing used, the nickel and lead are removed from solution in 10 minutes or less. Increasing the mass of resin used (from SF1 to SF2) in both the case of the bead resin and the crushed resin decreases the uptake time. In fact, the uptake is so fast on crushed resin that the sampling times used in the experiment could not accurately capture the decay curve.

These results show that decreasing particle size decreases the time to full adsorption of contaminants from solution. As discussed in the background material for this section, this is to be expected in both diffusion limited regimes, since time for both

film diffusion and particle diffusion are related to the size of the resin particle. However, this experiment does not provide any information on which diffusion regime is rate limiting, as there is no way to differentiate between the two mechanisms based on this data. Also, the data is incomplete due to lack of data in the initial decay periods of the crushed resin.

Additionally, it is clear that lead is taken up faster than copper and nickel. Greater selectivity for lead in strong acid cation exchange resins has been previously reported in the literature [79].

#### **4.4.2 Interruption test and effect of stir speed variation**

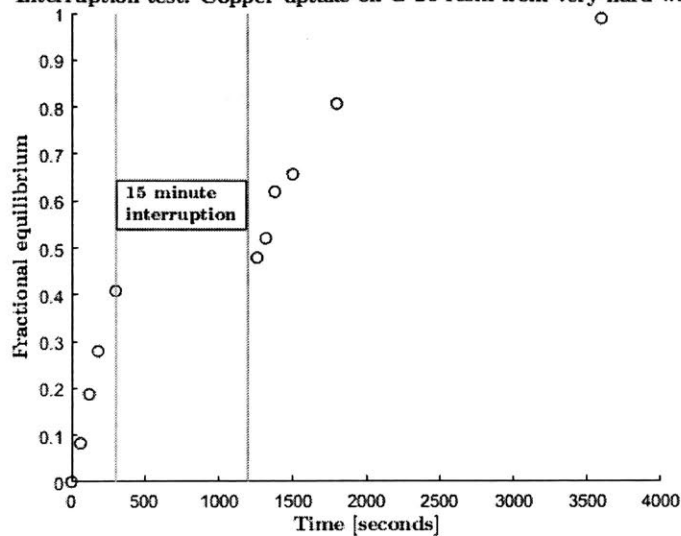
In order to determine the rate limiting diffusion mechanism, three kinetic experiments were performed. The first, the interruption test, is capable of distinguishing particle diffusion control from film diffusion control on the basis of concentration gradient type. By interrupting the kinetic test and removing the resin beads from contact with the water sample, any concentration gradients within the bead are leveled out during the interruption period. Upon being re-immersed in the solution, the rate of uptake should be greater than before interruption, if the transport is particle diffusion controlled. This manifests itself in a greater slope after interruption. However, if the transport is film diffusion controlled, the mechanism depends on the concentration difference across the film and is not sensitive to the interruption, providing film formation surrounding the beads is rapid [69].

As shown in Figure 4-6, the interruption test showed no obvious change in slope after interruption, suggesting that heavy metal uptake on G-26 cation exchange resin from very hard water is limited by film diffusion.

In the second kinetic experiment, the variation of stirrer speed affects the film thickness surrounding the beads. As shown in the background information, the film thickness is related to the fluid velocity by the dimensionless Sherwood number (Equation 4.2). Since the Reynolds number increases as fluid velocity increases (due to stir speed increase), the film thickness,  $\delta$  decreases as the stir speed is increased.

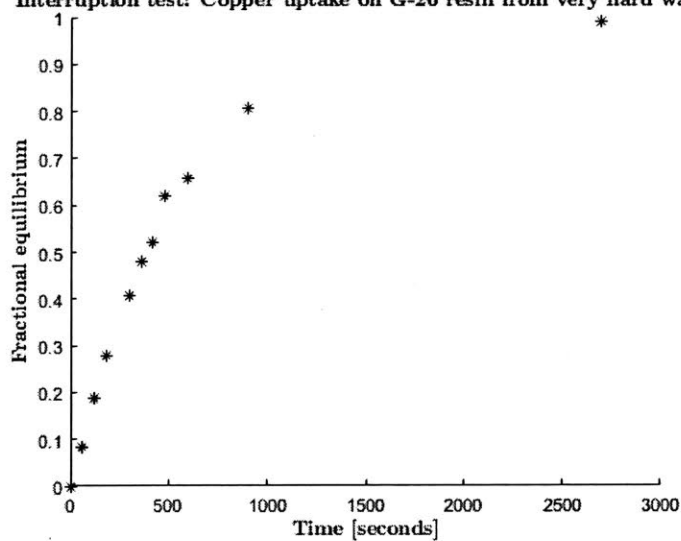
Therefore, if transport is controlled by film diffusion, the rate of counter-ion up-

Interruption test: Copper uptake on G-26 resin from very hard water



(a)

Interruption test: Copper uptake on G-26 resin from very hard water



(b)

Figure 4-6: Interruption test. (a) shows the raw data, with the interruption period included in the time. (b) subtracts the interruption period, so that the data immediately before and after the interruption can be more easily examined. There is no obvious change in slope after interruption, suggesting film diffusion control.

take should increase as the stir speed increases. In contrast, particle diffusion is not affected by the velocity of the fluid; therefore, if the counter-ion uptake rate does not vary with stir speed, the transport is particle diffusion controlled. However, the stir speed experiment is not as reliable as the interruption experiment, since at some fluid velocity, the limiting hydrodynamic efficiency may be obtained, at which changing the stir rate will have no effect on film limited diffusion transport [52].

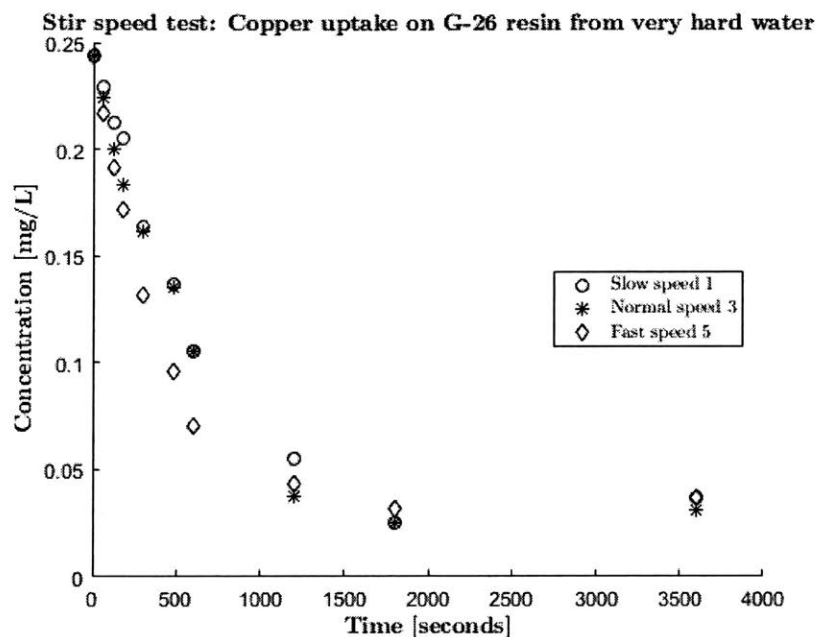


Figure 4-7: Stir speed test. While there is a slight increase in rate of uptake when the stir speed is fast, from zero to 500 seconds, saturation is reached in nearly the same time for all stir speeds (around 1800 seconds).

The results of the stir speed test (Figure 4-7) show a slight increase in uptake rate when the stir speed is fast; the slow and normal stir speeds remove copper at basically the same rate. All stir speeds cause the beads to saturate in around the same time, about 1800 seconds. These results are inconclusive; clearly, film diffusion is involved in the limiting the rate of uptake, but as the effect of increasing the stir speed is not very significant, particle diffusion can not be ruled out as a controlling mechanism. A more efficient stir speed test would confine the beads to a certain area within the bottle, so that the relative velocity of the fluid to the beads is large; however, those experiments are not performed here.

Additionally, knowing the actual impeller Reynolds number of the flow, computed based upon the rotations per minute (rpm) of the magnetic stir bar, would allow the film thickness to be estimated based upon correlations, such as Equation 4.2. The stir plates used in these experiments do not have an accurate stir speed readout and the attempt to measure the stir bar speed with a digital tachometer was unsuccessful due to the low contrast between the stir bar and the background environment.

From these experiments, it is concluded that the transport process limiting heavy metal uptake on G-26 resin likely a combination of particle and film diffusion.

#### **4.4.3 Effect of resin dosing on uptake time from very hard water**

Five masses of G-26 cation exchange resins (denoted SF0.5 to SF2.0) were used in kinetic experiments with 250mL of very hard water to examine the effect if amount of resin on kinetics. Representative results in Figure 4-8 show that the time to complete uptake of copper from solution decreases as the amount of ion exchange resin increases. This trend is also seen for calcium and magnesium, which are not contaminants of interest, but are present as hardness in all natural water samples and may have an effect on the rate of heavy metal cation uptake.

This effect is further shown by plotting the decay time constant (found using the MATLAB code discussed in Section 4.3.3) versus the number of beads in each experiment. While the number of beads is not precisely known, doubling the mass of beads used will double the number of beads because the density of the beads is constant and the bead mass used in each experiment is determined while the beads are in the wet state. Therefore, we choose an arbitrary number for the amount of beads used in SF1 and adjust it accordingly for each other SF.

The plot and time constants for copper uptake are shown in Figure 4-9. There is a strong linear relationship between the inverse decay time constant and the number of beads, such that doubling the number of beads cuts the decay time in half. In examining the time constant for each cation, it seems that early in the exchange

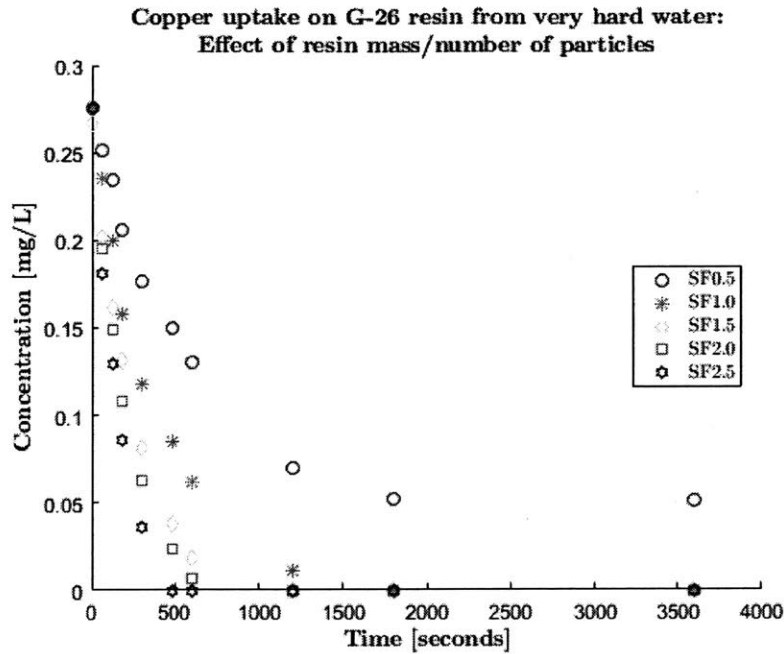


Figure 4-8: Effect of resin mass/particle number on uptake rate. As the resin mass is increased, the time to complete uptake decreases. More than doubling the mass of resin used (SF2.0) does not seem yield any significant additional rate decrease.

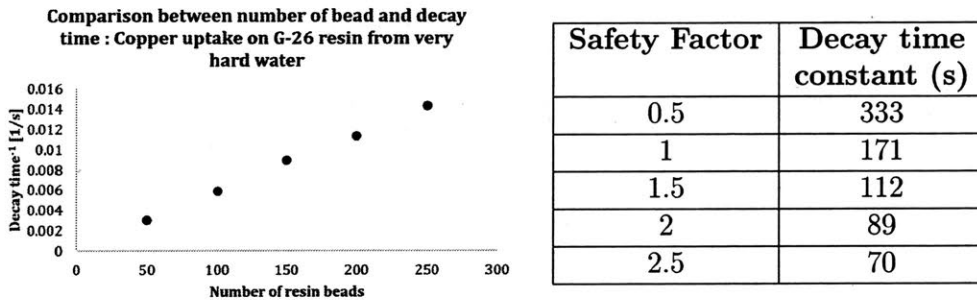


Figure 4-9: Comparison between number of resin particles in experiment and decay time constant. There is a strong linear dependence between the number of particles and the inverse of the time constant.



process the selectivity of the resin is not yet a factor, since decay times for all cations are relatively the same, falling between 160-200 seconds using SF1 resin mass (Table 4.4).

Table 4.4: Decay constants for divalent ions in uptake from very hard water on G-26 resin dosed at SF1.0. Time constants are similar for divalent cations

| Cation    | Decay time (s) |
|-----------|----------------|
| Copper    | 171            |
| Nickel    | 184            |
| Lead      | 160            |
| Calcium   | 182            |
| Magnesium | 200            |

#### 4.4.4 Effect of water matrix on uptake rate

To determine the effect of other normally occurring positively charged water matrix components, including calcium, magnesium, sodium and potassium, kinetic experiments were performed using three different synthetic water matrices: hard, very hard and high total dissolved solids (TDS). Results are shown in Figure 4-10 and a comparison of the decay times for each ion using SF1 resin mass are shown in Table 4.5.

Several notable trends are identified. First, the concentration of calcium and magnesium affects the uptake rate of the heavy metal cations of interest, with increasing hardness modestly increasing the decay time. This confirms the hypothesis that due to the divalent nature of calcium and magnesium and the specificity of G-26 resin for divalent cations, calcium and magnesium compete with the heavy metal cations for binding sites within the resin.

Second, increasing the monovalent cation concentration does not severely affect the rate of heavy metal cation uptake. Sodium and potassium are removed very fast initially, but then diffuse back out of the resin and into solution (Figure 4-11). The solution concentration of both monovalent ions recovers to 90% of the original starting concentration, so some of the monovalent ions remain trapped in the resin matrix. However, the concentration decay times during uptake from very hard water

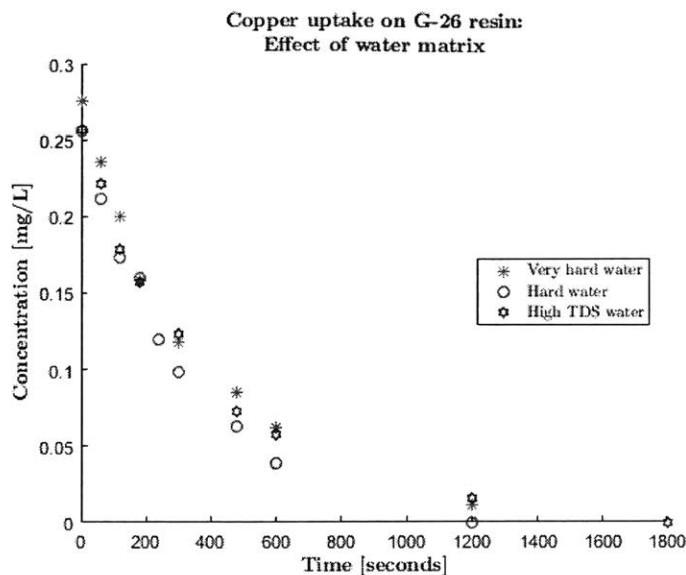


Figure 4-10: Effect of water matrix on copper uptake on G-26 resin dosed at SF1.0. Decreasing the hardness content of the water increases the rate of uptake.

Table 4.5: Decay constants for divalent ions in uptake from waters of various matrices on G-26 resin dosed at SF1.0. All data in seconds.

| Cation    | Very hard water | Hard water | High TDS water |
|-----------|-----------------|------------|----------------|
| Copper    | 171             | 152        | 176            |
| Nickel    | 184             | 137        | 192            |
| Lead      | 160             | 123        | 136            |
| Calcium   | 182             | 177        | 212            |
| Magnesium | 200             | 131        | 191            |

and high TDS water are very similar for all heavy metal cations, showing that this entrapment does not significantly affect the uptake rate or the resin capacity for the heavy metal cations.

This behavior likely has to do with the resin specificity for divalent cations over monovalent cations, as well as the faster diffusivity of sodium and potassium in the resin matrix. While the diffusivity of sodium and potassium in G-26 is not determined in this study, potassium and sodium have faster free solution diffusivities than calcium, magnesium, copper, lead and nickel (Table 4.7).

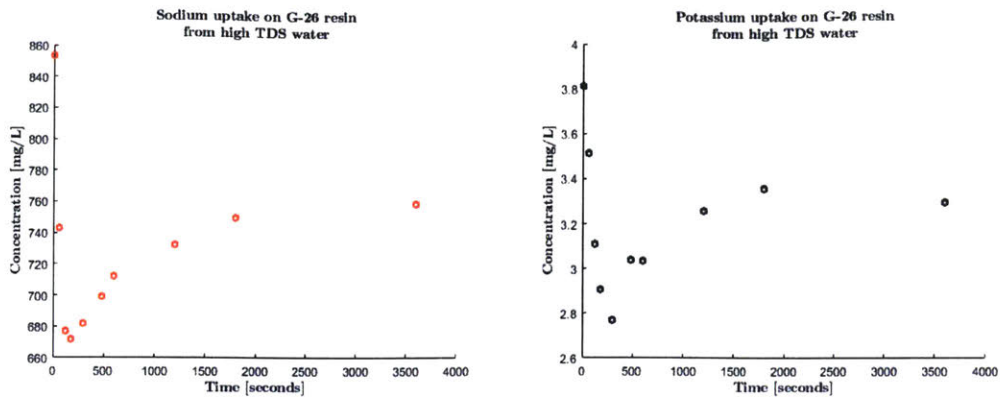


Figure 4-11: Uptake of sodium and potassium on G-26 resin dosed at SF1.0 from very hard water. After a very fast initial decay, the solution concentration recovers to 90% of the original, indicating that some monovalent ions remain trapped in the resin.

#### 4.4.5 Intraparticle diffusivity estimation

The transport of the heavy metals ions (present at trace level compared to calcium and magnesium) was shown to depend on the hardness of the water sample. Since the decay times are similar for all divalent cations, a combined diffusivity of calcium and magnesium is determined by combining the concentration versus time data for the two ions for each resin SF mass used in the above kinetic experiments and using the modified Fick's law model solution to estimate the combined diffusivity based on the slope of the graph (Figure 4-12), as described in Section 4.3.3. This analysis is performed for each kinetic experiment from moderately hard, very hard and high TDS experiments described in Section 4.4.4.

The film and particle diffusivities calculated by this method are shown in Table 4.6. The particle diffusivities calculated by this method are on the order of  $10^{-11}$   $m^2/s$ . This is slower than the free solution diffusivity (Figure 4.7), as would be expected, and is in good agreement with Fick's law exchange in the literature [80, 78, 81]. These diffusivities, however, are a lower bound estimate; they do not take into account the electrical potential effects or the differing ion mobilities. Additionally, in deriving the modified Fick's law model from Equation 4.10, only the first term in the summation was considered, which introduces error into this estimate, especially because the summation has been noted to not converge rapidly [69].

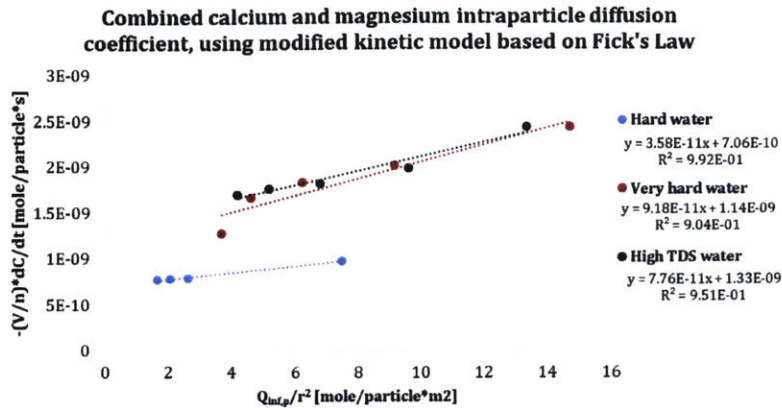


Figure 4-12: Graphical analysis of combined calcium/magnesium intraparticle diffusivities in different water matrices. The y axis variable is the change in concentration in the solution per particle. As predicted by revised model, the data is roughly linear and the intraparticle diffusivity can be estimated from the slope of the graph.

Table 4.6: Estimated combined calcium/magnesium intraparticle diffusivities.

| Water matrix    | Intraparticle diffusivity (m <sup>2</sup> /s) |
|-----------------|---|
| Hard water      | $5.97 \cdot 10^{-12}$                         |
| Very hard water | $1.53 \cdot 10^{-11}$                         |
| High TDS water  | $1.3 \cdot 10^{-11}$                          |

The estimated diffusivity in very hard water and high TDS water are very similar, indicating that the presences of large amounts of sodium and potassium do not negatively affect transport within the resin beads. This agrees with the data presented in previous sections.

#### 4.4.6 Estimation of Nernst film thickness from concentration decay data

The Nernst film thickness surrounding an ion exchange resin bead is inversely proportional to the fluid velocity by the correlation in Equation 4.2. This means that increasing the fluid velocity will decrease the film thickness, which decreases the resistance to mass transport across the film.

In trying to estimate the combined calcium/magnesium film diffusion coefficient, a slight experimental challenge arose in that the stir speed used in experiments was not accurately known. The stir plates used do not accurately control or have a way to convert the stir speed dial setting (for example, stir speed "3") to rpm of the magnetic stirrer. Because of this, the film thickness cannot be determined accurately and determining the film diffusivity using the model outlined cannot be performed.

However, typically film diffusion coefficients are on the order of free solution diffusivities. Therefore, in order to determine if the combined film diffusivity of calcium and magnesium could be estimated by their free solution diffusivities, the average of calcium free solution diffusivity and magnesium free solution diffusivity was used to estimate the Nernst film thickness,  $\delta$ , using Equation 4.17 and data from kinetic experiments in very hard, hard and high TDS water. Since all three solutions were stirred at the same stir speed dial setting, the estimation of  $\delta$  from each experiment should agree. In the literature,  $\delta$  is reported to be on the order of  $10^{-3}$ cm or  $10^{-5}$ m. Free solution diffusivities of all ions of interest in this study are shown in Table 4.7.

Figure 4-13 shows the graphs used to determine  $\delta$  and the estimated values of  $\delta$  using data from experiments performed in very hard, hard and high TDS water. All of the graphs are linear, which would be expected from Equation 4.17.  $R^2$  values for

Table 4.7: Free solution diffusivities of metal cations at 25°C and infinite dilution in water [82].

| Cation    | Diffusivity ( $\cdot 10^{-10} \text{ m}^2/\text{s}$ ) |
|-----------|---|
| Hydrogen  | 93.11   |
| Calcium   | 7.92  |
| Magnesium | 7.06  |
| Copper    | 7.14  |
| Nickel    | 7.05  |
| Lead      | 9.45  |
| Sodium    | 13.34   |
| Potassium | 19.57   |

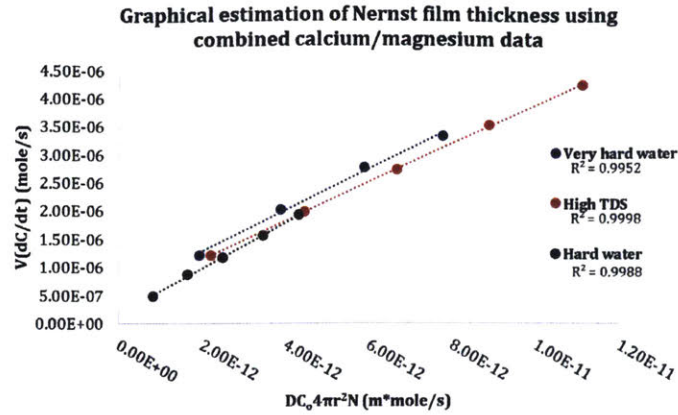
each data set are shown on the graph. Data from the all three waters falls nearly on one line, as expected since all experiments were performed using the same stir speed.

Estimation of  $\delta$  can be determined by the inverse of the slope of each line. As shown in Figure 4-13, using this method,  $\delta$  is estimated to be on the order of  $10^{-6}\text{m}$ , which is around an order of magnitude off from what is reported in literature. The free solution diffusivities used are those in solution at infinite dilution; it is likely an underestimate of the diffusivity of cations in water matrices containing other ions, where the electrical potentials developed could influence the movement of the ions.

Despite this, using the free solution diffusivity in later mass transport calculations would allow for safe estimates of device optimization and operation. Nevertheless, a more accurate estimate would be optimal and future work will seek to better estimate this diffusion coefficient.

## 4.5 Conclusion

To gain predictive capability of operational time for an eventual dry sampling device, the kinetics of copper, nickel and lead uptake on G-26 cation exchange resin were examined through a wide variety of experiments to determine the controlling diffusional regime, estimate the diffusivity and Nernst film thickness and examine the effect of changing system parameters on the uptake rate. All copper, nickel and lead, present at 5-25 times the maximum acceptable limit in a water samples, can be removed in



| Water matrix    | Slope  | $\delta$ (m)        |
|-----------------|--------|---------------------|
| Very hard water | 362224 | $2.8 \cdot 10^{-6}$ |
| Hard water      | 407325 | $2.5 \cdot 10^{-6}$ |
| High TDS        | 342417 | $3.0 \cdot 10^{-6}$ |
| <b>Average</b>  |        | $2.7 \cdot 10^{-6}$ |

Figure 4-13: Graphical determination of Nernst film thickness. Estimated film thicknesses are about an order of magnitude lower than what is reported in the literature.

10 minutes or less, depending upon the mass of resin used and the size of the resin particle. This operation time is in the ideal range.

These analyses revealed that the system at hand is likely controlled by a combination of film and particle diffusion. When the mass of resin is increased, the decay time constant was found to decrease linearly; however this kinetic benefit was seen to not be as significant beyond doubling the amount of resin needed. Increasing water hardness was found to increase the decay time constant for the heavy metals, while monovalent cation content did not significantly impact the kinetics. This is a hopeful finding, as it suggests that the dry preservation device could be operated in waters of high salinity without substantial protocol adjustment.

Furthermore, because the decay times for all divalent cations of interest were similar and water hardness was found to heavily influence the uptake time, a combined calcium and magnesium intraparticle diffusivity was estimated using a modified Fick's law model. These results give intraparticle diffusivities on the order of  $10^{-11}$  m<sup>2</sup>/s. Because this analysis assumed film diffusion was negligible compared to particle dif-



fusion, this estimate represent an upper bound on the diffusivity in the particle. One previous study has used G-26 resin in recovery of ions from wastewater, but used empirical models for kinetic estimates [83]; to date, no additional publications have been found reporting intraparticle diffusivities for this resin.

For this study, an estimate of the intraparticle diffusivity is sufficient because the device incorporating the resin sorbent will most likely affect the mass transport to the surface of the bead; the entire device kinetics will then be mass transport (film diffusion) limited and a more rigorous analysis of entire device kinetics is due. It was shown that, using the bulk solution diffusivity of calcium and magnesium, a simple film diffusion model predicted Nernst film thicknesses on the order of  $10^{-6}$ m. This analysis also gives an lower bound of film thickness (and thus, an upper bound on film diffusivity) since intraparticle diffusion was assumed to be negligible. The estimated film thickness differs from what is reported in literature; for future mass transfer coefficient calculations for designing a device, a more accurate estimate of the film diffusivity is needed.

However the effective diffusivity of the ions in the film could be up to 10 times higher, since the ion exchanged is hydrogen, whose free solution diffusivity is over ten times the diffusivity of the heavy metals of interest, as well as calcium and magnesium. The electrical potential due to hydrogen diffusion could effectively make the film thickness ten times greater. Other ions in solution will also affect the diffusivity. A more rigorous study would be required to more accurately estimate both the particle and film diffusion coefficients, which may be necessary in the future.



## Chapter 5

# Recovery of heavy metal ions after dry preservation on G-26 ion exchange resin

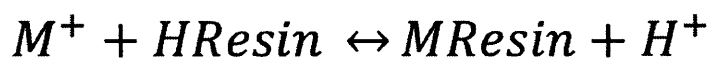
### 5.1 Introduction

The application of dry preservation technology depends on the ability of the preservation material to reliably bind and release metal cations after dry storage. The most applicable materials should be able to preserve cations over periods of time ranging from 6 months to one year. Ideally, the amount of contaminant recovered from the resin should be greater than 90%, so that lab results quantitatively reflect the amount of contaminant present in the sample.

Longer preservation periods also open the door for a dry preservation device to be used as a record keeper of contamination. If a contamination were discovered during routine monitoring, preserved samples collected and saved as a record could be analyzed retrospectively to determine when the contamination first appeared.

Regeneration protocols for cation exchange resins are well known and tested. Manufacturer information that comes with each ion exchange resin has a recommended regeneration protocol, usually consisting of elution with a moderate concentration of

strong acid. Although active sites in the resin have a higher affinity for metal ions, the presence of large amounts of hydrogen ion in solution reverse the thermodynamic potential for the chemical reaction, as shown by the reaction quotient (Figure 5-1). This allows the hydrogen ions to displace the bound metal cations, returning the resin to its initial form for reuse.



$$Q = \frac{\text{products}}{\text{reactants}} = \frac{[MResin][H^{+}]}{[HResin][M^{+}]}$$

Figure 5-1: Generic ion exchange reaction between a metal cation ( $M^{+}$ ) and hydrogen form resin ( $HResin$ ), and the reaction quotient,  $Q$ . When a concentrated solution of hydrogen ions is passed over the resin, the reaction quotient increases and the reaction now favors the reactants, displacing the metal ions and returning the resin to its original form.

This mechanism of regeneration could also be used for recovery of heavy metal cations at the lab for testing from a dry preservation device. The acid extraction from cation exchange resins is also appealing since water samples to be analyzed using ICP-OES or ICP-MS need to be acidified before analysis. Acid extraction would recover the heavy metal contaminants in a ready to analyze form, cutting down on processing time.

Therefore, the recovery of heavy metal cations, adsorbed onto G-26 ion exchange resin and stored at room temperature, was tested using published ion exchange regeneration protocols to elucidate the effect of dry storage length on recovery of heavy metals.

## 5.2 Materials and methods

### 5.2.1 Materials from previous experiments

All experimental materials from equilibrium capacity experiments (Chapter 3) and kinetic testing (Chapter 4) were saved and available for recovery testing. In the case of equilibrium capacity experiments, after samples for ICP-OES analysis were preserved, the rest of the test solution was removed from the culture dishes. The filter paper or ion exchange resin was left in the dish and as much of the adhesion liquid surrounding the materials was removed as possible. The dishes were then covered and stored on a lab bench at room temperature until recovery testing.

For kinetic experiments, the ion exchange resin was filtered from the test solution using VWR Grade 413 quantitative filter paper. The filter paper removed any additional liquid adhered to the surface of the beads. Carefully, using a polypropylene spatula, the resin beads were scraped off of the filter paper and deposited into 15mL propylene conicals. The conicals were left partially uncapped overnight to allow for further drying. Subsequently, they were sealed and stored upright on a lab bench at room temperature.

### 5.2.2 Sample preparation for testing of long term preservation

To test recovery efficiencies from the same source water over long periods of time, G-26 resin was used to adsorb copper, lead and nickel from 27 samples of the same water. Very hard water spiked with 0.250ppm each of copper, nickel and lead, was used as the test water (Table 3.7) and G-26 was dosed at twice the mass needed to completely remove all divalent ions in the test water (SF2, as outlined in Section 4.3). Resin and 30mL of test water were deposited into non tissue culture treated polypropylene dishes and left on an orbital shaker at 100rpm for 24 hours.

After incubation, 10mL of solution from each dish was collected and preserved in 2% TraceMetal grade nitric acid, following the same procedure as in Section 3.3.2. These samples were subsequently analyzed using ICP-OES to be sure that all copper,

lead and nickel were removed during the incubation period.

The remaining solution was poured out from each dish and the excess adhering water surrounding the beads was blotting away as much as possible. Dishes were then capped and stored at room temperature on a laboratory bench until recovery experiments.

A 10mL sample of the initial water was also preserved and analyzed using ICP-OES to determine the starting concentrations of copper, nickel and lead in the solution. Additionally, three control dishes, with no resin and only very hard test water spiked with the three heavy metals, were put through the same protocol as the experimental dishes, as described above. These controls were performed to make sure that copper, lead and nickel were not adsorbing to the polypropylene dishes and that the protocol of storing resins in their original dishes would not introduce error into the recovery measurement.

### 5.2.3 Regeneration of G-26 resin using hydrochloric acid

To return G-26 resin to its original form and recover the cations that had adsorbed, 30mL of 5% or 10% (v/v) TraceMetal Grade hydrochloric acid was deposited into each dish with preserved resin and incubated at room temperature on an orbital shaker at 100rpm for 2 hours. After incubation, a 10mL sample of acidic recovery solution was removed from each dish and preserved in 2% TraceMetal Grade nitric acid in previously prepared 15mL propylene conicals. Concentrations of copper, lead and nickel were determined via ICP-OES.

### 5.2.4 Recovery calculations

Using the calibration curve generated from the ICP-OES run, the concentration of each ion in the regenerated acid solution was calculated. Two measures of efficiency were calculated and combined to give an overall measure of the dry preservation process:

- **Removal efficiency ( $R_1$ ):** the ratio of the amount of cation removed from the

test solution and adsorbed on the resin to the initial amount of cation present in solution. This gives a measure of the uptake, ranging from zero (no uptake) to 1 (complete uptake).

- **Recovery ( $R_2$ ):** the ratio of the amount of cation present in solution after resin regeneration with hydrochloric acid to the amount adsorbed on the resin. Recovery shows how well the cation was dryly preserved and removed from the resin.

Overall dry preservation process efficiency,  $R_{eff}$  is defined as the product of removal efficiency and recovery:

$$R_{eff} = R_1 R_2 \quad (5.1)$$

For most samples of resin tested,  $R_1$  is equal to one, since the resin was dosed at a mass to ensure that all copper, nickel and lead was removed from the test solution.

## 5.3 Results

### 5.3.1 Initial recovery trial: 5% hydrochloric acid regeneration for G-26 resin and filter paper

For an initial trial of the recovery protocol, 5% hydrochloric acid concentration was selected, as this concentration is the middle of the recommended concentrations listed in product literature [54].

Figure 5-2 graphically shows the recoveries of copper from G-26 resin, Whatman Grade 1 filter paper and Grade 6 filter paper after 12 days of dry storage. Table 5.1 shows the removal efficiencies, recoveries and overall dry preservation efficiency for the same data. Recovery for copper fell between 90 and 100% for water matrices tested (hard or very hard, as described in Section 3.3.3) for both G-26 resin and Grade 1 filter paper. The overall efficiencies for the filter papers are due to the low removal efficiencies of copper from water matrices with hardness, as discussed in Chapter 3.

From this experiment, it was initially decided that 5% hydrochloric acid is sufficient for recovery and will be used in subsequent recovery experiments.

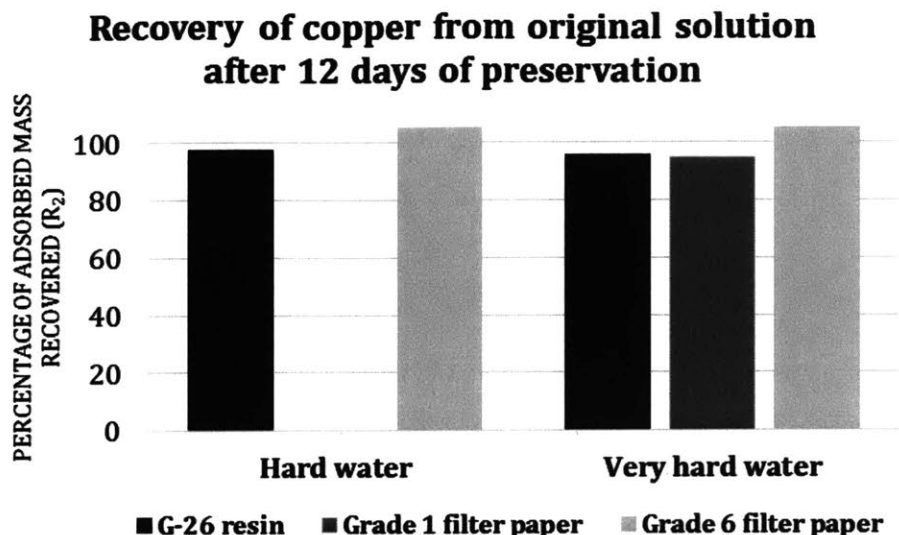


Figure 5-2: Initial recovery of copper from dry preservation sorbents after 12 days of dry storage. Over 90% of copper adsorbed on both Grade 1 filter paper and G-26 resin was recovered from very hard water. Grade 1 filter paper was not tested in hard water.

Of note, the copper recoveries from Grade 6 filter paper were consistently above 1, while recovery of copper from Grade 1 filter paper was in range. This greater than 1 recovery is concerning, because it suggests that there is some copper endogenously in the filter paper that could introduce error into the measurement of copper from a dry preservation device.

Table 5.1: Removal efficiency, recovery and overall recovery for initial preservation testing using G-26 resin and filter paper.

|                        | $R_1$ | $R_2$ | $R_{eff}$ |
|------------------------|-------|-------|-----------|
| <b>Hard water</b>      |       |       |           |
| G-26 resin             | 1     | 0.97  | 0.97      |
| Grade 6 filter paper   | 0.22  | 1.32  | 0.29      |
| <b>Very hard water</b> |       |       |           |
| G-26 resin             | 1     | 0.96  | 0.96      |
| Grade 1 filter paper   | 0.77  | 0.93  | 0.72      |
| Grade 6 filter paper   | 0.08  | 2.41  | 0.19      |

Upon further exploring product literature, it was found that filter paper can be

Table 5.2: Starting and ending concentration of heavy metals in solution after incubation for 24 hours with no sorbent. Intervals in the ending concentration is the standard deviation of three replicates. Copper and nickel are not adsorbed; however some lead gets adsorbed.

| <b>Cation</b> | <b>Starting concentration (mg/L)</b> | <b>Ending concentration (mg/L)</b> |
|---------------|--------------------------------------|------------------------------------|
| Copper        | 0.273                                | 0.279±0.004                        |
| Nickel        | 0.203                                | 0.204±0.001                        |
| Lead          | 0.201                                | 0.193±0.003                        |

contaminated with copper up to about 0.9 microgram per gram of filter paper for qualitative grades and can be as much as 8.2 micrograms per gram for quantitative grade papers, as per GE Whatman product literature. While lot analysis was not available for the Grade 6 filter paper used in these experiments, it is possible that copper contamination of the filter paper partly caused the recovery to be higher than 1 for copper.

### **5.3.2 Recovery from the same starting solution after different dry preservation periods**

Analysis of solutions from the three control dishes described in 6.2.2 showed that the polypropylene dishes do not adsorb copper and nickel (Table 5.2). Measurement of copper and nickel concentrations in the starting solution and after 24 hours of incubation were not significantly different and the starting measurements are within error or nearly within error of the ending measurement.

However, the polypropylene dish did adsorb approximately 10 ppb of lead. While this is a concerning finding for the recovery experiments, it was decided to go ahead as planned with the analysis of the prepared samples for an initial demonstration of recovery. For future experiments, a better material will be used during adsorption experiments. Other plastics may not adsorb lead, but are more expensive, which would have to be taken into account.

Each month, three dishes from the prepared samples described in 6.2.2 were subject to 5% hydrochloric acid regeneration treatment in order to evaluate the recovery

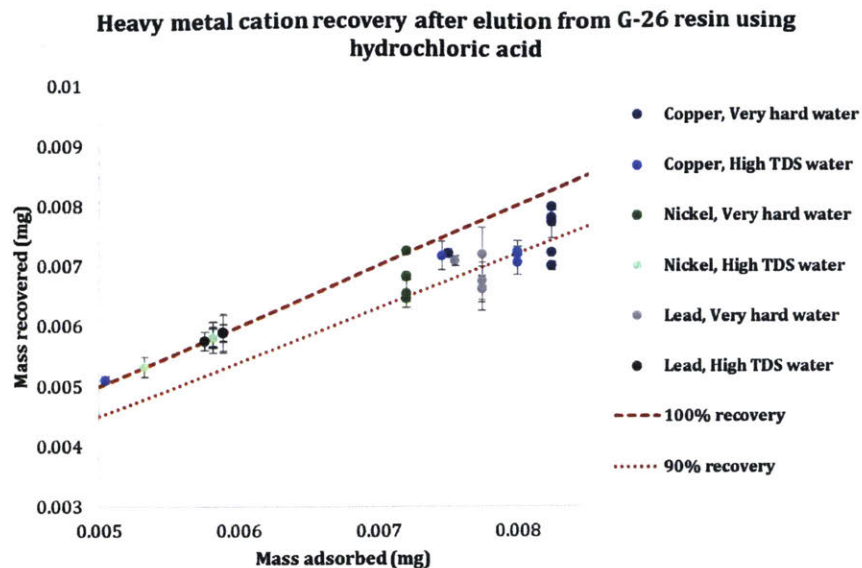


Figure 5-3: Heavy metal cation recovery from G-26 resin after up to 4 months of dry preservation. Error bars represent the standard error of three replicates. Most recovery values fall between 0.9 and 1.0.

and the error in measurement that could be expected, as well as the variation in recovery between samples.

Figure 5-3 shows recovery data ( $R_2$ ) from samples dryly preserved for up to 4 months, plotted as mass of cation recovered versus mass adsorbed to the resin. Table 5.3 expounds upon this data, showing the removal efficiency, recovery and the overall dry preservation efficiency for each cation after specific times of dry storage. Most recoveries fall in the range of 0.9-1, the threshold established earlier for the dry preservation device to yield quantitative results. Additionally, the matrix of the water sample does not seem to cause differences in recovery, as similar high recoveries were obtained for very hard water samples and high TDS samples. There is a slight trend towards less recovery as preservation time increases; further testing of samples preserved up to 9 months will show if this trend continues.

The cation that has the widest range in recovery and highest measurement error is lead. This could be for several reasons. For one, it is clear from kinetic data that lead is taken up faster than the other cations, suggesting that G-26 resin has a higher selectivity for lead than other cations; this is well established in ion exchange liter-



Table 5.3: Removal efficiency, recovery and overall preservation efficiency for initial preservation testing using G-26 resin for dry preservation periods up to 4 months. Intervals for  $R_2$  are standard errors of three replicates.

|                 | $R_1$ | $R_2$            | $R_{eff}$ |
|-----------------|-------|------------------|-----------|
| <b>1 month</b>  |       |                  |           |
| Copper          | 1     | $0.96 \pm 0.006$ | 0.96      |
| Nickel          | 1     | $1.0 \pm 0.008$  | 1         |
| Lead            | 1     | $0.94 \pm 0.018$ | 0.94      |
| <b>2 months</b> |       |                  |           |
| Copper          | 1     | $0.94 \pm 0.017$ | 0.94      |
| Nickel          | 1     | $0.95 \pm 0.001$ | 0.95      |
| Lead            | 1     | $0.85 \pm 0.047$ | 0.85      |
| <b>4 months</b> |       |                  |           |
| Copper          | 1     | $0.85 \pm 0.014$ | 0.85      |
| Nickel          | 1     | $0.91 \pm 0.003$ | 0.91      |
| Lead            | 1     | $0.87 \pm 0.040$ | 0.87      |

ature, and it is documented that strong cation exchange resins show higher affinity (and therefore, selectivity) for ions that are larger and carry more charge [67]. Therefore, it is possible that the concentration of hydrogen ions in 5% hydrochloric acid is not enough to displace lead from the resin and that a higher concentration is needed for better recovery.

Also, ICP-OES is not the most sensitive instrumentation for quantification of lead in solution and there is more measurement error in ICP-OES analysis for lead than for copper and nickel. This is demonstrated by the relatively low slope for lead in ICP-OES calibration curves. For more sensitive analysis of lead recovery, and for future experiments, ICP-MS could be used. An ICP-MS instrument is available at MIT. However, because ICP-MS is not universally available in water quality testing labs and has only recently been increasingly used in drinking water quality monitoring, it was decided that ICP-OES should be used for all initial analysis to be consistent in measurement method used.

### 5.3.3 Effect of hydrochloric acid concentration on cation recovery

To test if concentration of hydrochloric acid has an effect on the recovery, both 5% and 10% hydrochloric acid were used to extract cations from samples preserved for 4 months. A comparison of  $R_2$  for each cation when eluted with the different acid concentrations are shown in Table 5.4

For both copper and nickel, using 10% hydrochloric acid results in slightly more cation recovered, although the variance in the measurement is the same. This shows that the amount of hydrogen ions in 5% hydrochloric acid may limit the amount of recovery that can occur and saturating the system with hydrogen ions by doubling the concentration can help to be sure that the amount of hydrogen ion does not limit the recovery.

Table 5.4: Comparison of 5% and 10% hydrochloric acid in recovery of heavy metal cations from G-26 resin.

| Cation | $R_2$ , using 5% hydrochloric | $R_2$ , using 10% hydrochloric acid |
|--------|-------------------------------|-------------------------------------|
| Copper | $0.85 \pm 0.014$              | $0.87 \pm 0.014$                    |
| Nickel | $0.91 \pm 0.003$              | $0.95 \pm 0.007$                    |
| Lead   | $0.87 \pm 0.040$              | $0.85 \pm 0.029$                    |

For lead, 10% hydrochloric acid did not show as much of an improvement in the recovery or the variance of the recovery between dishes. This suggests that the resin selectivity and affinity for lead may be large enough to impede complete removal of the cation, so that some lead may always be left in the resin. If this amount is predictable and consistent between replicates and over different times of dry storage, then a correction factor could be introduced in calculating the original amount of lead in water sample (if the dry sampling device were to be used for quantitative measurements).

Based on these results, it is decided that the recovery protocol will now utilize 10% hydrochloric acid, for more reliable elution and more accurate quantification of certain metals.

## 5.4 Conclusion

Through recovery experiments using 5% hydrochloric acid regeneration of dry preservation sorbents, it was shown that high recovery of copper, nickel and lead, usually in the range of 0.9-1, is possible. This opens up the possibility of using the dry preservation device in quantitative evaluation of drinking water contamination. This recovery is, however, trending downward as the preservation time increases. Further experiments out to 9 months of preservation will help identify the maximum amount of time that the resin can be dryly stored before the recovery dips to an unacceptable amount.

Initial recovery experiments further helped rule out using Grade 6 filter paper as a material, due to appreciable endogenous copper contamination. From G-26 ion exchange resin, copper and nickel showed reliable recovery, while lead is the cation that shows the most variation in recovery. 10% hydrochloric acid yields slightly better recoveries, when compared with 5% hydrochloric acid; for all subsequent recovery tests, 10% hydrochloric acid will be used as the eluent.

To date, no analysis of the kinetics of acid regeneration have been performed, although they are likely similar to the time scales of uptake and the incubation time for cation elution could be decreased to under an hour. These kinetics need to be investigated through further experiments in order to optimize the recovery protocol for the most efficient dry sampling device use.



# Chapter 6

## Dry sampling device conceptualization and design

### 6.1 Introduction

The sorbents investigated in this thesis in their native forms are not in a format that is conducive to easy use. For example, ion exchange resins are small beads that become hard to contain when dry due to the static electrical forces that develop between them and cause them to scatter. It is necessary, then, to include the sorbent in a dry sampling device so that the sorbent can be easily applied to and removed from the water sample, as well as stored and transported easily and cleanly. Therefore, with a knowledge of the kinetics of uptake and outline of the preservation protocol, potential dry sampling devices incorporating G-26 ion exchange resin were ideated and prototyped. Initial testing of tea bag formats is presented here; however, this work is ongoing and optimization of device geometry and performance are the next major steps in the project.

### 6.2 Ideal device characteristics

Table 6.1 shows idea characteristics of the dry sampling device, with characteristics controlled by the design of the overall device bolded. Most importantly, the materials

Table 6.1: Ideal characteristics for dry preservation device. Characteristics specifically affected by the overall device geometry are bolded.

| Characteristic       | Ideal  |
|----------------------|--|
| Contaminant capacity | Adsorb 1-10mg of contaminant per gram of material<br>High fidelity/specificity for heavy metals over other ions<br>Consistent over relevant pH range (6.5-8) |
| Preservation process | Minimal addition of other reagents<br><b>Fast adsorption kinetics (&lt;30min)</b><br><b>Easy use and operation</b>   |
| Geometry             | <b>Compact; flat if possible</b><br><b>Total weight less than 10 grams</b>   |
| Availability         | <b>Commercially available components</b><br>or simple synthesis protocol<br><b>Low cost</b>  |

used in the device must be compatible with the entire dry preservation protocol. Where this is specifically important is in the recovery protocol, in which the device will be immersed in 5 to 10% hydrochloric acid. Therefore, usage of acid resistant materials is key in the success of a dry sampling device.

Materials used in the device should be cheap and easily sourced or lab synthesized. G-26 cation exchange resin itself is \$0.03 per gram when purchased in bulk and the materials for the dry sampling device should not bring the total cost of the device up to more than a few dollars. Additionally, if materials are easily available, manufacturing of the device could be localized and distributed, rather than all occurring at one manufacturing facility.

Using a mass of resin corresponding SF2, in very hard water, 6 grams of ion exchange resin would be required in a dry sampling device to sample from 1L of water. If the ideal device is no more than 10g total in weight, then the mass of the device materials should be also minimal in mass. Additionally, in order to facilitate allowing the device to be shippable, a compact device is desired; better yet would be if the device was relatively flat itself or could be folded into a slender shape.

Finally, to be able to incorporate different classes of sorbent for different classes of materials (heavy metals, organics, biologics, etc.), a device which could be configured to contain modules of different sorbents would be valuable. By connecting modules

into a single device, multiple types of contaminants could be preserved from a single sample of water in one step, allowing for comprehensive preservation and testing of micropollutants. Modules could then be disassembled and stored in or transported to different locations. While the current work only focuses on heavy metal cations, it is envisioned that sorbents for dry preservation of organics or biologics will be investigated in the future. It is therefore helpful to keep this modularity in mind when initially designing a dry sampling device.

### 6.3 Conceptualized ideas

Taking all of the aforementioned ideal characteristics into account, brainstorming yielded several different device conceptualizations which would fulfill the criteria outline above. A short description of the conceptualizations (some with figures) is provided below:

1. **Ion exchange resins in a tea bag** A tea bag is perhaps the simplest geometry for a dry sampling device (Figure 6-1a). A bag is fabricated from either a plastic mesh or fabric, with opening sizes smaller than the size of the resin, which is either in bead or crushed form. The bag is sealed using an acid resistant epoxy, sewn together using thread or melted together using a hot press. The tea bag can be inserted into the sampling container and stirred with the sample, either with the aid of a magnetic stir bar or through manual agitation.
2. **Resin coated or impregnated materials** Inspired by ion exchange resin paper, which was previously commercialized by Rohm and Haas and later GE Whatman [84], ion exchange resins could be crushed and incorporated into other support materials, such as paper or polymer membranes, as in heterogeneous cation exchange membranes (Figure 6-1b). Resin impregnated materials could be formed into different high surface area geometrical shapes, such as a flower or brush format. Crushed or bead resins could also be adhered to other porous materials and structures using a flexible acid resistant adhesive, which can with-

stand the stresses incurred when resins shrink during drying. Similar coating of structures with ion exchange resins has been performed to make air filters [85].

3. **Small packed bed resin cartridge** Similar to how ion exchange resins are typically used in water purification applications, resins could be packed in small modular cartridges, which could be connected together into a single packed bed to sample different classes of contaminants from the same water sample (Figure 6-1c). The packed bed cartridges would likely be operated in a flow through format.

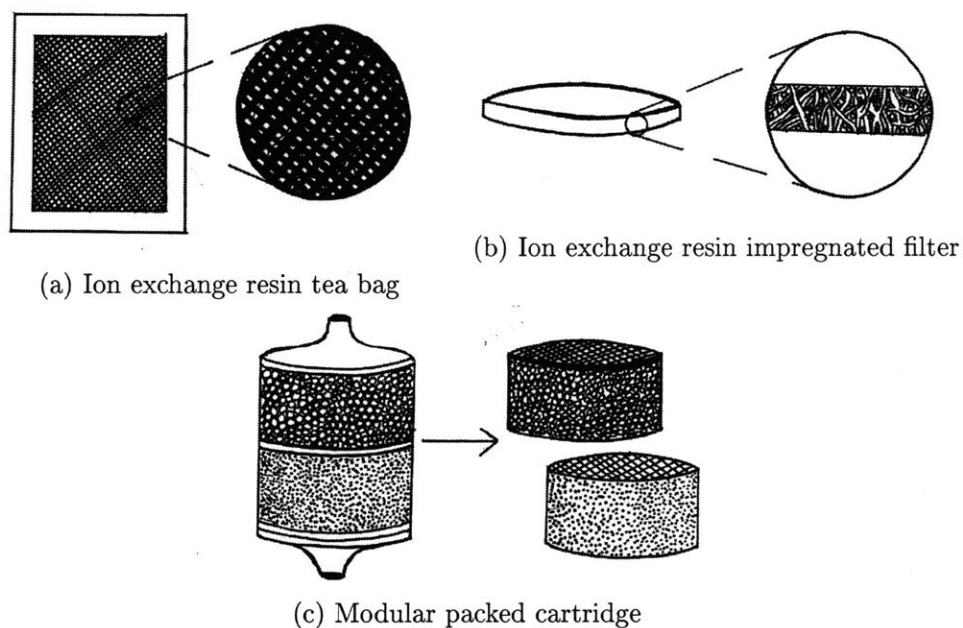


Figure 6-1: Sketches of potential dry sampling device geometries. Devices must somehow incorporate the dry sampling sorbent G-26 resin in such a way as to not provide a large resistance to mass transfer.

Several of these ideas were testing in initial prototyping, as described below, to test the feasibility and performance of each geometry.



## 6.4 Materials and methods

Polypropylene and nylon meshes, nylon thread and cotton fabric was purchased from McMaster Carr. 3M ScotchWeld epoxy adhesives 100 and 105 and Liquid Nails silicone adhesive were purchased from Amazon, Inc. Devcon 5 minute epoxy was purchased from VWR.

### 6.4.1 Fabrication of resin coated fabrics, meshes and strings

G-26 cation exchange resin was crushed and sieved in the wet state to a particle size of 300 to 400 $\mu\text{m}$ . Crushed resin and bead resin were then dried overnight in an oven at 50°C.

Materials to be coated were cut from the bulk purchased materials to the following sizes (dimensions in inches (in)):

- Cotton woven fabric, 0.026in thick: 2.5in by 1in rectangle; 6 rectangular strips 2.5in by  $\frac{1}{4}$ in each
- Nylon thread, 0.032in diameter: 2.5in
- Whatman Grade 1 cellulose filter paper, 180 $\mu\text{m}$  thick: 2.5in by 1in rectangle

Each material was manually coated with a thin layer of adhesive using a disposable tongue depressor. Crushed resins or bead resins were shaken in a petri dish with the adhesive coated material to coat the material with the resin. Adhesives used for coating the materials were:

- Devcon 5 minute epoxy
- 3M ScotchWeld DP105 flexible epoxy adhesive
- Liquid Nails silicon adhesive

After drying overnight, resin coated materials were soaked in ultrapure water for 6 hours to allow resins to swell. The amount of resin that came off of the material was noted.

### 6.4.2 Thermal testing of G-26 resin

A 1 gram sample of G-26 ion exchange resin in the wet state was placed in a 30mL glass scintillation vial and heated on a hot plate at 100°C. Every 20 minutes, the temperature of the hot plate was increased by 10°C and the resin was inspected for phase change by visual inspection and pressure testing. This testing was performed up until 260°C, the maximum temperature the hot plate can sustain.

### 6.4.3 Fabrication of ion exchange resin tea bags and tea bag testing in very hard water

Nylon mesh and polypropylene mesh were cut into various shapes for tea bags. Dimensions of tea bags are shown in Table 6.2. In the case of the polypropylene meshes, the bags had an extra two inches of mesh at the top to aid in holding the bags steady in the sample while stirring.

Table 6.2: Tea bag dimensions.

| Shape          | Dimensions (in) |
|----------------|-----------------|
| Rectangle      | 2.5 x 1.75      |
| Long rectangle | 3 x 1.25        |
| Circle         | 2 (diameter)    |

Three sides of the bag were sealed using either Devcon 5 minute epoxy (nylon bags) or ScotchWeld DP105 (polypropylene bags). After the adhesive dried overnight, G-26 resin at SF2 mass for very hard water, weighed out in wet form, was deposited into each of the tea bags. The final edge of each bag was then sealed with the respective epoxy and the resin tea bag was hung to dry overnight.

To test tea bag performance in adsorbing heavy metal cations of interest, kinetic experiments were performed using the tea bags in a 250mL sample of very hard water (composition the same as described in Section 3.3.3). Nylon tea bags were immersed in the solution and allowed to freely move as the solution was stirred, whereas polypropylene tea bags were held stationary in the solution through use of the extra mesh extending from the tea bag (Figure 6-2). In all experiments, a 1.5in

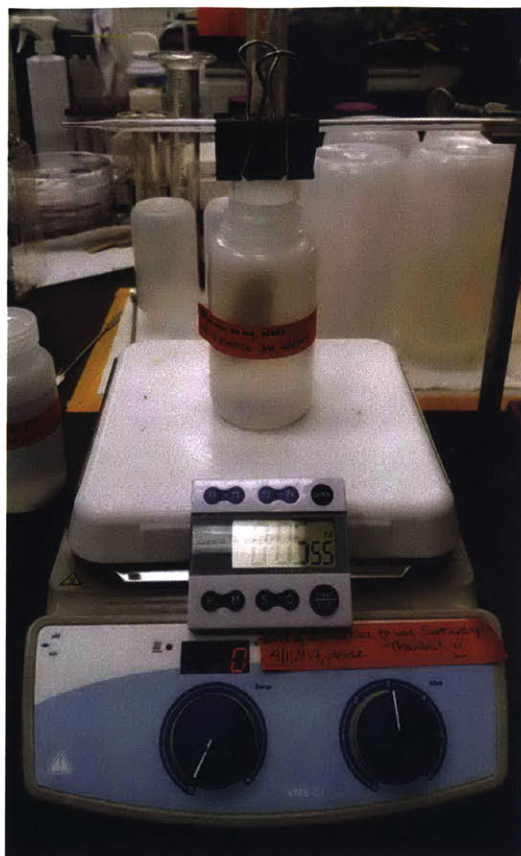


Figure 6-2: Polypropylene tea bag testing setup. Using a binder clip and serological pipette, tea bags were held stationary by the excess material.

magnetic stir bar and 250mL low density polyethylene bottle was used and the stir speed was set at 3, as in other kinetic experiments.

Over the course of each experiment, eleven 2mL solution samples were taking and preserved in a 2% (v/v) TraceMetal Grade nitric acid solution. Samples from all experiments were analyzed using ICP-OES and calibrated each time using suitable standards, as outlined in Section 3.3.2.

## 6.5 Results

### 6.5.1 Swelling and stability of resin coated materials

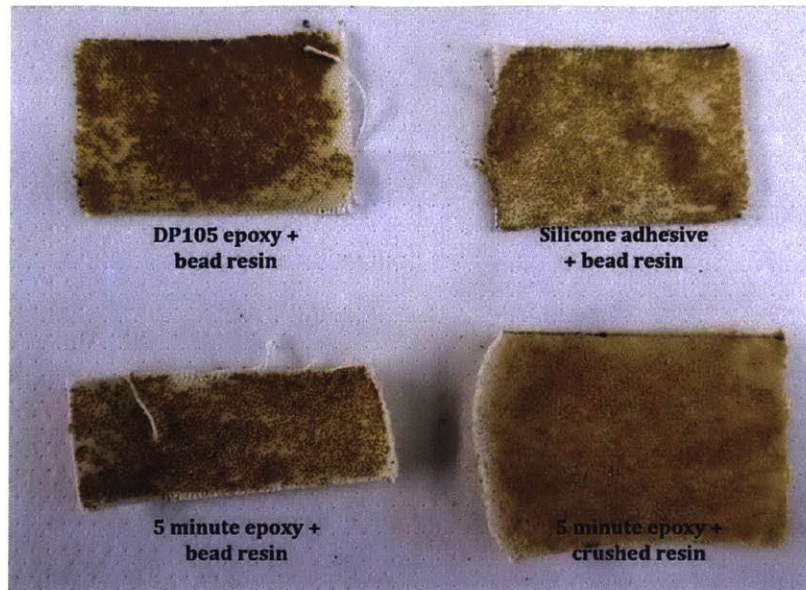
Due to the ion exchange resin swelling during immersion in water and shrinking during drying out, any coated material must be able to accommodate the stresses

that occur during this shrinking and swelling process, so as to keep the resin bound to the surface. This is particularly impacts the choice of adhesive, which must be flexible in the cured state. Furthermore, coating of the material should occur when resins are in the dried state and at their smallest. If resins were coated while in the wet state, adhesion sites would accommodate the larger size of the resin. Upon drying of the resin, the adhesive may not shrink with the resin and the dried resin particle may pop out of the binding site.

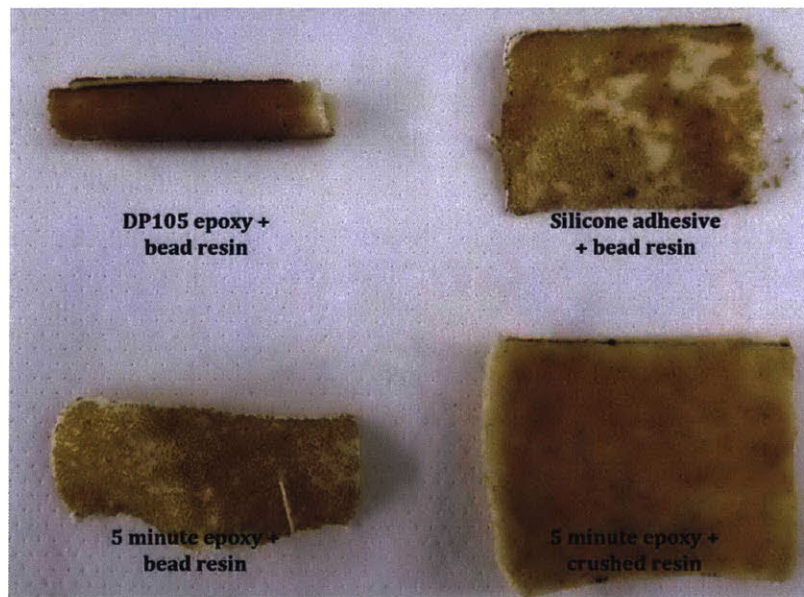
These hypothesis were confirmed through testing of the performance of resin coated materials in a swell/shrink cycle. Figure 6-3 shows coated fabrics in their dried/shrunk state and wet/swelled state. A number of notable observations come from this brief experiment. First, despite being coated with adhesive, most adhesives still permit the resins to swell when immersed in water. The only coated materials that did not swell were those in which silicone adhesive was used. In addition to being flexible, silicone adhesives are notable for being waterproof and are often used in applications where adhesives should also serve as sealants. In the case of a dry sampling material, this makes silicone adhesives a poor choice, since resins must swell in order for water carrying cations to penetrate the resins.

As predicted, hard cure epoxies lost more beads during swelling than flexible epoxies. After swelling, resin beads could be easily rubbed off of the materials which used the hard cured epoxy as an adhesive. On the other hand, materials coated with flexible epoxies did not lose nearly as many beads, suggesting that the flexibility of the epoxy is able to accommodate the size change in resin as it swells and shrinks.

On the basis of these experiments, coating materials with cation exchange resin using flexible epoxy is the most promising method of obtaining resin coated materials. However, the process of making these materials needs to be optimized. For example, shaking the adhesive coated materials with the dried resins to coat the materials is inefficient and leads to uneven coating of the resin on the material. It was observed that the majority of the beads that came off of the materials with flexible epoxy came from sites in which beads were clumped or did not make full contact with the coated adhesive surface. A method in which the resins are uniformly sprinkled on the



(a) Resin coated fabrics in dry form



(b) Resin coated fabrics in after soaking in water

Figure 6-3: Resin coated fabrics in dry and wet swelled form. Resin bead and particles come off of fabric when 5 minute epoxy is the adhesive; beads adhered with silicone adhesive do not seem to swell. Using flexible epoxy keeps the majority of the beads secured in a shrink/swell cycle.



adhesive coated surface would need to be investigated to ensure minimal resin slough off.

### 6.5.2 Thermal formability of native G-26 ion exchange resin

Figure 6-4 shows a sample of G-26 resin in its native amber transparent wet bead form and a sample of the same resin after incremental heating to 260°C. Despite an increased tendency for the resin beads to form small clumped clusters after heating, the resin did not become moldable during the entire heating process. Additionally, the resin turned into hard black spheres, signifying a chemical change that may have negatively impacted the exchange ability of the resin.

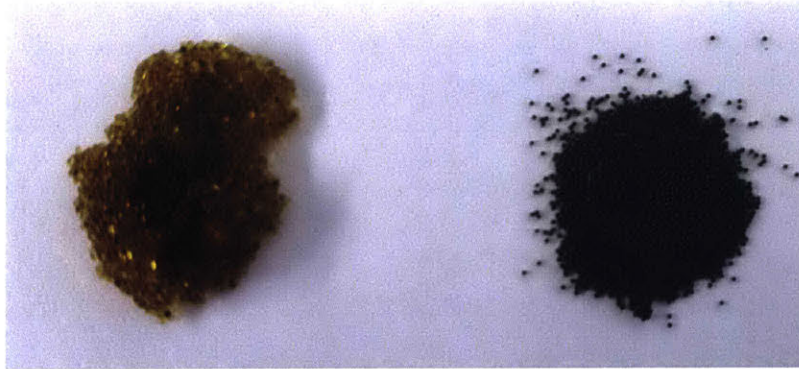


Figure 6-4: Comparison of G-26 resin in native form and after incremental heating to 260°C. Resin turns black after heating, indicating a possible chemical of resin structure.

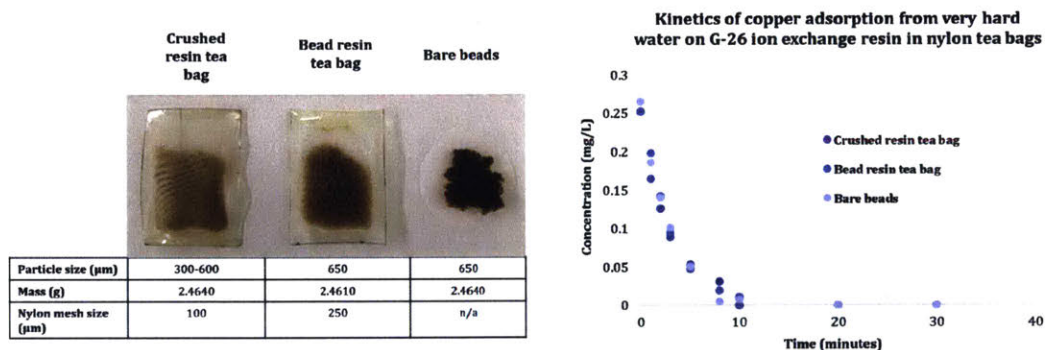
This shows that G-26 resin in its commercial form cannot likely be thermoformed into another flat shape or monolith to incorporate into a dry sampling device. This was expected; although the resin is made from an easily formed thermoplastic, polystyrene (glass transition temperature near 100°C [86], depending on molecular weight), the crosslinking reaction with divinylbenzene converts the polystyrene to a very stable solid material, unresponsive to thermal or chemical modifications. This crosslinking allows ion exchange resins to operate in fluid samples with temperatures approaching degrees of 500°C [54].

Therefore, in order for native G-26 resin to be formed into a different shape for a dry sampling device, the G-26 resin would need to be combined with another polymer

binder, which can be molded through thermal or chemical processes.

### 6.5.3 Initial tea bag testing

Although nylon is not compatible with hydrochloric acid treatment as used in the cation recovery protocol, nylon tea bags were fabricated and tested first to observe the tea bag structure's effect on uptake kinetics. Kinetics using tea bag enclosed whole bead and crushed resin in comparison with free bead resin is shown in Figure 6-5. It can be seen that enclosing the resin in a plastic mesh does not significantly affect the rate of uptake on the resin, showing that the resistance to mass transfer to the bead posed by the plastic mesh is likely negligible. However, these results also show that the kinetic benefit in using smaller resin particles does not occur when these particles are enclosed in a plastic mesh. All three tea bags performed similarly.



(a) Fabricated nylon tea bags and G-26 bare beads

(b) Copper uptake kinetics using nylon tea bags

Figure 6-5: Fabricated nylon tea bags and their kinetic performance. All three formats achieved total copper uptake in a similar amount of time, although the kinetic advantage in using crushed resin seen in previous kinetic testing, is not apparent in this experiment.

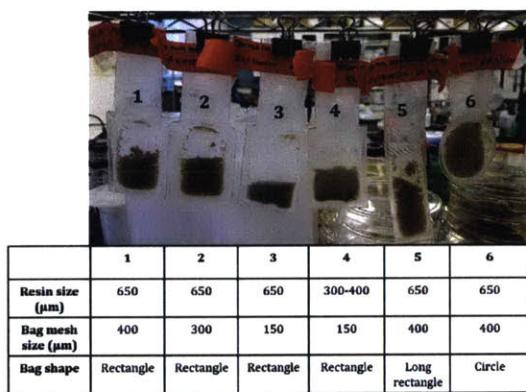
To further observe the effect of resin particle size and tea bag mesh on kinetic performance, polypropylene bags were fabricated using different opening size meshes. These bags were held stationary in the solution (instead of freely moving as the solution stirred, as with the nylon bags), so that the relative velocity of the beads compared to that of the solution was minimized. This, in theory, permits better mass



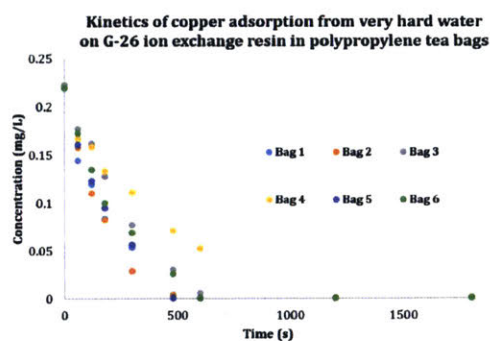
transfer to the beads, by reducing the size of the stagnant liquid film surrounding the beads.

In agreement with the results from the nylon tea bag test, enclosing the resin in polypropylene mesh did not seem to negatively impact the kinetics of uptake (Figure 6-6). Further, the size of the polypropylene mesh opening also does not significantly affect the uptake rate, with 400, 300 and 150  $\mu\text{m}$  mesh tea bags with bead resin adsorbing all of the copper from solution within 10 minutes. The rectangle bag made with 300  $\mu\text{m}$  mesh (Bag 2) and the long rectangle mesh bag (Bag 5) slightly outperform the other bead resin bags. The long rectangle bag may be more efficient at keeping the resins in place and presenting more resin surface area for mass transfer.

Most apparent in these tests, and consistent to what was observed when using nylon tea bags, is that crushed resins in the tea bag formats tested take up heavy metal cations slower than whole bead resins in tea bags. This shows that cation adsorption in a tea bag format is a mass transport (film diffusion) limited process. The smaller resin particles are able to pack together with less space between them, thus providing less void area for fluid to flow through and limiting mass transfer to the surface of the particles.



(a) Fabricated polypropylene tea bags



(b) Copper uptake kinetics using polypropylene tea bags

Figure 6-6: Fabricated polypropylene tea bags and their kinetic performance. All three formats achieved total copper uptake in a similar amount of time, although the kinetic advantage in using crushed resin seen in previous kinetic testing, is also not apparent in this experiment.

Optimized tea bag shapes and fabrication methods will help to limit resistance to



mass transport. The bags tested in this short study permitted the resin to settle at the bottom of the bag. A better constructed bag, perhaps with small compartments or modules, could hold resins in place in a single layer. This would greatly increase the free surface area exposed for mass transport. If crushed resins were placed in such a format so that the space between the particles was maximized, it is likely that the kinetic advantage that was seen in using freely moving crushed particles could be realized in the tea bag format.

## 6.6 Conclusion

Incorporating the dry sampling sorbent in a device format that is easy to use, compact and preserves rapid kinetics is key in realizing the dry sampling paradigm for water quality monitoring. From the short investigation presented in this section, a tea bag seems to be the most straightforward format in which to incorporate cation exchange resins for a dry sampling device. The resins in their native form are crosslinked and chemically/thermally inert, preventing the resins from being molded into a structure themselves without another polymeric filler or binder. While resin coated materials are promising device formats, major optimization of the fabrication protocol is needed to make sure the necessary amount of resin adheres sufficiently to the surface. Overall, this section presented the initial steps in device fabrication and testing; ongoing work over the next year will seek to optimize the tea bag format for the lowest pressure drop across the bag with the highest mass transfer coefficient, as well as continue testing of different resin coated materials.



# Chapter 7

## Conclusion

### 7.1 Summary of thesis

Rural and resource limited settings, in India and elsewhere around the world, suffer from limited access to improved drinking water sources. Furthermore, testing for contaminants from already existing sources is hampered by the lack of testing ability at local labs, necessitating preservation of water samples at the source and long distance transport to centralized labs. This high labor and time process limits water quality monitoring in such settings.

The goal of this thesis was to explore and develop a dry sampling technology that would allow contaminants of interest in a water sample to be preserved in a dry compact format, suitable for storage, manual transport or shipping to a centralized laboratory. It is hypothesized that such a sorbent, incorporated into an easy to use device, would greatly expand the ease and reach of water quality monitoring.

- An overview of water quality monitoring systems, testing methods and preservation protocols were described in **Chapter One**. Through understanding and identifying gaps in water quality monitoring protocols, especially for rural and resource limited settings, dry sampling of drinking water samples was identified as a potential solution to enable centralized water quality monitoring of the hardest to reach source, much like dried blood spotting revolutionized clinical

trials for rural areas.

- In **Chapter Two**, an overview of the existing water quality monitoring infrastructure in India, as understood from travels and meetings with stakeholders, was presented. Through this exploration, it became clear that the framework for easy-to-test parameters, such as hardness and total dissolved solids, is intact and functioning closely to the prescribed structure in the Uniform National Drinking Water Quality Monitoring Protocol. However, there a lack of testing for micropollutants, such as heavy metals, organics or biological pollutants, due to the high capital instrumentation needed to test these pollutants, which restricts their location to centralized state labs. While there is a framework for testing these contaminants included in the UDWQMP, a disconnect between labs at the district level and at the state level exists such that, despite the concern for these harmful pollutants, they are not tested. Therefore, the scope of the dry sampling technology was refined to preservation of micropollutants, specifically heavy metals.
- In **Chapter Three**, different materials were evaluated in their potential to be dry sampling sorbents. Ideal characteristics for a dry sampling sorbent include high contaminant capacity, low cost and wide availability of materials. From literature review, cellulose, modified cellulose and ion exchange polymers were identified as potential sorbents for heavy metal cations. While promising in initial tests, cellulose did not possess enough capacity to make a low weight dry sampling device and cellulose's performance as a sorbent was sensitive to pH changes. Citric acid modified cellulose showed very high initial capacities, but the chemistry of citric acid modification was not repeatable. Cation exchange resins were shown to have large capacity for divalent cations of interest and perform well over a wide range of water hardness levels. Therefore, the cation exchange resin that performed the best, DOWEX G-26, was selected for further testing as a heavy metal sorbent.
- Kinetics of heavy metal uptake were the subject of **Chapter Four**, in which

the limiting diffusional mechanism in heavy metal uptake using G-26 ion exchange resin was characterized. In performing multiple experiments to try to elucidate if film diffusion or particle diffusion limits the rate of adsorption, experiments provided evidence that both phenomena likely contribute to the rate of uptake. Experiments examining the effect of resin mass, particle size and water matrix components showed that increasing the mass of resin or decreasing the resin particle size both increase the rate of cation uptake from solution. All divalent cations in solution, including the two major divalent components of water, calcium and magnesium, have similar concentration decay constants during adsorption and the water hardness largely influences the rate of heavy metal uptake. Because of this, a combined calcium and magnesium diffusivity was estimated using Fick's law models. The intraparticle diffusivity was found to be on the order of  $10^{-11}\text{m}^2/\text{s}$ . Additionally, the Nernst film thickness was estimated by approximating the film diffusivity by the free solution diffusivity. This analysis yielded film thicknesses on the order of  $10^{-6}\text{m}$ , which is an order of magnitude less than what is reported in literature. In future calculations for mass transport in the device, this will need to be taken into account.

- **Chapter Five** presented experimental evidence of the efficacy of using G-26 cation exchange resin as a dry sampling sorbent due to the high recovery of metals adsorbed after elution using hydrochloric acid. Greater than 80% of copper, lead and nickel can be recovered after adsorption to G-26 cation exchange resin and dry storage at room temperature for up to 4 months. Using 10% (v/v) hydrochloric acid instead of 5% (v/v) hydrochloric acid results in slightly greater recovery of cations. Of the three cations, lead has the lowest recovery overall; this is likely due to the high selectivity of cation exchange resins for lead. Repeatable high recoveries from cation exchange resins open the door for quantitative analysis of contaminants after dry preservation, instead of a presence/absence qualitative assessment.
- Conceptualization and initial prototyping of a dry sampling device is discussed

in **Chapter Six**. Several different geometries of dry sampling device, including a tea bag, resin coated surfaces and packed modular columns, were identified for their potential agreement with ideal device characteristics. For resin coated surfaces, the adhesive and material used is key, as they need to be able to accommodate that stresses that come from the shrinking and swelling of the resin when it is dried and rehydrated. Tea bags were identified as the most straightforward device geometry and shown to be a mass transport limiting format, necessitating the future optimization of the tea bag geometry to have the lowest pressure drop with the highest mass transfer coefficient.

## 7.2 Future work

This thesis represents significant progress in the development of a dry sampling device for heavy metal cations, but there is still significant work to be performed in order to field test the technology and, hopefully, commercialize it. These experiments include:

- Additional kinetic testing in other water matrices, including those with organic and buffering content
- A short optimization of tea bag geometry, using packed bed models and mass transfer correlations, to determine the best geometry for the lowest pressure drop across the tea bags that results in the highest mass transfer coefficient
- Fabrication technique identification for resin coated materials; capacity and kinetic testing of these materials and comparison with tea bags
- Longer term recovery testing, examining the recovery from G-26 resin after a year of dry storage; establishment of a recovery protocol after kinetic recovery testing
- Extensive testing of optimized teabag format to check repeatability and reliability in uptake time and recovery, both using synthetic water samples and real water samples; comparison with the current preservation and testing methods

- Collaboration with stakeholders in India (and potentially elsewhere) to get their feedback on device usability, geometry and usage; continued prototyping based on their needs





# Bibliography

- [1] World Health Organization. Guidelines for Drinking Water Quality, Fourth Edition. 2011.
- [2] United Nations. The Millennium Development Goals Report. pages 1—72, 2015.
- [3] UNICEF; WHO. Progress on Drinking Water and Sanitation, 2012 Update. Technical report, 2012.
- [4] WWAP. The United Nations World Water Development Report 2016: Water and jobs. Technical report, 2016.
- [5] Food and Agricultural Organization of the United Nations. How to Feed the World 2050. pages 1–4, 2009.
- [6] Center for Affordable Water and Sanitation Technology. 2013 Annual Report. Technical report, 2013.
- [7] Robert Bain, Jamie Bartram, Mark Elliott, Robert Matthews, Lanakila McMahan, Rosalind Tung, Patty Chuang, and Stephen Gundry. A summary catalogue of microbial drinking water tests for low and medium resource settings. *International Journal of Environmental Research and Public Health*, 9(5):1609–1625, 2012.
- [8] Patty Chuang, Stephanie Trottier, and Susan Murcott. Comparison and verification of four field-based microbiological tests: H<sub>2</sub>S test, Easygel<sup>®</sup>, Colilert<sup>®</sup>, Petrifilm<sup>™</sup>. *Journal of Water Sanitation and Hygiene for Development*, (1):68–85.
- [9] Water Testing Laboratories, Public Health Engineering Department, Government of West Bengal. <http://www.wbphed.gov.in/main/index.php/water-testing-laboratories>. Accessed: 2015-09-30.
- [10] Johnny Crocker and Jamie Bartram. Comparison and cost analysis of drinking water quality monitoring requirements versus practice in seven developing countries. *International Journal of Environmental Research and Public Health*, 11(7):7333–7346, 2014.

- [11] Robert Guthrie and Ada Susi. A simple phenylalanine method for detecting phenylketonuria in large populations of newborn infants. *Pediatrics*, 32(3):338–343, 1963.
- [12] S Chaorattanakawee, O Natalang, H Hananantachai, M Nacher, a Brockman, S Krudsood, S Looareesuwan, and J Patarapotikul. Storage duration and polymerase chain reaction detection of *Plasmodium falciparum* from blood spots on filter paper. *American Journal of Tropical Medicine and Hygiene*, 69(1):42–44, 2003.
- [13] V. Michaud, P. Gil, O. Kwiatek, S. Prome, L. Dixon, L. Romero, M. F. Le Potier, M. Arias, E. Couacy-Hymann, F. Roger, G. Libeau, and E. Albina. Long-term storage at tropical temperature of dried-blood filter papers for detection and genotyping of RNA and DNA viruses by direct PCR. *Journal of Virological Methods*, 146(1-2):257–265, 2007.
- [14] Ujjwal Neogi, Soham Gupta, Rashmi Rodridges, Pravat Nalini Sahoo, Shwetha D. Rao, Bharat B. Rewari, Suresh Shastri, Ayesha De Costa, and Anita Shet. Dried blood spot hiv-1 rna quantification: A useful tool for viral load monitoring among infected hiv-infected individuals in india. *Indian Journal of Medical Research*, 136(6):956–962, 2012.
- [15] Abishek Sharma, Swati Jaiswal, Mahendra Shukla, and Jawahar Lal. Dried blood spots: Concepts, present status, and future perspectives in bioanalysis. *Drug Testing and Analysis*, 6(5):399–414, 2014.
- [16] P N Nyambi, K Fransen, H De Beenhouwer, E N Chomba, M Temmerman, J O Ndinya-Achola, P Piot, and G van der Groen. Detection of human immunodeficiency virus type 1 (HIV-1) in heel prick blood on filter paper from children born to HIV-1-seropositive mothers. *Journal of clinical microbiology*, 32(11):2858–2860, 1994.
- [17] M. Burger, S. Raskin, S. R. Brockelt, B. Amthor, H. K. Geiss, and W. H. Haas. DNA fingerprinting of *Mycobacterium tuberculosis* complex culture isolates collected in Brazil and spotted onto filter paper. *Journal of Clinical Microbiology*, 36(2):573–576, 1998.
- [18] Véronique Vacchina, Vincent Huin, Sébastien Hulo, Damien Cuny, Franck Broly, Gilles Renom, and Jean-Marc Perini. Use of dried blood spots and inductively coupled plasma mass spectrometry for multi-element determination in blood. *Journal of Trace Elements in Medicine and Biology*, 28(3):255–259, 2014.
- [19] UNEP/WHO. *Water Quality Monitoring - A Practical Guide to the Design and Implementation of Freshwater Quality Studies and Monitoring Programmes*, volume 2. 1996.

- [20] Leslie A DeSimone, Pixie A Hamilton, and Robert J Gilliom. Quality of water from domestic wells in principal aquifers of the United States, 1991—2004: Overview of major findings. Technical report, 2009.
- [21] Patricia L Toccalino, Julia E Norman, and Kerie J Hitt. Quality of Source Water from Public-Supply Wells in the United States , 1993—2007: Scientific Investigations Report 2010. Technical report, 2010.
- [22] Pallav Sengupta. Potential health impacts of hard water. *International Journal of Preventive Medicine*, 4(8):866–875, 2013.
- [23] Centers for Disease Control and Prevention. Achievements in Public Health, 1900-1999 : Fluoridation of Drinking Water to Prevent Dental. *Journal of the American Medical Association*, 283(10):1283–1286, 2000.
- [24] United States Department of Health and Human Services Federal Panel on Community Drinking Water Fluoridation. U.S. Public Health Service Recommendation for Fluoride Concentration in Drinking Water for the Prevention of Dental Caries. *Public Health Reports*, 130(4):318–31, 2015.
- [25] S Ayoob and A K Gupta. Fluoride in Drinking Water : A Review on the Status and Stress Effects. *Critical Reviews in Environmental Science and Technology*, 36(6):433–487, 2006.
- [26] World Health Organization. Fluoride in Drinking-water: Background document for development of WHO Guidelines for Drinking-water Quality. Technical report, 2004.
- [27] Lorna Fewtrell. Drinking-water nitrate, methemoglobinemia, and global burden of disease: A discussion. *Environmental Health Perspectives*, 112(14):1371–1374, 2004.
- [28] Paul B Tchounwou, Clement G Yedjou, Anita K Patlolla, and Dwayne J Sutton. Heavy Metals Toxicity and the Environment. *EXS*, 101(June):133–164, 2012.
- [29] Bureau of Indian Standards. Drinking Water - Specification IS 10500:2012. Technical report, 2012.
- [30] Robert Bain, Ryan Cronk, Jim Wright, Hong Yang, Tom Slaymaker, and Jamie Bartram. Fecal contamination of drinking-water in low- and middle-income countries: a systematic review and meta-analysis. *PLoS Medicine*, 11(5):e1001644, 2014.
- [31] Li Liu, Hope L. Johnson, Simon Cousens, Jamie Perin, Susana Scott, Joy E. Lawn, Igor Rudan, Harry Campbell, Richard Cibulskis, Mengying Li, Colin Mathers, and Robert E. Black. Global, regional, and national causes of child mortality: An updated systematic analysis for 2010 with time trends since 2000. *The Lancet*, 379(9832):2151–2161, 2012.

- [32] United States Environmental Protection Agency. Handbook for sampling and sample preservation of water and wastewater. Technical report, 1982.
- [33] David Duncan, Fiona Harvey, Michelle Walker, and Australian Water Quality Center. *EPA Guidelines: Regulatory monitoring and testing, Water and wastewater sampling*, volume 3. 2007.
- [34] Hans Hermann Rump. *Laboratory Manual for the Examination of Water, Waste Water and Soil, 3rd Edition*. Wiley, 2000.
- [35] G. E. Batley and D. Gardner. Sampling and storage of natural waters for trace metal analysis. *Water Research*, 11(9):745–756, 1977.
- [36] J. R. Garbarino and H. E. Taylor. Inductive-Coupled Plasma Atomic-Emission Spectrometric Method for Routine Water Quality Testing. *Appl Spectrosc*, 33(3):220–226, 1979.
- [37] John R. Garbarino and Tedmund M. Struzeski. Methods of Analysis by the USGS National Water Quality Laboratory– Determination of Elements in Whole-Water Digests Using Inductively Coupled Plasma-Optical Emission Spectrometry and Inductively Coupled Plasma-Mass Spectrometry. Technical report, 1998.
- [38] Roland De Marco, Graeme Clarke, and Bobby Pejic. Ion-selective electrode potentiometry in environmental analysis. *Electroanalysis*, 19(19-20):1987–2001.
- [39] PerkinElmer. Atomic spectroscopy: a guide to selecting the appropriate technique and system. Technical report, 2008.
- [40] Government of India and Ministry of Drinking Water and Sanitation. National Rural Drinking Water Programme: Movements towards ensuring people’s Drinking Water Security in Rural India. page 126, 2013.
- [41] Website of the National Rural Drinking Water Program, Ministry of Drinking Water and Sanitation, Government of India. <http://indiawater.gov.in/IMISReports/>. Accessed: 2015-09-30.
- [42] Government of India and Ministry of Drinking Water and Sanitation. Uniform Drinking Water Quality Monitoring Protocol. Technical report, 2013.
- [43] Sanna Hokkanen, Amit Bhatnagar, and Mika Sillanpaa. A review on modification methods to cellulose-based adsorbents to improve adsorption capacity. *Water Research*, 91:156–173, 2016.
- [44] David William O’Connell, Colin Birkinshaw, and Thomas Francis O’Dwyer. Heavy metal adsorbents prepared from the modification of cellulose: A review. *Bioresource Technology*, 99(15):6709–6724, 2008.
- [45] Samuel D. Faust and Osman M. Aly. *Adsorption Processes for Water Treatment*. Butterworth, 1987.

- [46] K.Y. Foo and B.H. Hameed. Insights into the modeling of adsorption isotherm systems. *Chemical Engineering Journal*, 156(1):2–10, 2010.
- [47] Ayhan Demirbas. Heavy metal adsorption onto agro-based waste materials: A review. *Journal of Hazardous Materials*, 157(2-3):220–229, 2008.
- [48] Filiz Nuran Acar and Zeynep Eren. Removal of Cu(II) ions by activated poplar sawdust (Samsun Clone) from aqueous solutions. *Journal of Hazardous Materials*, 137(2):909–914, 2006.
- [49] K. S. Low, C. K. Lee, and S. M. Mak. Sorption of copper and lead by citric acid modified wood. *Wood Science and Technology*, 38(8):629–640, 2004.
- [50] S. Pitsari, E. Tsoufakis, and M. Loizidou. Enhanced lead adsorption by unbleached newspaper pulp modified with citric acid. *Chemical Engineering Journal*, 223:18–30, 2013.
- [51] Dowex Ion Exchange Resins: Fundamentals of Ion Exchange. Technical report, 2000.
- [52] Vassilis Inglezakis and Stavros Pouloupoulos. *Adsorption, Ion Exchange and Catalysis, First Edition*. Elsevier Science, 2006.
- [53] Erol Pehlivan and Turkan Altun. The study of various parameters affecting the ion exchange of  $\text{Cu}^{2+}$ ,  $\text{Zn}^{2+}$ ,  $\text{Ni}^{2+}$ ,  $\text{Cd}^{2+}$ , and  $\text{Pb}^{2+}$  from aqueous solution on Dowex 50W synthetic resin. *Journal of Hazardous Materials*, 134(1-3):149–156, 2006.
- [54] Dow Chemical Company. DOWEX G-26 (H) Product Information. Technical report.
- [55] Dow Chemical Company. DOWEX Marathon C Resin. Technical report.
- [56] Dow Chemical Company. DOWEX MAC-3 Resin. Technical report.
- [57] Carlos M. H. Ferreira, Isabel S. S. Pinto, Eduardo V. Soares, and Helena M. V. M. Soares. (Un)suitability of the use of pH buffers in biological, biochemical and environmental studies and their interaction with metal ions — a review. *RSC Adv.*, 5(39):30989–31003, 2015.
- [58] Sanna Hokkanen, Eveliina Repo, Terhi Suopajarvi, Henriikki Liimatainen, Jouko Niinimaa, and Mika Sillanpaa. Adsorption of Ni(II), Cu(II) and Cd(II) from aqueous solutions by amino modified nanostructured microfibrillated cellulose. *Cellulose*, 21(3):1471–1487, 2014.
- [59] Upendra Kumar and Manas Bandyopadhyay. Sorption of cadmium from aqueous solution using pretreated rice husk. *Bioresource Technology*, 97(1):104–109, 2006.

- [60] Pavel Janoš, Sezen Coskun, Věra Pilařová, and Jaroslav Rejnek. Removal of basic (Methylene Blue) and acid (Egacid Orange) dyes from waters by sorption on chemically treated wood shavings. *Bioresource Technology*, 100(3):1450–1453, 2009.
- [61] Marina Šćiban, Mile Klačnja, and Biljana Škrbić. Modified softwood sawdust as adsorbent of heavy metal ions from water. *Journal of Hazardous Materials*, 136(2):266–271, 2006.
- [62] Daisy Setyono and Suresh Valiyaveetil. Functionalized paper-A readily accessible adsorbent for removal of dissolved heavy metal salts and nanoparticles from water. *Journal of Hazardous Materials*, 302:120–128, 2016.
- [63] Woo Shin Eun and Roger M. Rowell. Cadmium ion sorption onto lignocellulosic biosorbent modified by sulfonation: The origin of sorption capacity improvement. *Chemosphere*, 60(8):1054–1061, 2005.
- [64] Sang Youn Oh, Il Yoo Dong, Younsook Shin, Chul Kim Hwan, Yong Kim Hak, Sik Chung Yong, Ho Park Won, and Ho Youk Ji. Crystalline structure analysis of cellulose treated with sodium hydroxide and carbon dioxide by means of X-ray diffraction and FTIR spectroscopy. *Carbohydrate Research*, 340(15):2376–2391, 2005.
- [65] Saima Q. Memon, Najma Memon, S. W. Shah, M. Y. Khuhawar, and M. I. Bhangar. Sawdust-A green and economical sorbent for the removal of cadmium (II) ions. *Journal of Hazardous Materials*, 139(1):116–121, 2007.
- [66] Lihua Chen, Anas Ramadan, Lili Lu, Wenjing Shao, Fang Luo, and Ji Chen. Biosorption of methylene blue from aqueous solution using lawn grass modified with citric acid. *Journal of Chemical and Engineering Data*, 56(8):3392–3399, 2011.
- [67] Spiro D. Alexandratos. Ion-Exchange Resins: A Retrospective from Industrial and Engineering Chemistry Research. *Industrial & Engineering Chemistry Research*, 48(1):388–398, 2009.
- [68] Andrei Zagorodni. *Ion Exchange Materials: Properties and Applications*. Elsevier Science, 2006.
- [69] Friedrich Helfferich. *Ion Exchange*. McGraw-Hill, 1962.
- [70] Vassilis J. Inglezakis and Helen P. Grigoropoulou. Applicability of Simplified Models for the Estimation of Ion Exchange Diffusion Coefficients in Zeolites. *Journal of colloid and interface science*, 234(2):434–441, 2001.
- [71] Carla Heitner-Wirguin and J. Kandler. Kinetic behaviour of chelating resins with phosphonic functional groups. *Journal of Inorganic and Nuclear Chemistry*, 33:3119–3129, 1971.

- [72] G Patzay. A simplified numerical solution method for the Nernst-Planck multicomponent ion exchange kinetics model. *Reactive & Functional Polymers*, 27(1):83–89, 1995.
- [73] Anatoly M. Dolgonosov, Ruslan Kh Khamizov, Anna N. Krachak, and Andrei G. Prudkovsky. Macroscopic model for multispecies ion-exchange kinetics. *Reactive and Functional Polymers*, 28(1):13–20, 1995.
- [74] Konrad Dorfner. *Ion Exchangers*. Walter de Gruyter, 1991.
- [75] F. Helfferich and M. S. Plesset. Ion Exchange Kinetics. A Nonlinear Diffusion Problem. *The Journal of Chemical Physics*, 28:418, 1958.
- [76] M.S. Plesset, F. Helfferich, and J.N. Franklin. Ion exchange kinetics. A nonlinear diffusion problem. II. Particle diffusion controlled exchange of univalent and bivalent ions. *The Journal of Chemical Physics*, 29(5):1064–1069, 1958.
- [77] Yng Long Hwang and Friedrich G. Helfferich. Generalized model for multispecies ion-exchange kinetics including fast reversible reactions. *Reactive Polymers*, 5(3):237–253, 1987.
- [78] G.E. Boyd, A.W. Adamson, and L.S. Myers Jr. The exchange adsorption of ions from aqueous solutions by organic zeolites. II. Kinetics. *Journal of the American Chemical Society*, 69(11):2836–2848, 1948.
- [79] Erol Pehlivan and Turkan Altun. Ion-exchange of  $Pb^{2+}$ ,  $Cu^{2+}$ ,  $Zn^{2+}$ ,  $Cd^{2+}$ , and  $Ni^{2+}$  ions from aqueous solution by Lewatit CNP 80. *Journal of Hazardous Materials*, 140(1-2):299–307, 2007.
- [80] D Reichenberg. Properties of ion-exchange resins in relation to their structure. III. Kinetics of exchange. *Journal of the American Chemical Society*, 75(3):589–597, 1953.
- [81] G.E Boyd and B.A. Soldano. Self-diffusion of cations in and through sulfonated polystyrene cation-exchange polymers. *Journal of the American Chemical Society*, 75(24):6091–6099, 1954.
- [82] David R. Lide and Henry V. Kehiaian. *CRC Handbook of Thermophysical and Thermochemical Data*. CRC Press, Inc., 1994.
- [83] Nghiem Van Nguyen, Jae chun Lee, Manis Kumar Jha, Kyoungkeun Yoo, and Jinki Jeong. Copper recovery from low concentration waste solution using Dowex G-26 resin. *Hydrometallurgy*, 97(3-4):237–242, 2009.
- [84] Charles H. McBurney and Erich F. Meitzner. Cellulosic paper containing ion exchange resin and process of making the same, October 4, 1960. U.S. Patent 2 955 067.

- [85] Teruzi Yamazaki, Toshiro Nakano, and Imai Akihiro. Method for manufacturing chemical filter, February 3, 2005. U.S. Patent 0 025 884.
- [86] Serope Kalpakjian and Steven R. Schmid. *Manufacturing Engineering and Technology, 7th edition*. Pearson Education, 2014.